

Optimization of Soft Interference Cancellation in DS-CDMA Receivers

Pascal G. Renucci

Thesis submitted to the Faculty of the
Virginia Polytechnic Institute and State University
in partial fulfillment of the requirements for the degree of

Master of Science
in
Electrical Engineering

Dr. Brian D. Woerner, Chairman

Dr. Theodore S. Rappaport

Dr. Charles W. Bostian

May 8, 1998

Blacksburg, Virginia

Keywords: Code Division Multiple Access, Multiuser Receivers, Interference Cancellation,
Spread Spectrum Communications, Mobile Radio

Copyright 1998, Pascal G. Renucci

Optimization of Soft Interference Cancellation in DS-CDMA Receivers

Pascal G. Renucci

Abstract

Parallel interference cancellation for DS-CDMA has been shown to suffer from biased amplitude estimates if a matched-filter estimator is used [1, 2]. The bias magnitude is proportional to the number of interfering users. For heavy system loads, the bias has been shown to adversely effect the accuracy of the interference cancellation process, thereby impairing BER after cancellation. Empirical simulation work [1, 2, 3] has demonstrated that weighting down interference estimates can improve BER performance.

This thesis substantiates these BER improvements by modelling and analyzing a soft interference cancellation technique which mitigates the effects of the bias by minimizing BER after cancellation in a bit-synchronous parallel interference cancellation CDMA receiver. We analyze system decision metrics with down-scaled interference estimates and determine both the mean and variance of the biased decision statistics. From these two metric moments, system BER is evaluated, and the optimal interference scaling function which minimizes BER is derived. We demonstrate BER performance enhancements by simulating this soft interference cancellation technique in systems under perfect power control and in the near-far situation. We further discuss the applicability of the results to asynchronous systems.

Dedication

This work is dedicated to the one and only Ron Rohrer.

Ron, if you still have doubts about my liking math, check-out Chapter 4!

Acknowledgements

For quite some time now I have been looking forward to writing this part of my thesis, for so many people worthy of mention have contributed to my graduate education and my well-being at Virginia Tech.

In October of 1995, I first approached Brian Woerner to tell him I wanted to become his student. Dr. Woerner had proven to me a gifted instructor and a very nice person outside of class, so I thought that since his research interests were consistent with mine, I should try to join his team. As it turns out, I could not have been any luckier. Dr. Woerner took a chance by taking me as his student and has provided me ever since with an ideal setting for learning. He has made my graduate experience in wireless communications everything I had hoped for and more. He gave me the opportunity to work at HP during the summer of 1997, and was most supportive of the pursuit of my own research ideas which ultimately lead to this thesis. Through Dr. Woerner's tutelage, I have sharpened my analytical and research skills, and feel that I have become a genuine member the world of research and development. Dr. Woerner is a veritable paradigm of academic altruism and my work with him has been the most thrilling intellectual experience of my life.

I would like to extend my gratitude as well to my two other committee members, Dr. Theodore Rappaport and Dr. Charles Bostian, for their insights into my research and its documentation in this thesis. Acknowledgment is due as well to several organizations who have funded me during my tenure at MPRG. First and foremost, I would like thank The Defense Advanced Research Projects Agency (DARPA) for funding most of my research

at MPRG. Further, I thank The US Office of Naval Research (ONR) and Hewlett-Packard Company (HP) for their support.

The staff at MPRG including Rennie Givens, Anjala Krishen, Hilda Reynolds, Aurelia Scharnhorst, and Lori Hughes deserve praise for their help throughout my graduate education. Rennie Givens has been extremely helpful in handling affairs ranging from getting me registered for a conference (an ordeal, trust me) to convincing Foxridge Apartments not to evict me! Further, Anjala Krishen was always eager to tender help for every computer crisis I ran across.

Many students at MPRG have enriched my learning experience. Neiyer Correal helped introduce me into the realm of MPRG's interference cancellation multiuser receiver, explaining the algorithm to me, and the famed "back-off factor" which has turned out to be my research bread and butter. Nitin Mangalvedhe has always been particularly generous with his time, imparting to me his more senior understanding of communications theory. Francis Dominique and Nishith Tripathi were commensurately generous and I have missed them both since their departure.

I was fortunate to have an office my final year at MPRG and got to know my colleague Matt Valenti a good deal better. Matt, whom I had always thought of as Mr. Turbo Code, provided for stimulating conversations on my own research and also helped me see parallels between our respective research areas. Matt has been a valuable source of friendship and I look forward to calling him Professor Valenti in the not-so-distant future!

Outside of MPRG, I have enjoyed the friendship of Florenz Plassmann who, through his giving nature, has become like a big brother to me. Our Beer & Pizza evenings at the Cellar are some my most treasured memories of Virginia Tech.

Looking ahead to the future, I await with breathless anticipation starting a new life in northern California. I look forward to joining the "Bay Area Happy Family" with my great friends Chinarut Ruangchotvit, Eugene Feinberg, Martin Frankel, Tao Ye, and of-course, Munazza-Ouh-La-La Bukhari.

Finally, I would like to thank my parents for their constant encouragement throughout my studies, both undergraduate and graduate, and for fostering my aspirations to the highest levels of education.

Contents

1	Introduction	1
1.1	Trends in Personal Communications	1
1.2	Multiple Access Fundamentals	2
1.3	Attributes of CDMA	5
1.4	CDMA Pitfalls	8
1.5	CDMA Receivers	9
1.6	Research Contributions	10
1.6.1	Organization of Thesis	12
2	Spread Spectrum and CDMA Multiuser Detection	14
2.1	Spread Spectrum Schemes	15
2.2	Fundamentals of DS-SS	16
2.2.1	The Single User DS-SS Transmitter	16
2.2.2	PN Sequences	20
2.2.3	The Conventional Correlation Receiver for DS-SS	22
2.3	CDMA Receiver Structures	24

2.3.1	Single User CDMA Receivers	24
2.3.2	Multuser CDMA Receivers	28
2.4	Summary	33
3	Analysis of Brute Parallel Interference Cancellation	34
3.1	Model of Brute Parallel Interference Cancellation	36
3.1.1	Transmitter Model	36
3.1.2	Brute Parallel Interference Cancellation Receiver	38
3.2	Analysis of Receiver Performance	41
3.2.1	First Stage	42
3.2.2	Second Stage	45
3.3	Discussion of Bias	50
3.4	Summary	54
4	Analysis of Soft Parallel Interference Cancellation	55
4.1	Model of Soft Parallel Interference Cancellation	56
4.1.1	Transmitter Model	57
4.1.2	Soft Interference Cancellation Receiver	58
4.2	Metric Characterization and Bias Analysis	60
4.2.1	First Stage	61
4.2.2	Second Stage	62
4.3	Chapter Summary	71

5	Interpretation of the Soft Cancellation Factor and Simulation Results	72
5.1	Evaluation of the SCF	72
5.2	Limiting Cases	74
5.3	Perfect Power Control	76
5.4	The Near-Far Case	85
5.5	Chapter Summary	87
6	Conclusions	88
6.1	Summary and Contributions	88
6.2	Future Work	90

List of Figures

1.1	The Three Principle Multiple Access Methods	5
2.1	BPSK-based Single User DS-SS Transmitter	16
2.2	Signal at Different Stages of Transmitter	18
2.3	Power Spectrum Comparison of Data and CDMA Signals	19
2.4	Sample Auto- and Cross-Correlation Functions of PN Codes ($N = 128$)	21
2.5	BPSK-based Conventional Correlation DS-SS Receiver	22
2.6	CDMA Communication System	25
2.7	BPSK-based Conventional Single User CDMA Receiver	26
2.8	BPSK-based Rake CDMA Receiver for a Given User	27
2.9	General Multiuser Receiver Structure	29
2.10	BPSK-based Optimal CDMA Receiver	30
2.11	BPSK-based General Purpose Interference Cancellation CDMA Receiver	32
3.1	CDMA Transmitter Model [4]	37
3.2	Interference Cancellation CDMA Receiver – One Stage of Cancellation	39
3.3	Asynchronous Time Relationship Between Users	47

3.4	Average Magnitude of Second Stage Metric versus Number of Simultaneous Users (K) for Perfect Power Control ($P_k = 1$ W for all Users) with Processing Gain $N = 15$ and $E_b/N_o = 10$ dB	52
3.5	BER versus Number of Simultaneous Users (K) in Perfect Power Control System ($P_k = 1$ W for all Users) with Processing Gain $N = 15$ and $K = 15$ Users	53
3.6	BER versus E_b/N_o in Perfect Power Control Asynchronous System ($P_k = 1$ W for all Users) with Processing Gain $N = 15$ and $K = 15$ Users	54
4.1	CDMA Bit-Synchronous Transmitter Model	57
4.2	CDMA Bit-Synchronous Soft Interference Cancellation Receiver Model	59
5.1	Soft Cancellation Factor (SCF) versus Number of Simultaneous Users (K) and versus $\frac{E_b}{N_o}$ for Processing Gain $N = 15$	77
5.2	Soft Cancellation Factor (SCF) versus Number of Simultaneous Users (K) and versus $\frac{E_b}{N_o}$ for Processing Gain $N = 31$	78
5.3	Average Second Stage Decision Metric $E \left[\left Z_{k,i}^{(2)} \right \right]$ versus Number of Simultaneous Users (K) for Processing Gain $N = 15$, $P_k = 1$ W for all Users, and $E_b/N_o = 10$ dB	79
5.4	Soft Cancellation Factor versus $\frac{E_b}{N_o}$ for $N = 15$ and $K = 15$	80
5.5	BER Comparison with Several SCFs for Processing Gain $N = 15$ and for Number of Simultaneous Users $K = 15$	81
5.6	Soft Cancellation Factor versus Number of Simultaneous Users (K) for Processing Gain $N = 15$ and for $\frac{E_b}{N_o} = 10$ dB	82

5.7	BER Comparison of Soft Cancellation, Cancellation when $\xi = 1$, and Cancellation when $\xi = 1$ with Unbiased Estimates for Processing Gain $N = 15$ and for $\frac{E_b}{N_o} = 10$ dB	83
5.8	BER versus Soft Cancellation Factor (SCF) Across Various System Loads (K) for Both Synchronous and Asynchronous Systems with Processing Gain $N = 31$ and $E_b/N_o = 10$ dB	84
5.9	Soft Cancellation Factor versus Power Disparity in dB for Processing Gain $N = 31$ and for $\frac{E_b}{N_o} = 10$ dB	86
5.10	BER Comparison of Soft Cancellation versus Brute Cancellation ($\xi = 1$) for Processing Gain $N = 31$ and for $\frac{E_b}{N_o} = 10$ dB	87

Chapter 1

Introduction

The landmark inventions of the transistor, and soon thereafter, of the integrated circuit are the building blocks of much of today's technology. They enabled the explosion of the personal computer industry in the early 80's in response to the pervasive demand for more computing power. More recently still, they have allowed for the development of the wireless personal communications industry to feed the insatiable need for communications capability any place and anytime.

1.1 Trends in Personal Communications

The growth of the wireless personal communications industry has been astronomical. Today, the most widely available media for commercial wireless personal communication are the cellular telephone and the pager. By mid-August 1997, there were 50 million cellular telephone subscribers in the United States alone, compared to less than 500,000 in 1987, demonstrating the cellular industry's exponential expansion [5]. The paging industry has commensurately exploded with the number of subscribers mushrooming from 1 million in 1980 to an expected 63 million in the year 2000 [5].

In the early 90's, The Federal Communications Commission (FCC) auctioned a portion of frequency spectrum dedicated to the Personal Communications Services (PCS) industry. The PCS industry's goal is to expand upon the capabilities of current second generation cellular systems to provide an enhanced set of services such as wireless facsimile, e-mail, and bank transactions. Looking further ahead, third generation personal communication systems under planning now will afford the much sought after capability of communicating with whomever, whenever, and very importantly, wherever one may be [6].

While there is still some distance to cover before reaching this point, many developing PCS technologies are key in achieving the ultimate third generation goals. These technologies include adaptive antenna arrays (smart antennas), adaptive equalization, speech coding, propagation prediction, and advanced signal processing techniques for mitigating interference effects. PCS subscriber growth is predicted to shoot from 500,000 in April 1997 all the way to 50 million in 2001 [5], a growth rate as yet unparalleled in the personal communications industry.

1.2 Multiple Access Fundamentals

If the growth of the personal communications industry is to continue as it has for the past decade, methods need to be devised to allow increasing number of customers to share the available communications bandwidth. First and second generation (analog and digital, respectively) cellular telephone systems faced the same problem.

Many first generation systems solved the problem by using *Frequency Division Multiple Access (FDMA)* technology. The basic idea behind FDMA is decades old. AM and FM radio stations have long used Frequency Division Multiplexing (FDM) [7] for their simplex channels, which amounts to using a unique frequency band for each radio station to transmit in. For cellular telephony, the concept was extended for full duplex channels. FDMA allows multiple users to access the communications channel by allotting two distinct frequency

bands to each transmitter and receiver pair. Many of the world's first widely deployed cellular systems successfully used FDMA, such as The Advanced Mobile Phone Service (AMPS) in the US, The Extended European Total Access Cellular System (ETACS) in Europe, and The Nippon Telephone and Telegraph (NTT) system in Japan [7].

While the technical accomplishments of first generation cellular systems are significant, the subscriber base of these systems demanded improved quality and an enlarged range of services. Indeed, FDMA has been shown to have hard capacity limits and to perform poorly in many cellular radio environments [8, 9, 10]. In addition, analog components are notorious not only for their intolerance of changes in ambient temperature, but also for their performance degradation as they age. These impediments motivated the cellular industry to shift towards digital technology for its second generation systems [11]. There are a number of advantages afforded by the use of digital systems. Some include digital modulation and speech coding which can provide better spectral efficiency, error correction coding which insulates the transmission from channel impairments, encryption which protects the signal from unauthorized eavesdropping, and digital signal processing which is more flexible, simpler to implement, and more resistant to changes in temperature than analog signal processing.

Along with the change from analog to digital came new multiple access techniques implemented digitally in second generation cellular systems. The most commonly used multiple access technique in early second generation systems was *Time Division Multiple Access (TDMA)*. TDMA separates users by assigning each user a short time slot during which only that user's signal is transmitted; during the next time slot another user's signal is transmitted and so forth [7]. The nature of TDMA entails intense switching among users and correspondingly, circuitry capable of delivering fast and accurate switching between various users' data streams. It would be considerably more difficult to design analog circuits with such performance than it is to design digital circuits for that purpose, leading to the digital realization for TDMA.

Examples of second generation systems include the pan-European Groupe Spécial Mobile

(GSM) standard, The United States Digital Cellular (USDC) standard (also known as The Intermediate Standard-54, or IS-54), and The Pacific Digital Cellular (PDC) standard in Japan [7]. The GSM system is particularly noteworthy as it was the world's first fully digital cellular system. GSM went online in 1990 after almost a decade of political and technical negotiation between a multitude of European nations.

An alternative competitor to TDMA emerged in later second generation wireless systems. The competing multiple access technique is called ***Code Division Multiple Access (CDMA)*** and is based upon spread spectrum technology (the associated cellular telephone standard is known as IS-95). The spread spectrum concept is in fact almost as old as the FDM idea, however spread spectrum was limited primarily to military endeavors from World War II to as recently as the last decade. The development of VLSI technology has made spread-spectrum economical for commercial applications.

The principle CDMA relies upon to isolate users from one another is less intuitive than that of FDMA and TDMA. In FDMA and TDMA, users are orthogonalized along frequency and time. FDMA allots separate *frequency* slots for users while TDMA allots separate *time* slots for users. In contrast, CDMA signals all overlap in both time and frequency, but are distinguishable by their *signature codes* (i.e. the *codes* in *Code Division Multiple Access*). Each user is assigned a unique high rate signature code which isolates it from all other users. For each user, the code signal multiplies the data signal, and since the code rate is much higher than the data rate, the resulting signal bears a higher rate than the data rate. The increased rapidity of time domain changes induces a frequency spreading effect upon the original data signal (ergo, the *spread* spectrum) [12]. In the IS-95 standard, the bandwidth of the CDMA signal is 1.25 MHz. The newer ETSI proposal for a third generation CDMA-based standard calls for a 5 MHz bandwidth (wide-band CDMA or WCDMA). The differences between the three discussed flavors of multiple access are depicted graphically in Figure 1.

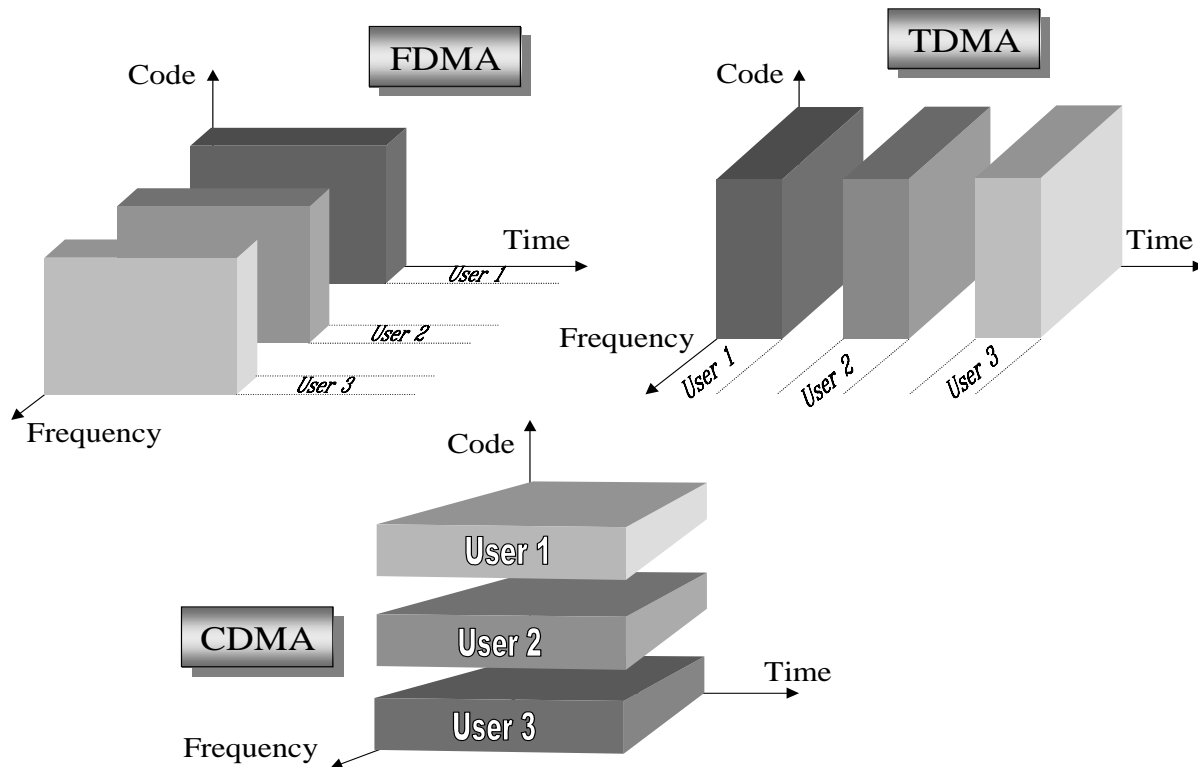


Figure 1.1: The Three Principle Multiple Access Methods

1.3 Attributes of CDMA

CDMA signals and systems possess many attributes distinguishing them from their FDMA and TDMA counterparts. These distinguishing features have motivated many cellular and PCS providers to consider CDMA for their systems.

The most immediate advantage to employing CDMA signalling techniques stems from the spread nature of the spectrum of a CDMA signal. When considered over its spreading band, a CDMA signal appears noise-like. The almost white spectral feature arises from the high rate signature codes which modulate the data signal. In fact, these codes are often called Pseudo-Noise codes or PN codes. CDMA signals therefore provide a degree of free message privacy or protection since they are in effect camouflaged in noise, and can even pass unnoticed in instances where the spread power spectrum creeps below the noise floor. It is these *anti-jamming and Low Probability of Intercept (LPI)* properties in particular

that decades ago drew military attention to spread spectrum communications.

More recently, myriad other advantages of CDMA have been discovered. Key among them is the ***resistance of CDMA to multipath fading***. Indeed, in an FDMA system, if the frequency band of a given user is subject to a particularly severe fade, that user's signal can be unrecoverable. In CDMA however, every user is spread over a wide bandwidth and so if a small portion of the band is faded, every user does feel the fade, but most of the spectrum remains intact preserving message signal integrity for all users. The wider the spread bandwidth is, the more resistant to multipath fading the system becomes, thus the inherent advantage of the wide-band CDMA standard. Moreover, multiple signal paths can serve as a source of diversity reception for CDMA, instead of a bane as they are for FDMA and TDMA. If the *RMS* delay spread of the arriving time-delayed multipath components is significantly greater than the CDMA symbol (chip) time, the multipath components are resolvable (i.e. they do not constructively or destructively combine) and can be filtered in a number of ways to enhance reception in ***Rake CDMA receivers*** [13].

Some have suggested that CDMA systems offer the possibility of ***overlay capability*** [14] because of their immunity to interference. Since the CDMA power spectrum is spread below that of narrowband systems, a CDMA signal overlaid onto a narrowband one poses little threat; moreover, CDMA is inherently resistant to narrowband interference. Therefore, a CDMA system and a narrowband system might be capable of coexisting without harm to each other. This, although not universally accepted, feature is most attractive as it eases the transition from analog to digital cellular telephony.

From a cost and time perspective, CDMA requires less ***frequency planning*** as compared to its FDMA cousin. The process of allocating just enough frequencies to base stations and separating the base stations sufficiently for an FDMA system to maintain its 18 dB signal to interference ratio (S/I) is long, costly, and arduous. In contrast, CDMA can operate at a much reduced S/I ; in fact, all cells in a CDMA system can employ the same carrier frequency, thus CDMA's famed ***universal frequency reuse***.

The issue of handoff is yet another strong suit of CDMA. In first generation analog systems, handoff is a risky operation. If the mobile's signal is subject to a deep fade during the handoff, there is the potential of a *call drop* if the base station cannot perceive the mobile's signal. CDMA however employs universal frequency reuse, and so a mobile's signal is recognizable by more than just one base station. CDMA takes advantages of this and employs ***soft handoff***. The mobile in fact transmits to two base stations simultaneously during handoff, and the base station receiving the stronger signal ultimately keeps the user. This greatly reduces the number of call drops as compared to handoff in FDMA.

CDMA systems also take advantage of the human voice duty cycle being about 40%. Due to the nature of a CDMA signal being a multiplexed stream of users, digital vocoder technology can periodically cease transmitting in instances of voice inactivity. During this portion of time, the interference level is effectively reduced which in CDMA converts directly into a capacity increase [9].

However, perhaps the most significant performance advantage that CDMA offers is ***capacity***. Certainly, the driving force behind lucrative cellular businesses is the number of subscribers a provider can give quality service to. The more subscribers a provider can serve for a fixed cost, the better. It is often said that CDMA performance degrades gracefully as the system is gradually loaded up, providing a smooth instead of abrupt performance decline [15]. CDMA thus provides a ***soft capacity*** limit, instead of a hard capacity limit as in the case of FDMA and TDMA. This is certainly a great attribute for if an FDMA or a TDMA system is loaded beyond its designed capacity, some users' data would be destroyed, resulting in one or more forced call drops. In fact, several publications estimate a 10 to 18 times improvement in capacity for CDMA over FDMA [9, 16].

1.4 CDMA Pitfalls

As with any system, CDMA presents a few potential difficulties which we discuss here briefly. The performance of a CDMA system depends, among other factors, upon the *auto- and cross-correlation properties* of its PN codes. Ideally, different PN codes would be perfectly orthogonal, but practically generating perfectly orthogonal codes is impossible. Consequently, a CDMA system's performance will depend on how close its PN codes approximate full orthogonality.

Since there is almost always a finite non-zero degree of correlation among all users in an asynchronous CDMA system, each user's decision statistic will reflect this other-user intrusion, termed *self-interference*. If one considers a single cell system, both FDMA and TDMA preserve inter-user orthogonality in frequency and in time, respectively, whereas CDMA exhibits a degree of self-interference. But even though FDMA and TDMA perform better in a single cell environment, their performance falters as compared to CDMA when extending the system to several cells, as FDMA and TDMA encounter co-channel and adjacent-channel interference [17].

One additional limitation in CDMA is the *near-far* problem. It occurs when a signal originating from a mobile very far from the base station (near a cell boundary for instance) is received with significantly less power than another mobile transmitting very close to the base station. In this instance, the received power from the closer mobile can be much greater than that of the farther mobile. A user experiencing the near-far effect is in danger of not being received by the base station¹. Accordingly, tight power control must be exercised by the mobile and/or by the base station to mitigate this effect. However, perfect power control is difficult to implement and unfortunately, small power disturbances such as 1 or 2 dB can cut capacity down 15-35% [16, 18].

¹The near-far effect is more of a concern on the reverse link (from mobile to base) than on the forward link (from base to mobile) where all signals originate from a common base station.

1.5 CDMA Receivers

As discussed in Section 1.3, CDMA's principle forte is its soft capacity limit. Where exactly this limit is drawn depends upon the number of interferers a given user perceives in the system. As such, CDMA is *interference limited*: the greater the level of interference, the less capacity the system can support. In fact, the Bit-Error-Rate (BER) in CDMA has been found to increase approximately linearly with the percent of capacity overload. Therefore, any suppression of interference roughly translates linearly into a capacity increase [9].

Seeking to capitalize upon this fact, researchers have endeavored for several years now to innovate methods of reducing interference levels in CDMA systems. CDMA would be interference-free if the codes were ideal, however it is impossible to design perfectly orthogonal codes for an asynchronous reverse link. Therefore, less of an effort has been made to design nearly optimal PN codes, for the near-far problem could still harm performance despite almost perfect codes. Efforts have therefore delved more into designing CDMA receiver algorithms capable of mitigating interference effects.

Classical textbook receiver design as taught for many years has emphasized the use of *The Maximum A Posteriori (MAP)* decision rule to minimize BER, and the matched-filter to best recognize digital pulses in white noise [19]. The conventional CDMA receiver uses this correlation operation to recover the users from the received CDMA signal. However, use of the correlation receiver is based upon the premise of Additive White Gaussian Noise (AWGN) corrupting the transmitted signal. In CDMA, the desired user is corrupted by interference from other users in addition to AWGN, the aggregate of which is not exactly Gaussian distributed. Therefore, classical receiver theory does not suffice to take full advantage of the inherent structure of a CDMA signal to isolate its constituent users. In fact, if the structure of the multiple access interference is known, significantly improved reception is possible.

Most recent CDMA receiver algorithms attempting to mitigate interference were designed using a novel approach to signal detection: multiuser detection [20, 21]. A CDMA signal is

a mix of multiple users' signals linearly summed together, all users overlapping in both time and frequency. For any time duration, the entire spreading bandwidth contains information about all the users in the system. To recover a given user, the receiver could therefore not only seek the desired user directly (conventional CDMA detection), but it could also use information about the interfering users to aid in the recovery of the desired one. Multiuser receivers distinguish themselves from conventional ones in their use of interfering users' information to help detect the desired user. Many multiuser receivers have been analyzed in the literature and the principle categories will be briefly reviewed in the following chapter.

The optimal multiuser receiver algorithm for CDMA was derived by Verdù [22]. Verdù showed that to produce lowest probability of error, the receiver algorithm needs to perform *Maximal Likelihood Sequence Estimation (MLSE)* over the entire duration of the received signal and correspondingly, decode the entire received sequence of symbols within a trellis using the Viterbi Algorithm. Such a procedure is exponentially complex in the number of users and translates into a receiver structure that is not practically realizable. Consequently, the role of Verdù's receiver structure has become that of a benchmark against which to compare less optimal receiver algorithms. Since then, the search for high performance sub-optimal receiver structures with reasonable complexity that has dominated research efforts in multiuser detection.

1.6 Research Contributions

In this thesis, we analyze a particular type of sub-optimal multiuser receiver termed a *parallel interference cancellation* receiver. In essence, such a receiver attempts to concurrently (i.e. in *parallel*) estimate interfering users' signals and to subtract them from the received signal, leaving only the desired user's signal. The idea was originally proposed by Varanasi and Aazhang [23]. Since then, research has documented the potential performance gains of interference cancellation over conventional CDMA detection.

This research considers a multistage parallel interference cancellation CDMA receiver structure originally proposed by Striglis, *et al.* [24]. The multistage structure consists of a conventional receiver for the first stage, followed by one or more interference cancellation stages. The role of the first stage is to supply first order amplitude estimates of each user's transmitted signal to the second stage. The second stage then reconstructs transmitted signal estimates for the interfering users based upon The Gaussian Approximation for the probability distribution of the interferers. Signal reconstruction is followed by the subtraction of these signal estimates from the received signal, producing then a "reconstructed" cleaner received signal containing the desired user, residual interference, and thermal noise. The new received signal is then matched-filtered to obtain an enhanced (second order) amplitude estimate of the desired user. The second stage can be repeated several times, however each new iteration brings about less improvement. Ultimately, hard bit decisions are made based upon the enhanced matched-filter outputs.

Initial analysis was carried out under the assumption of unbiased first and second stage amplitude estimates [24, 25]. However, it was later discovered that the amplitude estimates at the second stage are in fact biased in direct proportion to the number of interfering users [1]. The bias acts to the detriment of system BER, particularly under severe loading conditions. Previously derived analytical BER is consistent with simulation BER for light system loads, when bias magnitude is small. But as the system load grows larger, a disparity between analytical and simulation BER arises, with simulation BER diving below predicted BER due to the greater bias magnitude.

In an effort to reduce the effects of the bias, empirical Monte-Carlo simulation trials were carried out using down-scaled first stage amplitude estimates, for use in second stage interference cancellation (instead of cancelling using the original estimated amplitudes from the first stage). The motivation behind this technique is that if interference estimates are unreliable due to biasing, then perhaps using them partially as opposed to integrally may improve performance. Results from such experiments were most encouraging, so much so that a simulation study was conducted to find the optimal scaling factor for a given system.

The scaling factor, termed the *Soft Cancellation Factor* or *SCF*, giving lowest BER was found to depend roughly linearly upon system loading: the greater the loading, the smaller the SCF. Similar experimental results have been observed by other researchers with comparable improvements [3].

The contribution of this thesis is to substantiate analytically the observed BER improvements after one stage of interference cancellation. For a synchronous and asynchronous system, we analyze system decision statistics at both the first and second stages, showing the presence of the bias at the second stage. Through a series of simulations, we demonstrate the harmful effects of the bias on system performance. For a synchronous system, we then analyze the interference cancellation algorithm with interference estimates down-scaled by SCFs. We derive both the mean and variance of the biased amplitude estimates from which an expression for second stage BER is determined in terms of the SCFs. The SCFs that minimize second stage BER are then computed. We compare the resulting BER with that produced by a system employing an unbiased amplitude estimator.

1.6.1 Organization of Thesis

The rest of the thesis is structured as follows.

Chapter 2 begins with an expository of the fundamentals of direct sequence spread spectrum communications and continues with a review of the various multiuser CDMA receiver structures discussed in the literature, highlighting their salient features.

Chapter 3 presents our model of an asynchronous CDMA system employing the aforementioned interference cancellation receiver. We analyze the decision statistics of the receiver, determining the mean of first and second stage metrics. First stage statistics are shown to be genuinely unbiased, but second stage statistics are proven to be biased, with a bias magnitude proportional to the number of interferers. We document the effect of the bias with plots of averaged second stage decision statistic magnitudes under various user loads,

and show how the actual mean decays with loading from the desired mean due to the bias. Further, we compare BER from simulation (affected by the bias) with BER from analysis in [25] which assumes the bias does not exist, and show the degradation in BER in the biased system as compared to the unbiased system. We finish Chapter 3 by motivating our soft interference cancellation solution to mitigating the effect of the bias upon BER.

Chapter 4 models and analyzes a bit-synchronous version of our CDMA system using soft interference cancellation. We begin by detailing our bit-synchronous soft interference cancellation system model and then delve into an analysis of system metrics. The mean and variance of both first and second stage statistics are derived in terms of the soft cancellation factors. As before, first stage statistics are shown to be unbiased while second stage statistics are biased in proportion to loading. With second stage mean and variance at hand, we express second stage BER in terms of the soft cancellation factors, and finally proceed to derive the set of soft cancellation factors minimizing this BER.

In Chapter 5, a performance evaluation of the soft cancellation technique is done. We begin with general issues regarding the evaluation of the soft cancellation factors and their validity. We then move to specific systems and demonstrate the performance enhancements associated with soft cancellation. We first deal with systems operating under perfect power control and then with those subject to the near-far effect. In our treatment of perfect power control systems, we include a discussion of how well the derived soft cancellation factors in our bit-synchronous system can be applied to an asynchronous system (to the end of minimizing BER).

Chapter 6, the conclusions and summary chapter, terminates this work.

Chapter 2

Spread Spectrum and CDMA Multiuser Detection

The previous chapter presented some of the characteristics of spread spectrum systems. There are in fact several ways to spread the signal spectrum, each with its own particular set of advantages [26]. The common measure among them is called the Processing Gain (PG) which reflects the degree of spectral spreading. The PG can be defined as the ratio of the spread signal bandwidth to the data signal bandwidth. The realization of the PG within a particular system depends upon the specific type of spread spectrum system. In this chapter, we begin with a brief overview of the basic types of spectrum spreading schemes, and then focus upon Direct-Sequence Spread Spectrum signals and the receivers used to despread them.

2.1 Spread Spectrum Schemes

There are three principle types of spectrum spreading techniques:

1. Direct Sequence Spread Spectrum (DS-SS):

DS-SS systems are currently the most commercially important class of spread spectrum systems. In DS-SS, each user's data signal is multiplied by its unique high rate signature sequence waveform, thus the title *direct sequence*. The spreading operation is in fact a layer of phase modulation on top of the digital modulation format used for transmission (usually BPSK or QPSK) [27]. The additional modulation permits users be distinguished from one another at the receiver. The PG in DS-SS can be measured as the ratio of the code rate to the data rate. In this thesis, we concentrate upon DS-SS systems solely.

2. Frequency Hopped (FH):

FH systems are reasonably popular and achieve spectral spreading by transmitting the narrowband message signal at successively different carrier frequencies. The *hopping pattern* is pseudo-random in nature and is determined by the spreading code. In FH systems, the PG is determined by the total number of different carrier frequencies in the hopping pattern.

3. Time Hopped (TH):

TH systems are analogous to FH in that TH systems use a pseudo-random code to specify at which times to transmit the narrowband message signal. Here, the PG is the total number of different transmission times.

There are also hybrid spread spectrum system formats which use the above in combination. However, these only occur sparsely and we shall deal only with DS-SS systems in this thesis.

2.2 Fundamentals of DS-SS

In this section, we briefly survey the principles of DS-SS systems, and introduce a mathematical notation for describing such systems. We begin with an example of a basic single user DS-SS transmitter and continue with desirable PN code properties. We finish this section with the single user DS-SS receiver.

2.2.1 The Single User DS-SS Transmitter

For ease of exposition, we select the BPSK digital modulation format for our DS-SS transmitter. Figure 2.1 depicts a single user BPSK DS-SS transmitter model.

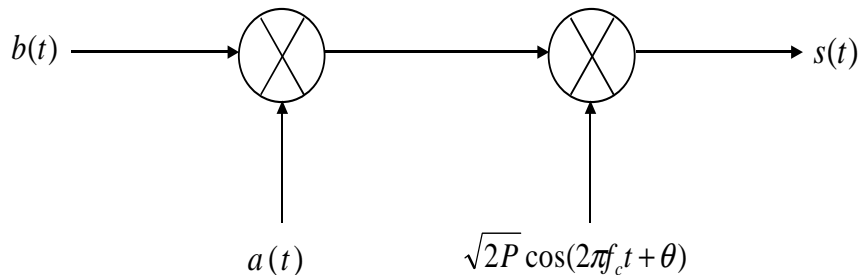


Figure 2.1: BPSK-based Single User DS-SS Transmitter

The data signal $b(t)$ can be expressed as

$$b(t) = \sum_{i=-\infty}^{\infty} b_i p_T(t - iT), \tag{2.1}$$

where $\{b_i\}$ is a set of independent identically distributed (*i.i.d.*) Bernoulli random variables. The symbol b_i represents the i^{th} data bit with $b_i \in \{-1, +1\}$ and

$Pr[b_i = -1] = Pr[b_i = +1] = 1/2$. The unit rectangular pulse $p_T(t)$ is given by

$$p_T(t) = \begin{cases} 1, & 0 \leq t < T \\ 0, & \text{otherwise,} \end{cases} \quad (2.2)$$

where T is the duration of the data bit. The data signal is spread by the PN code waveform $a(t)$ denoted as

$$a(t) = \sum_{j=-\infty}^{\infty} a_j p_{T_c}(t - jT_c), \quad (2.3)$$

where a_j is identically distributed to b_i . Therefore, we assume that the spreading code $\{a_j\}$ is randomly generated, although known at both the transmitter and the receiver. The elements of $\{a_j\}$ are called code *chips* and there are usually many chips per bit, i.e $T_c \ll T$.

We denote the system processing gain by N . As mentioned previously, we can define N as the ratio of the chip rate to the data rate, $N = R_c/R$, which can also be expressed as the ratio of the bit duration to the chip duration, $N = T/T_c$. Many systems' code sequences repeat for each bit of a given user. Such systems are called *code on pulse* (each bit being a pulse) and their code waveforms are periodic in T . The IS-95 system however does not operate this way, and many DS-SS system simulations use aperiodic code sequences.

Continuing with the DS-SS transmitter model, the spread data signal $b(t)a(t)$ is modulated onto an RF carrier. The time-averaged bandpass power of the carrier is P , the carrier frequency is f_c , and the carrier phase is θ . The resulting transmitted signal $s(t)$ then has the form

$$s(t) = \sqrt{2P}b(t)a(t) \cos(2\pi f_c t + \theta). \quad (2.4)$$

Figure 2.2 shows a time domain example of a train of three bits as it passes through a single user DS-SS transmitter. For ease of illustration, we use a code on pulse system with $N = 7$. The data sequence is chosen as $\{b_i\} = \{+1, -1, +1\}$, and the code sequence is set to $\{a_j\} = \{-1, -1, +1, -1, +1, +1, -1\}$. Figure 2.3 shows the frequency domain viewpoint of the process.

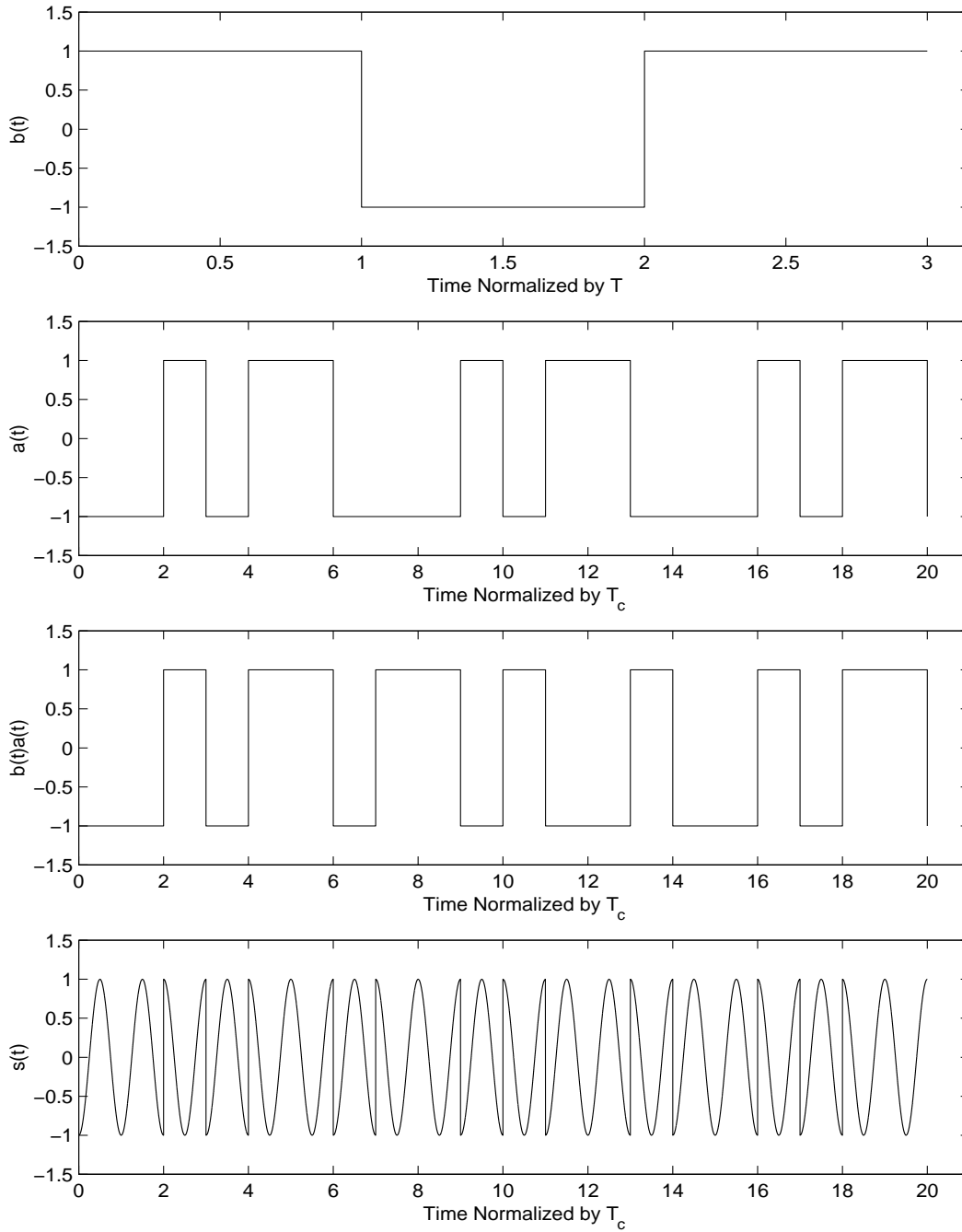


Figure 2.2: Signal at Different Stages of Transmitter

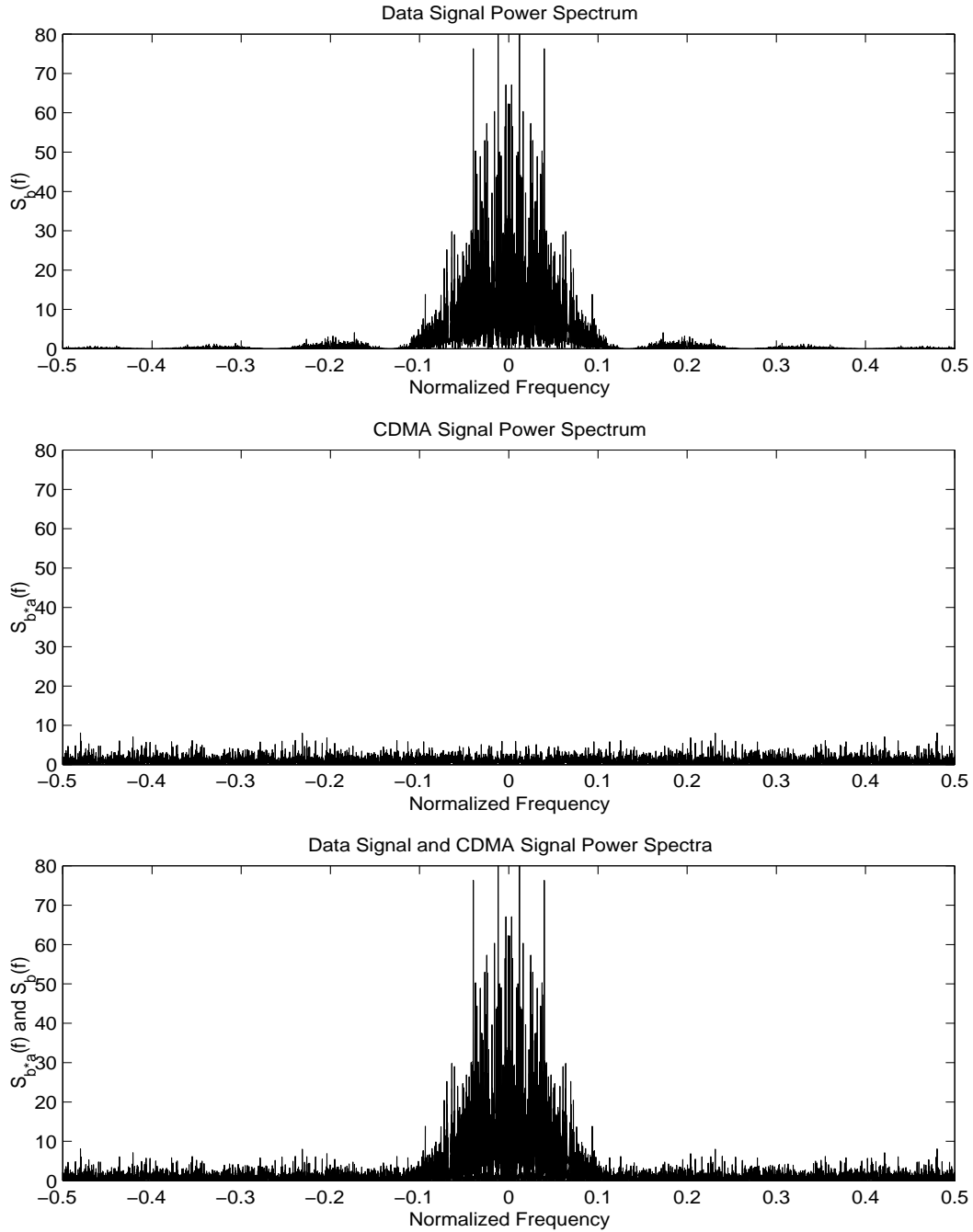


Figure 2.3: Power Spectrum Comparison of Data and CDMA Signals

2.2.2 PN Sequences

PN sequences are a vital part of a DS-SS system as their characteristics directly impact system performance. Ideally, PN sequences would permit multiple users to share bandwidth without interfering with each other at all. Unfortunately, achieving this ideal is impossible from a practical perspective, and so codes with *near-ideal* properties are sought after.

The quality of the PN codes is often gauged by computing their auto- and cross-correlation functions. PN code design seeks to minimize auto-correlation for non-zero delay and to minimize cross-correlation over all delays. Optimally, the auto-correlation would be zero for non-zero delay and the cross-correlation would be zero over all delays. The degree to which PN code properties approach this, determines the degree to which users interfere with one another, and consequently, decides the system performance.

Low auto-correlation is important for determining performance in fading channels and low synchronization time. Mathematically stated for a PN code sequence $\{a_j\}$, we seek the auto-correlation property

$$R_{a_j}[\delta] = \frac{1}{2N-1} \sum_{n=1-N}^{N-1} a_n a_{n+\delta} \simeq 0 \quad \delta \neq 0. \quad (2.5)$$

Shifting now to the requirement of low interference between users, we desire that the cross-correlation between any two distinct (l and m , $l \neq m$) users' PN sequences $\{a_{l,j}\}$ and $\{a_{m,k}\}$ obey

$$R_{a_{l,j} a_{m,k}}[\delta] = \frac{1}{2N-1} \sum_{n=1-N}^{N-1} a_{l,n} a_{m,n+\delta} \simeq 0 \quad \forall \delta, \quad (2.6)$$

where $a_{l,j}$ is the j^{th} chip of l^{th} user's PN sequence.

Figure 2.4 shows empirically computed sample auto- and cross-correlation functions for random codes in an $N = 128$ system.

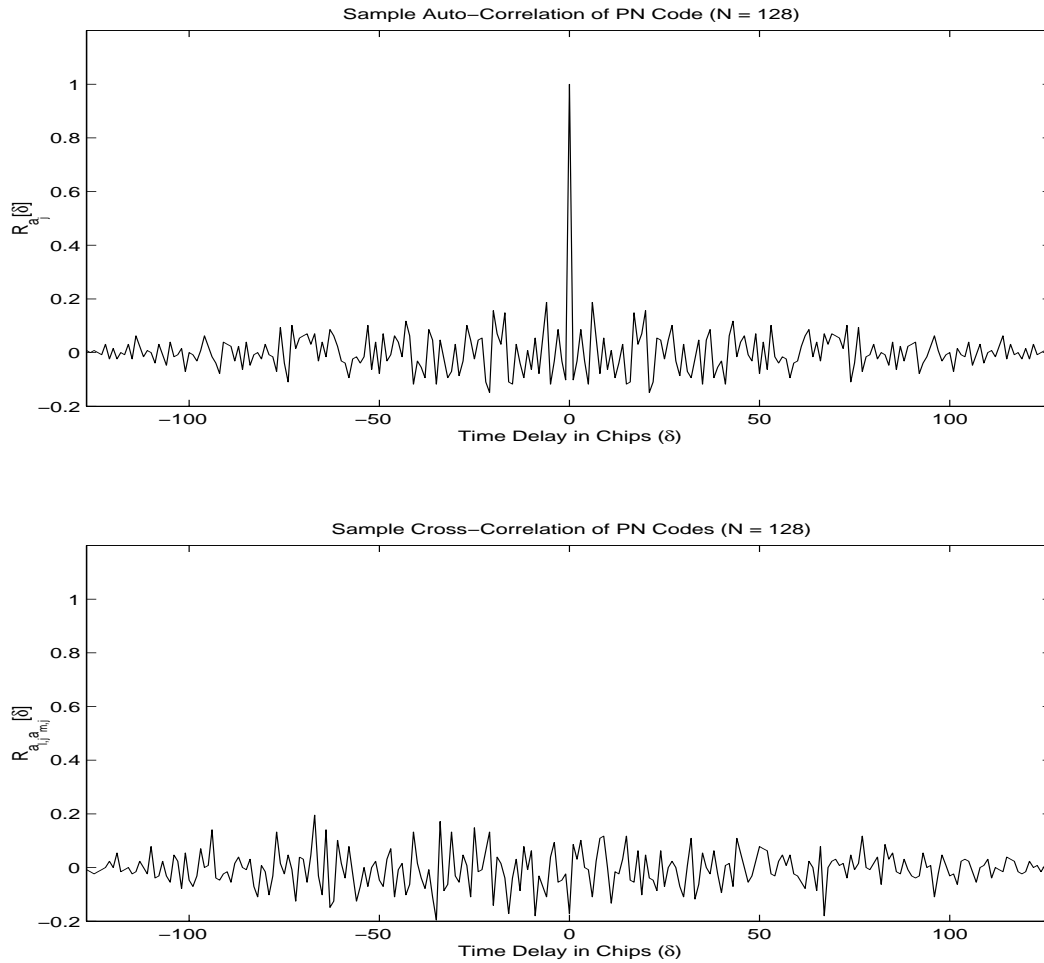


Figure 2.4: Sample Auto- and Cross-Correlation Functions of PN Codes ($N = 128$)

While not completely ideal, random codes do exhibit good auto- and cross-correlation properties. Such codes have great utility in DS-SS system modelling and analysis. In real systems however, PN codes are usually generated by a finite state machine such as a linear-feedback shift register. *Maximal Length Sequences* or *m-sequences* are a common class of PN codes created by a shift register. Other types of PN sequences can be derived from *m-sequences* such as *Gold Codes* and *Kasami Sequences* [12]. Each type of code has a particular advantage and depending upon system requirements, various performance parameters can be traded-off by the use of one code type over another.

2.2.3 The Conventional Correlation Receiver for DS-SS

The receiver’s function is to absorb the incoming signal and to recover the transmitted bit stream while making the least possible amount of incorrect bit decisions. Its success in this endeavor depends upon its detection algorithm, the aforementioned PN code properties, and the channel conditions as well.

Here, a suitable channel model inserts a finite propagation delay τ into the transmitted signal $s(t)$ producing $s(t - \tau)$, and corrupts the transmitted signal with additive white Gaussian noise (AWGN) $n(t)$. The input to the receiver is the sum of the delayed transmitted signal and the AWGN. Maintaining consistency with our BPSK-based DS-SS transmitter, the received signal is modelled by

$$\begin{aligned} r(t) &= s(t - \tau) + n(t) \\ &= \sqrt{2P}b(t - \tau)a(t - \tau) \cos(2\pi f_c(t - \tau) + \theta) + n(t). \end{aligned} \tag{2.7}$$

Figure 2.5 depicts a BPSK-based conventional DS-SS receiver.

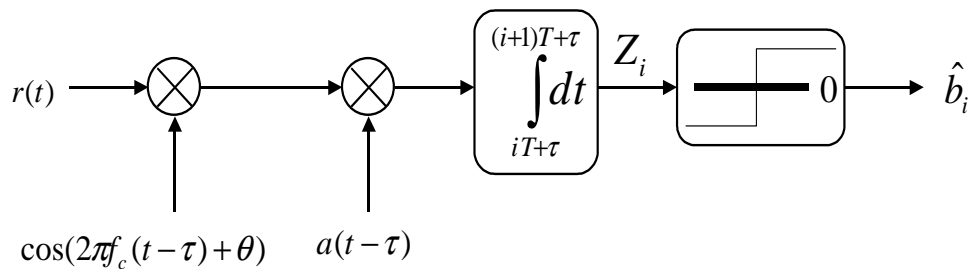


Figure 2.5: BPSK-based Conventional Correlation DS-SS Receiver

Its chain of operations essentially undoes those of the transmitter: demodulation followed by despreading (and ultimately decision making). For effective demodulation, the receiver’s carrier replica must be synchronized with that of transmitter’s. Once the receiver has achieved carrier lock, the receiver must then regenerate a synchronous copy of the PN code waveform

$a(t - \tau)$ to fully despread the incoming signal. Once despread, the signal passes through a correlator which produces a *decision statistic* or *metric* Z_i for the i^{th} transmitted data bit, computed as

$$Z_i = \int_{iT+\tau}^{(i+1)T+\tau} r(t)a(t - \tau) \cos(2\pi f_c(t - \tau) + \theta)dt. \quad (2.8)$$

The information stream to be recovered is embedded, along with AWGN, within $r(t)$. From an intuitive viewpoint, the above correlation integral gauges the degree of similarity between $a(t - \tau)$ and the baseband version of $r(t)$, much like an inner product operation. If the AWGN level is reasonable, the correlation operation will be sufficiently capable of recognizing the code hidden in $r(t)$.

Following the correlator is a non-linear threshold device, modelled as a hard limiter, which yields an estimate of the transmitted bit \hat{b}_i ,

$$\begin{aligned} \hat{b}_i &= \text{sgn}[Z_i] \\ &= \begin{cases} -1, & Z_i < 0 \\ +1, & Z_i \geq 0. \end{cases} \end{aligned} \quad (2.9)$$

It can be shown that such a correlation receiver, usually implemented as a matched-filter, is optimal (lowest BER) when attempting to detect a known signal $a(t)$ in AWGN $n(t)$ [19]. Therefore, a correlation receiver is indeed optimal when attempting to recover a single DS-SS user in AWGN.

However, when multiple DS-SS users are transmitting simultaneously, the channel then becomes a CDMA channel. The problem of recovering a given user then shifts from detection of a DS-SS user in AWGN, to detection of a DS-SS user amidst AWGN *and* all interfering DS-SS users. If interference from other users in a CDMA channel may be modelled as Gaussian, then the matched-filter receiver would still be optimal. Unfortunately, other user interference is not exactly Gaussian and so a matched-filter receiver is in fact not optimal. The conventional CDMA receiver however does assume a Gaussian distribution for interference and employs the above receiver structure for each user.

Since the inception of the conventional CDMA receiver, there have been novel receiver architectures proposed whose performance surpasses that of the conventional receiver. In the next section, we briefly survey the major CDMA receiver structures, and the remainder of the thesis will concentrate on one type of structure of interest.

2.3 CDMA Receiver Structures

The change from a single user communications environment to a multiple user environment necessarily entails a modification in receiver design if high performance is to be maintained. The communication system model depicted by Figure 2.1 and Equation 2.7 is no longer valid and the multiple users sharing the channel must be accounted for in the design of the receiver.

Figure 2.6 is a general model of a CDMA communication system. It is comprised of K single user DS-SS transmitters simultaneously transmitting over a linear AWGN channel. The channel attenuates and delays each signal and corrupts the aggregate transmission with AWGN. This noisy composite of delayed and attenuated signals $r(t)$ arrives at the CDMA receiver whose job it is to recover each user's data stream.

2.3.1 Single User CDMA Receivers

Early work in CDMA receiver design simply assimilated interference into AWGN channel noise and detected each user with a single user DS-SS receiver. Such a design is called a *single user receiver* since it assumes that only one user is transmitting and treats other user interference as additional AWGN channel noise. We look at two types of single user receivers.

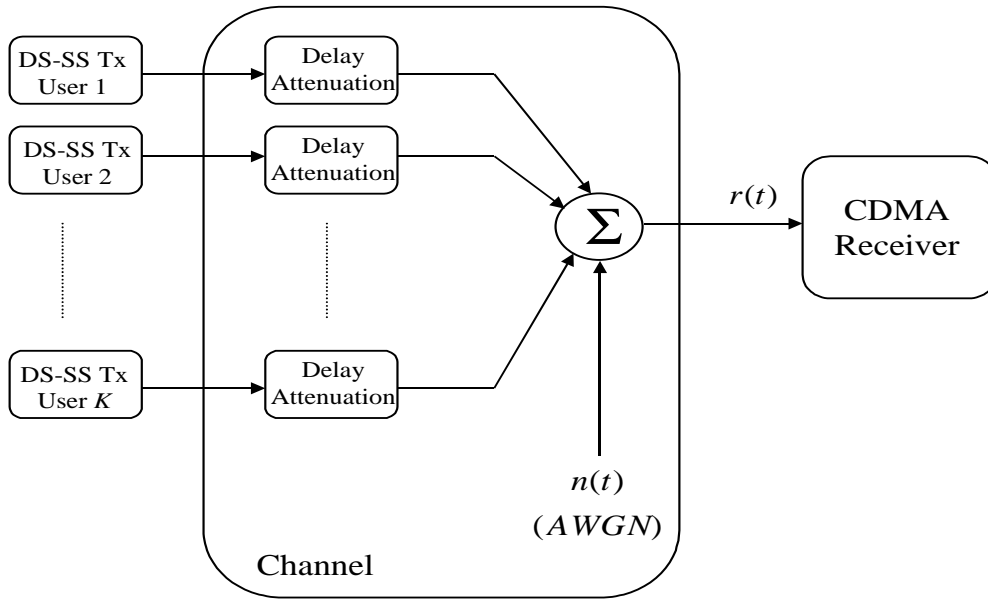


Figure 2.6: CDMA Communication System

- **Correlation Receivers:**

The correlation receiver is the conventional CDMA receiver, proposed for use in the IS-95 standard. Such receivers offer relatively low complexity at the cost of lesser performance. Correlation receivers use a bank of single user DS-SS receivers for each user, implemented as a bank of matched-filters. These correlation outputs are fed to decision devices that form transmitted bit estimates. Figure 2.7 shows a conventional BPSK-based CDMA receiver.

- **Rake Receivers**

The second type of single-user receiver is actually a variant of the standard correlation receiver. Rake receivers were introduced by Price and Green [13] and take advantage of multipath diversity in a frequency selective fading CDMA channel. In frequency selective fading, the coherence bandwidth of the channel is significantly smaller than the bandwidth of the transmitted wideband CDMA signal, and so the arriving multipath

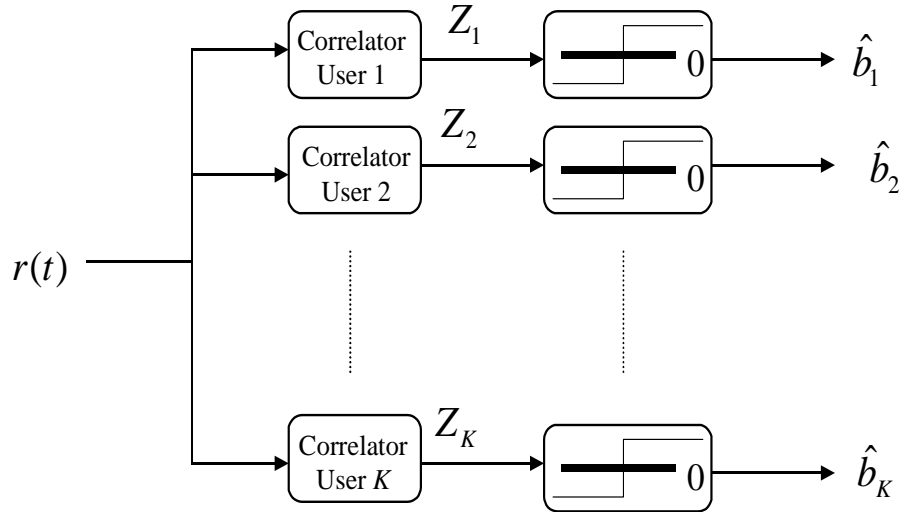


Figure 2.7: BPSK-based Conventional Single User CDMA Receiver

signal components are distinguishable [7]. The Rake receiver locks onto each arriving multipath component and, for a given bit, filters the components to produce a final decision statistic on that bit.

Figure 2.8 shows the Rake receiver structure for a given user. The name *Rake* is derived by analogy to a generic garden rake. The M “fingers” of the rake receiver are to track the M multipath components of each user. The first part of the receiver is much like the conventional correlation receiver except that the bank of correlators is dedicated to the M multipath components of each user, resulting in a total of $M \cdot K$ matched-filters. In a K user system, there are M such filter banks, one for each user. The correlators produce a set of preliminary decision statistics $\{Z_i\}$ which reflect the strength and reliability of a given multipath component. Based upon the multipath structure of the channel, appropriate FIR filter weights $\{w_i\}$ are chosen to maximize the fidelity of the

final decision statistic Z , computed as

$$Z = \sum_{i=1}^M w_i Z_i. \tag{2.10}$$

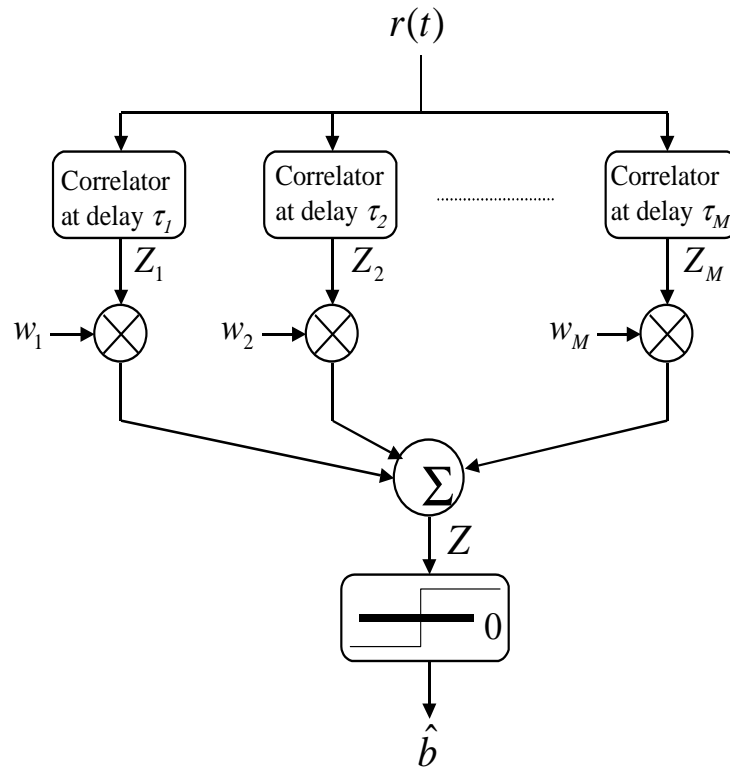


Figure 2.8: BPSK-based Rake CDMA Receiver for a Given User

The IS-95 standard proposes a four finger rake receiver at the base station and a three finger Rake receiver at the mobile unit [28].

There have been other single user receiver structures proposed in the literature [29, 30]. These are usually adaptive filtering techniques more sophisticated than the simple matched-filter which take advantage of the cyclostationarity properties of code on pulse CDMA signals. A comprehensive survey of such techniques can be found in [31].

2.3.2 Multiuser CDMA Receivers

As mentioned previously, single user detectors are not optimal for CDMA because they process other user interference, termed *multiple access interference (MAI)*, as unstructured channel noise. To design better CDMA receivers, the specific structure of MAI needs to be more fully exploited. To such an end, novel receiver structures have been proposed over the years that take advantage of knowledge of MAI signal parameters. Such receivers are termed multiuser receivers. Multiuser receivers are more complex than conventional ones because of their added capability of using MAI signal information to help recover the desired user. For the foreseeable future, multiuser receiver structures are only suitable for use at the base station where additional complexity may be supported.

A mold that most multiuser detectors fit, depicted in Figure 2.9, is composed of an initial correlation stage followed by a set of additional stages where a multiuser detection algorithm is implemented. It is shown by Verdù [22] that the set of correlator outputs for each user forms a set of sufficient statistics that, if processed properly, can lead to an optimal multiuser decision. All multiuser detectors in this thesis are consistent with this structure. A comprehensive survey of the main types of multiuser receivers can be found in [20, 21]. The remainder of this chapter gives a brief overview of the most commonly researched multiuser detectors in the literature.

- **The Optimal Detector:**

Verdù derived the optimal CDMA receiver in 1986 [22], seven years after multiuser detection was actually introduced by Schneider back in 1979 [32]. The optimal structure, shown in Figure 2.10, consists of a bank of matched-filters providing first order user amplitude estimates to a Viterbi decision algorithm. Verdù showed that the optimal structure afforded significant performance improvement over the conventional structure. Further, he also showed that the optimal receiver was not affected by the near-far problem, an asset called *near-far resistance*. This led to the conclusion

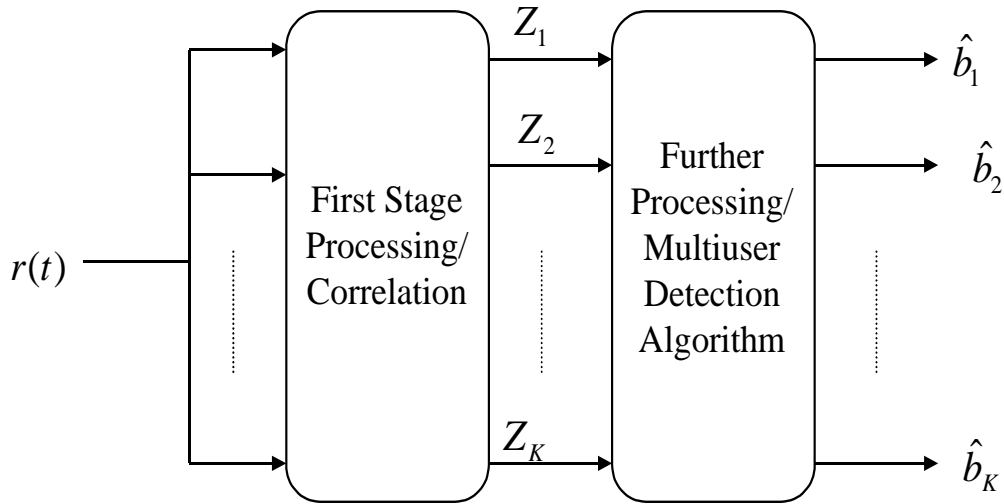


Figure 2.9: General Multiuser Receiver Structure

that the near-far effect is not inherent to CDMA, but a consequence of the receiver structure.

The extraordinary performance enhancements however come at a price. The optimal receiver assumes *a priori* knowledge of received signal amplitudes as well as delays; in practice, such ideals are usually not attainable. More burdensome yet is the receiver's use of the Viterbi decision algorithm, where the bulk of its complexity resides. The Viterbi decision algorithm performs *Maximal Likelihood Sequence Estimation* over the entire sequence of received message bits, thereby decoding the whole message sequence in a trellis with 2^K states. The computational complexity per bit decision then becomes exponential in the number of users, clearly rendering the optimal receiver impractical for implementation.

Due to its prohibitively expensive complexity, the role of the optimal receiver has been relegated to that of a benchmark against which to compare sub-optimal CDMA detectors exhibiting more reasonable computational complexity. We now consider three

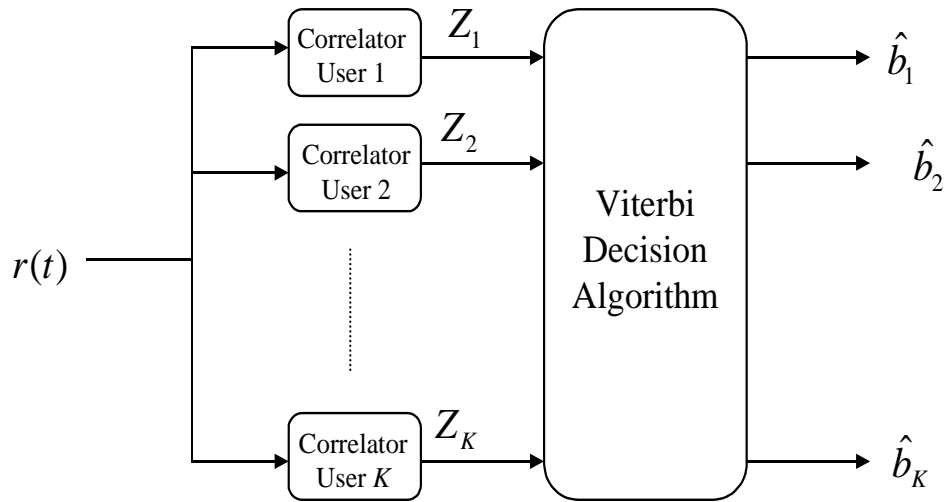


Figure 2.10: BPSK-based Optimal CDMA Receiver

such sub-optimal multiuser receivers.

- **The Decorrelator:**

The decorrelator is a linear multiuser detector with an upper bound on complexity of K^2 . It functions by applying a linear transformation to the set of matched-filter outputs obtained from the first stage. As its name implies, the receiver seeks to undo the various inter-user correlations so as to isolate users from one another. This decorrelation attempt is carried out by computing PN code waveform cross correlation values and storing these in $K \times K$ matrix, and multiplying the inverse of this matrix by the vector of matched-filter outputs from the first stage. The decorrelator does not require knowledge of signal amplitudes and is completely insensitive to the near-far effect. In general, the decorrelator provides substantial performance and capacity gains over the conventional receiver [21], however, it has many drawbacks and as a result is not widely used.

Its K^2 complexity stems from the $K \times K$ matrix storage requirement; and while not exponential, such complexity is formidable nonetheless. This matrix is time varying as users come on and drop off of the system, thereby making updates on such a large matrix expensive. Further, this correlation matrix needs to be inverted, bringing about the issue of singularity. The decorrelator relies upon accurate PN code correlation values, and if the inverse correlation matrix becomes unstable or undefined even, then the detector ceases to function adequately. Of concern as well is a noise enhancement produced by the decorrelation operation, rendering decision statistics more noisy.

- **The Minimum Mean Square Error (MMSE) Detector:**

The MMSE detector, like the decorrelator, operates by applying a linear transformation to the set of first stage matched-filter outputs. It seeks to minimize the averaged square error between actual data and the soft outputs from the first stage. In doing so, it rectifies the decorrelator's shortcoming of enhancing noise, but at the cost of requiring knowledge of signal amplitudes. In general though, the MMSE receiver's BER is better than that of the decorrelator's. However, in the limit as the noise level drops to zero, the MMSE detector's performance approaches that of the decorrelator's. The MMSE receiver provides many of the advantages of the decorrelator and is similar in computational complexity. However, its near-far resistance is slightly less than that of the decorrelator's, and it shares many of the decorrelator's problems due to the necessity of computing a matrix inverse.

- **Interference Cancellation Detectors:**

Interference cancellation has received a great deal of attention in the literature and the remainder of this thesis will deal with an interference cancellation algorithm. First proposed by Varanasi and Aazhang [23], interference cancellation detectors seek to remove interference by actually subtracting estimates of interfering signals from the received signal. A general interference cancellation receiver is depicted in Figure 2.11. It comprises of an initial stage of matched-filters, like the other multiuser receivers,

followed by stages of interference cancellation.

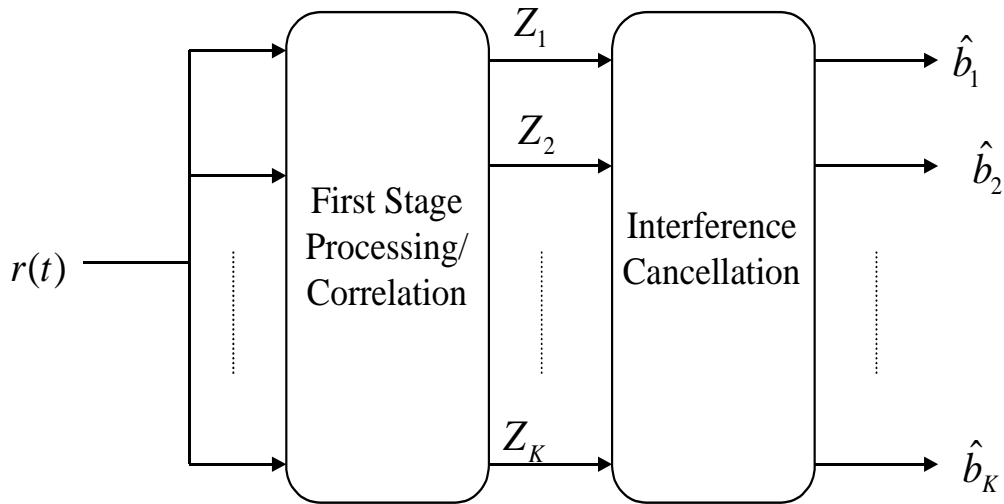


Figure 2.11: BPSK-based General Purpose Interference Cancellation CDMA Receiver

Interference cancellation receivers typically come in two flavors: **parallel** [23] and **successive** [33]; the parallel scheme is the one originally proposed by Varanasi and Aazhang. In parallel interference cancellation, all interfering users are cancelled (subtracted) concurrently (*in parallel*) from the received signal. In the successive approach proposed by Holtzman, users are cancelled serially in descending order of estimated received power, from strongest to weakest.

Both detectors have been shown to improve performance and capacity over conventional detection, and both have distinct sets of advantages over one another [21]. From a computational viewpoint, parallel cancellation is more advantageous as it can usually be implemented with complexity linear in K . Further, since all users are cancelled concurrently, the cancellation process is faster than in the successive canceller which incurs a delay in subtracting out each interferer one after the other. Such an ordering of cancellation in the successive case entails an expensive K^2 computational complexity.

The parallel scheme also performs better than its successive counterpart under perfect power control.

However, for severe power variations, the successive scheme has advantages over the parallel one. Successive interference cancellation was designed to mitigate the near-far effect. In cancelling by descending order of estimated received power, the stronger users are cancelled first. The reason for this design is that the stronger users' amplitude estimates are more reliable than the weaker users' amplitude estimates. Therefore, cancellation is done in order of signal estimate reliability which enhances the accuracy of the interference cancellation. Such a scheme performs better in severe near-far situations than does the parallel approach. However, in a cellular environment, rough power control can be assumed. Therefore, we focus on parallel cancellation.

In conclusion, interference cancellation performance enhancements do not come at the price of a priori knowledge of signal amplitudes, unstable mathematical operations, or prohibitive computational complexity. Many authors have even suggested that interference cancellation is one of the most promising types of multiuser detectors and merit a great deal more investigation [34]. Indeed, the following chapters will address an issue associated with parallel interference cancellation.

2.4 Summary

We have reviewed the general principles of spread spectrum systems and have covered the two main types of CDMA receivers, conventional single user CDMA detectors as well as multiuser detectors. We have pointed out the general features of these receivers, focusing on the enhancements provided by multiuser receivers over conventional single user receivers, particularly those employing interference cancellation. We will now focus much more narrowly on a parallel interference cancellation approach.

Chapter 3

Analysis of Brute Parallel Interference Cancellation

In the previous chapter, we noted the deficiencies of conventional matched-filter receivers for CDMA, and motivated the need for multiuser reception to improve receiver performance. In particular, we focused upon the interference cancellation flavor of multiuser receiver design. In this chapter, we delve into a particular approach to parallel interference cancellation originally put forth by Striglis *et al.* [24, 35].

The proposed receiver structure consists of an initial stage of matched-filter reception, followed by an arbitrary number of interference cancellation stages (a structure consistent with Figure 2.9). The first stage provides first order amplitude estimates (decision statistics) of each user which are fed to the second stage. The second stage then constructs MAI signal estimates based upon first stage amplitude estimates and cancels this reconstructed MAI from the original received signal. The MAI reconstruction and cancellation process can be repeated if desired.

This receiver was first analyzed in [24, 35, 25], where it was assumed that all amplitude estimates were completely unbiased. It was later discovered in [1], where the receiver was

analyzed much more extensively, that amplitude estimates after cancellation are in fact biased in proportion to the amount of interfering users¹. This revelation accounted for the overly optimistic analytical BER in [25] (particularly for high system loads), as compared to simulation BER which reflects the bias effects.

This chapter presents a baseband model for the interference cancellation receiver in [24, 35, 25] and analyzes its decision metrics. The mean and variance of the first stage statistics are found for an asynchronous channel, permitting us to write first stage BER (corresponding to conventional CDMA receiver BER). The first stage analysis largely follows that of [25]. However, beginning at the second stage, our analysis deviates from [25] as we more accurately model the interference cancellation algorithm, showing the presence of the bias in MAI estimates. Continuing with an asynchronous system, we derive the mean of the second stage statistic, demonstrating the bias source. The effects of the bias on system performance are then shown.

In an effort to mitigate bias effects, Kaul *et. al.* carried out simulation experiments where interference estimates were down-scaled by a scalar. Promising initial results of this sort of interference cancellation were documented in [1] and later in [2]. In Chapter 4, we analyze this idea for a bit-synchronous system by analytically modelling interference estimate down-scaling. Ultimately, we derive the down-scaling factors yielding the lowest BER for a given system. For now, we concentrate on analyzing the performance of *brute* interference cancellation, where no interference estimate down-scaling is done.

¹When considering parallel interference cancellation structures in general, the first account of biasing was actually documented by Divsalar and Simon [36].

3.1 Model of Brute Parallel Interference Cancellation

This section presents the interference cancellation transceiver model which provides the basis for the remainder of this thesis. While taken mostly from [25], the following model is slightly different in that it is a *baseband* transceiver representation and that all matched-filter outputs are normalized by the bit duration T . Even though a baseband representation is used to dispense with the frequency translation associated with a carrier waveform, we do account for carrier phase effects. We consider first the transmitter model and then describe the interference cancellation algorithm of the receiver. An analysis of the algorithm is postponed until the next section.

3.1.1 Transmitter Model

A block diagram for the transmitter is shown in Figure 3.1. It is indeed very similar to the transmitter model in Figure 2.6. Our model, based on [4], accounts for K single-user DS-SS transmitters communicating simultaneously over a linear AWGN channel to a brute parallel interference cancellation CDMA receiver.

Each of the K users transmits a binary data stream, with the k^{th} user's bit stream modelled as

$$b_k(t) = \sum_{i=-\infty}^{\infty} b_{k,i} p_T(t - iT), \quad (3.1)$$

where $\{b_{k,i}\}$ is a set of independent identically distributed (*i.i.d.*) Bernoulli random variables. The k^{th} user's i^{th} data bit is represented by $b_{k,i}$ where $b_{k,i} \in \{-1, +1\}$ and $Pr[b_{k,i} = -1] = Pr[b_{k,i} = +1] = 1/2$. The unit pulse $p_T(t)$ of duration T is described in the previous chapter.

The k^{th} user's binary data stream is spread by its unique signature code waveform $a_k(t)$, given by

$$a_k(t) = \sum_{j=-\infty}^{\infty} a_{k,j} p_{T_c}(t - jT_c), \quad (3.2)$$

where $a_{k,j}$ is identically distributed to $b_{k,i}$. We will assume in all further analysis that $b_k(t)$

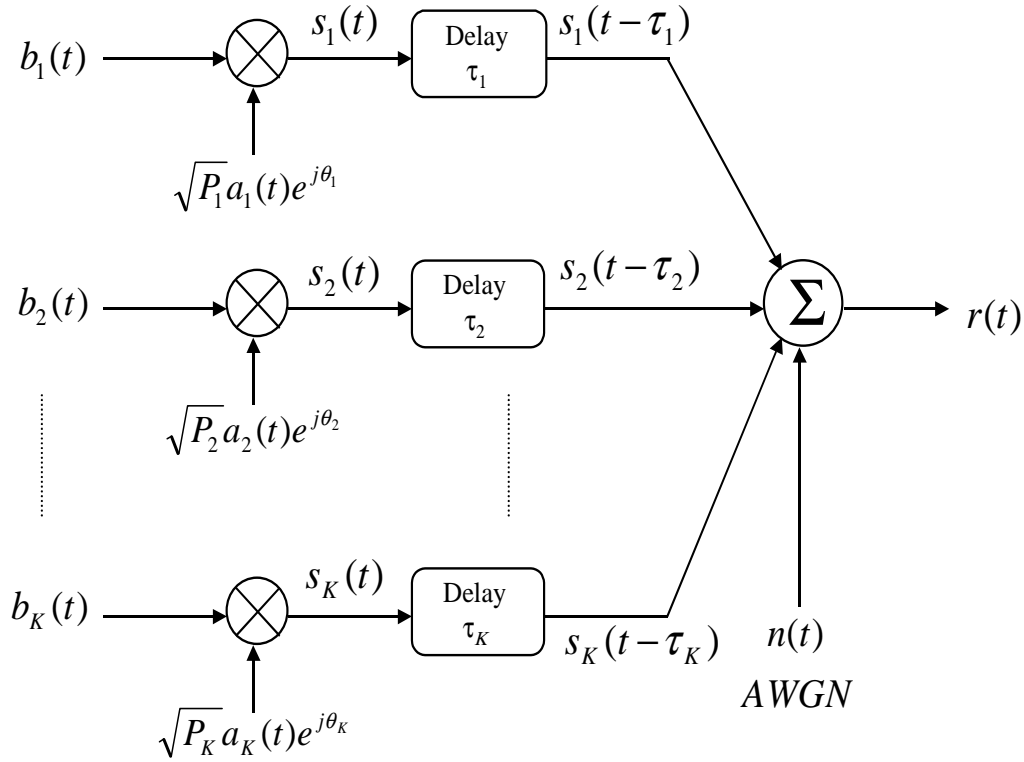


Figure 3.1: CDMA Transmitter Model [4]

and $a_k(t)$ are statistically independent random processes. The ratio of the bit duration T to the chip duration T_c is the system processing gain $N = T/T_c$.

Once each user’s binary data stream is spread by its PN code waveform, the resulting spread signal is phase shifted to account for the carrier phase, producing the k^{th} user’s transmitted signal $s_k(t)$ given by

$$s_k(t) = \sqrt{P_k} b_k(t) a_k(t) e^{j\theta_k}, \tag{3.3}$$

where P_k is the baseband power of the k^{th} user’s signal and θ_k is its associated carrier phase, modelled as a random variable uniformly distributed over $[0, 2\pi)$.

The channel inserts a propagation delay τ_k into each signal $s_k(t)$ and corrupts the aggregate

transmission with AWGN $n(t)$. The received signal $r(t)$ is expressed as

$$\begin{aligned} r(t) &= \sum_{k=1}^K s_k(t - \tau_k) + n(t) \\ &= \sum_{k=1}^K \sqrt{P_k} b_k(t - \tau_k) a_k(t - \tau_k) e^{j\phi_k} + n(t). \end{aligned} \tag{3.4}$$

The noise $n(t)$ is modelled as a zero-mean ergodic (and therefore stationary) complex AWGN process with one-sided power spectrum magnitude N_o . Each signal's propagation delay τ_k is modelled as a random variable uniformly distributed over $[0, T)$. The received phase of each user ϕ_k is assumed to be different than θ_k , but identically distributed to θ_k .

3.1.2 Brute Parallel Interference Cancellation Receiver

Now that we have described the transmitter model and the channel, we come to the multiuser interference cancellation CDMA receiver. The receiver structure is shown below in Figure 3.2.

First Stage:

The first stage, as with many multiuser detectors, is a conventional correlator. The received signal $r(t)$ is correlated with a synchronous copy of each user's spreading waveform $a_k(t - \tau_k)$. The resulting correlation value is then normalized by the bit duration T , producing a first stage decision statistic $Z_{k,i}^{(1)}$ for the i^{th} bit of the k^{th} user, as given by²

$$Z_{k,i}^{(1)} = \frac{1}{T} \int_{iT + \tau_k}^{(i+1)T + \tau_k} \Re \left\{ r(t) a_k(t - \tau_k) e^{-j\phi_k} \right\} dt, \tag{3.5}$$

where $\Re\{\cdot\}$ denotes the real part operator. The normalization by T removes the dependence of the decision statistic upon the bit duration, and will simplify subsequent analysis.

²From here onwards, we assume that the receiver has achieved both carrier and code lock before decision statistic computation.

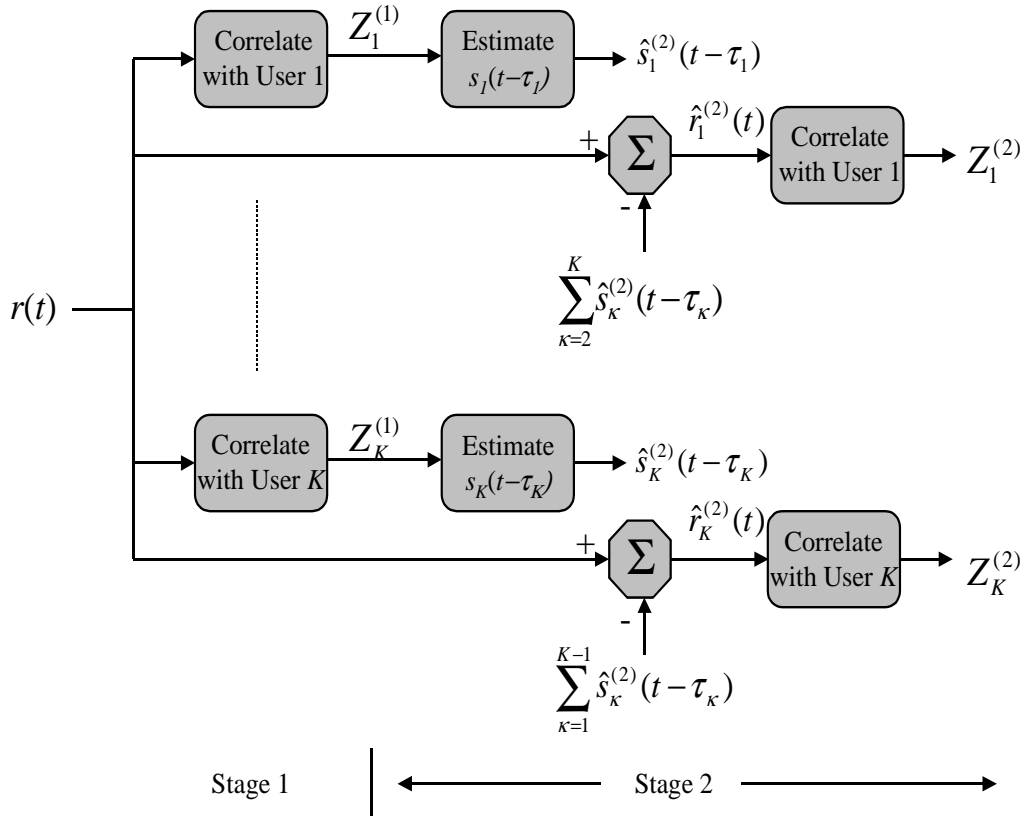


Figure 3.2: Interference Cancellation CDMA Receiver – One Stage of Cancellation

Second Stage:

The second stage begins by constructing transmitted signal estimates which constitute the MAI signal estimates that will later be cancelled. To construct these estimates, first stage decision metrics are used as first order amplitude measures of each user’s transmitted signal.

We will dissect the first stage correlation metric in detail in the next section, but for purposes of explaining the receiver algorithm, it suffices here to state that $Z_{k,i}^{(1)}$ can be modelled by a Gaussian random variable if we assume the Gaussian approximation for MAI [4]. When conditioned upon the i^{th} transmitted bit of the k^{th} user $b_{k,i}$, $Z_{k,i}^{(1)}$ can be shown to have mean

$$E [Z_{k,i}^{(1)} | b_{k,i}] = \sqrt{P_k} b_{k,i}. \tag{3.6}$$

The implication of this result is that on the ensemble average, for a given transmitted bit,

first stage metrics are equal to the signed amplitude of the given user's transmitted signal. It therefore becomes simple to form an unbiased estimator of each user's transmitted signed amplitude $b_{k,i}\widehat{\sqrt{P_k}}$, for each transmitted bit, given by

$$b_{k,i}\widehat{\sqrt{P_k}} = Z_{k,i}^{(1)}. \quad (3.7)$$

Further, since the receiver has knowledge of each user's PN code waveform, the receiver is now armed with enough information to construct a first order estimate of each user's transmitted delayed signal $\hat{s}_k^{(2)}(t - \tau_k)$ expressed as

$$\hat{s}_k^{(2)}(t - \tau_k) = \left[\sum_{i=-\infty}^{\infty} Z_{k,i}^{(1)} p_T(t - \tau_k - iT) \right] a_k(t - \tau_k) e^{j\phi_k}. \quad (3.8)$$

It should be noted that under the Gaussian approximation, each transmitted signal estimate (MAI signal estimate) becomes an unbiased estimate of the corresponding transmitted signal, or

$$E \left[\hat{s}_k^{(2)}(t - \tau_k) \right] = s_k(t - \tau_k). \quad (3.9)$$

Once all signal reconstructions complete, the second stage proceeds with brute interference cancellation. Brute interference cancellation is implemented by the subtraction of interfering users' signal estimates from the received signal $r(t)$, to form a new reconstructed received signal for the k^{th} user $\hat{r}_k^{(2)}(t)$, like so

$$\hat{r}_k^{(2)}(t) = r(t) - \sum_{\substack{\kappa=1 \\ \kappa \neq k}}^K \hat{s}_\kappa^{(2)}(t - \tau_\kappa). \quad (3.10)$$

A new reconstructed received signal is generated for each user, since each user is the desired user at some point. The new received signals are cleaner versions of $r(t)$, for each user respectively.

Much of the effectiveness of the cancellation operation lies in the degree of accuracy of the reconstructed MAI signals: the closer the estimates are to the actual transmitted signals, the better receiver performance becomes. Equation (3.9) indicates that MAI estimates, on the ensemble average, are equal to actual transmitted signals. However, despite this equality

in the mean sense, performance can suffer if MAI signal estimates wander around this mean significantly, as gauged by the variance of reconstructed MAI.

The new received signals are passed through a bank of correlators identical to that in the first stage, producing a second stage decision statistic for each user according to

$$Z_{k,i}^{(2)} = \frac{1}{T} \int_{iT+\tau_k}^{(i+1)T+\tau_k} \Re \left\{ \hat{r}_k^{(2)}(t) a_k(t - \tau_k) e^{-j\phi_k} \right\} dt. \quad (3.11)$$

We would like for $\hat{r}_k^{(2)}(t)$ to contain the least possible amount of MAI for the correlator following the cancellation operation is optimal only when AWGN corrupts the desired signal.

In general, the cancellation of interference in first stage metrics enhances the quality of second stage metrics. Interference cancellation can be repeated any number of times, however, most of the performance enhancement is already achieved after the second stage. The additional performance improvement lessens from stage to stage as the fundamental performance limit imposed by the system processing gain impedes further isolation of desired signal from MAI. In fact, processing beyond four stages is worth neither the computational burden nor the incurred delay. Figure 3.2 shows a two stage implementation (one stage of interference cancellation) and correspondingly, the rest of this thesis will analyze the receiver's performance up to and including the second stage.

3.2 Analysis of Receiver Performance

In this section, we analyze receiver performance by characterizing the decision statistics at both the first and second stages. In first stage analysis, based upon [4, 25], we compute both the mean and the variance of the decision statistic, which allows us to write first stage BER.

The characterization of first stage metrics provides a basis for comparison of second stage metric moments, in which we demonstrate the existence of a bias. We show the potentially severe effects of this bias in the next section. For all the following analysis, we set user 1 as our desired user to make notation less cumbersome, and for convenience we set user 1's

propagation delay to zero $\tau_1 = 0$.

3.2.1 First Stage

Before attempting to compute first stage decision statistic moments, we first break up the correlation integral in Equation (3.5) into its three constituent parts: desired user, MAI, and noise due to AWGN. Substituting the expression for $r(t)$ from Equation (3.4) into Equation (3.5) and setting the desired user to user 1 yields

$$\begin{aligned}
 Z_{1,i}^{(1)} &= \frac{1}{T} \int_{iT}^{(i+1)T} \Re \left\{ r(t) a_1(t) e^{-j\phi_1} \right\} dt \\
 &= \frac{1}{T} \int_{iT}^{(i+1)T} \Re \left\{ \left[\sum_{k=1}^K \sqrt{P_k} b_k(t - \tau_k) a_k(t - \tau_k) e^{j\phi_k} + n(t) \right] a_1(t) e^{-j\phi_1} \right\} dt \\
 &= \underbrace{\frac{1}{T} \int_{iT}^{(i+1)T} \Re \left\{ \sqrt{P_1} b_1(t) a_1(t) e^{j\phi_1} a_1(t) e^{-j\phi_1} \right\} dt}_{\text{Desired User}} \\
 &\quad + \underbrace{\frac{1}{T} \int_{iT}^{(i+1)T} \Re \left\{ \left[\sum_{k=2}^K \sqrt{P_k} b_k(t - \tau_k) a_k(t - \tau_k) e^{j\phi_k} \right] a_1(t) e^{-j\phi_1} \right\} dt}_{\text{MAI}} \\
 &\quad + \underbrace{\frac{1}{T} \int_{iT}^{(i+1)T} \Re \left\{ n(t) a_1(t) e^{-j\phi_1} \right\} dt}_{\text{Noise}} \\
 &= A_1 + \sum_{k=2}^K I_k^{(1)} + \eta, \tag{3.12}
 \end{aligned}$$

where A_1 , $I_k^{(1)}$, and η are the contributions from the desired user, first stage interference from the k^{th} user, and the noise due to AWGN, respectively.

From an intuitive perspective, first stage amplitude estimates are composed of a desired component, accompanied by MAI and noise due to AWGN. The matched-filter's ability to rid MAI from $r(t)$ is determined by the processing gain and is influenced by the relative powers of desired user versus MAI.

The three components in the decision metric are statistically independent random variables,

and as a result, we can compute their means and variances separately, yielding

$$E [Z_{1,i}^{(1)} | b_{1,i}] = E [A_1 | b_{1,i}] + E \left[\sum_{k=2}^K I_k^{(1)} \middle| b_{1,i} \right] + E [\eta | b_{1,i}] \quad (3.13)$$

and

$$\text{Var} [Z_{1,i}^{(1)} | b_{1,i}] = \text{Var} [A_1 | b_{1,i}] + \text{Var} \left[\sum_{k=2}^K I_k^{(1)} \middle| b_{1,i} \right] + \text{Var} [\eta | b_{1,i}]. \quad (3.14)$$

Desired User:

$$E [A_1 | b_{1,i}] = E \left[\frac{1}{T} \int_{iT}^{(i+1)T} \Re \left\{ \sqrt{P_1} b_{1,i} a_1^2(t) e^{j\phi_1} e^{-j\phi_1} \right\} dt \right] \quad (3.15)$$

$$\begin{aligned} &= E \left[\frac{1}{T} T \Re \left\{ \sqrt{P_1} b_{1,i} \right\} \right] \quad (3.16) \\ &= \sqrt{P_1} b_{1,i}. \end{aligned}$$

Since we are conditioning upon the desired bit $b_{1,i}$, the variance of the desired user term is zero,

$$\text{Var} [A_1 | b_{1,i}] = 0. \quad (3.17)$$

MAI:

$$\begin{aligned} E \left[\sum_{k=2}^K I_k^{(1)} \middle| b_{1,i} \right] &= E \left[\frac{1}{T} \int_{iT}^{(i+1)T} \Re \left\{ \left[\sum_{k=2}^K \sqrt{P_k} b_k(t - \tau_k) a_k(t - \tau_k) e^{j\phi_k} \right] a_1(t) e^{-j\phi_1} \right\} dt \right] \\ &= E \left[\frac{1}{T} \int_{iT}^{(i+1)T} \Re \left\{ \sum_{k=2}^K \sqrt{P_k} b_k(t - \tau_k) a_k(t - \tau_k) a_1(t) e^{j(\phi_k - \phi_1)} \right\} dt \right] \\ &= \frac{1}{T} \int_{iT}^{(i+1)T} \sum_{k=2}^K \sqrt{P_k} E [b_k(t - \tau_k) a_k(t - \tau_k) a_1(t - \tau_1) \cos(\phi_k - \phi_1)] dt \\ &= 0, \end{aligned}$$

since we are assuming both random bit and signature sequences.

The computation of the variance of the MAI term was done in [25] under the Gaussian assumption for MAI and we simply state the result here, adapting it to our baseband model as well as our normalized decision statistics,

$$\text{Var} \left[\sum_{k=2}^K I_k^{(1)} \middle| b_{1,i} \right] = \frac{1}{3N} \sum_{k=2}^K P_k. \quad (3.18)$$

Noise:

$$E[\eta|b_{1,i}] = E\left[\frac{1}{T}\int_{iT}^{(i+1)T}\Re\{n(t)a_1(t)e^{-j\phi_1}\}dt\right] \quad (3.19)$$

$$\begin{aligned} &= \frac{1}{T}\int_{iT}^{(i+1)T}\Re\{E[n(t)a_1(t)e^{-j\phi_1}]\}dt \\ &= 0, \end{aligned} \quad (3.20)$$

since we model AWGN as a zero mean random process.

The noise term variance is computed to be

$$\begin{aligned} \text{Var}[\eta|b_{1,i}] &= E[\eta^2|b_{1,i}] \quad (3.21) \\ &= E\left[\frac{1}{T}\int_{iT}^{(i+1)T}\Re\{n(t)a_1(t)e^{-j\phi_1}\}dt \cdot \frac{1}{T}\int_{iT}^{(i+1)T}\Re\{n(\lambda)a_1(\lambda)e^{-j\phi_1}\}d\lambda\right] \\ &= \frac{1}{T^2}E\left[\int_{iT}^{(i+1)T}\int_{iT}^{(i+1)T}a_1(t)a_1(\lambda)\Re\{n(t)e^{-j\phi_1}\}\Re\{n(\lambda)e^{-j\phi_1}\}dtd\lambda\right] \\ &= \frac{1}{T^2}E\left[\int_{iT}^{(i+1)T}\int_{iT}^{(i+1)T}\left[\frac{n(t)e^{-j\phi_1} + n^*(t)e^{j\phi_1}}{2}\right]\left[\frac{n(\lambda)e^{-j\phi_1} + n^*(\lambda)e^{j\phi_1}}{2}\right]dtd\lambda\right] \\ &= \frac{1}{4T^2}\int_{iT}^{(i+1)T}\int_{iT}^{(i+1)T}E[n(t)n^*(\lambda) + n^*(t)n(\lambda)]dtd\lambda \\ &= \frac{1}{4T^2}\int_{iT}^{(i+1)T}\int_{iT}^{(i+1)T}2\delta(t-\lambda)dtd\lambda \\ &= \frac{1}{2T^2}\int_{iT}^{(i+1)T}N_o dtd\lambda \\ &= \frac{N_o}{2T}, \end{aligned}$$

where $(\cdot)^*$ denotes complex conjugation. We can now finally write the first stage mean and variance. Following Equations (3.13) and (3.14), we have

$$E[Z_{1,i}^{(1)}|b_{1,i}] = \sqrt{P_1}b_{1,i}, \quad (3.22)$$

and

$$\text{Var}[Z_{1,i}^{(1)}|b_{1,i}] = \frac{1}{3N}\sum_{k=2}^K P_k + \frac{N_o}{2T}. \quad (3.23)$$

We focus the reader's attention upon Equation (3.22) which indicates that first stage metrics are unbiased amplitude estimates of each user's signal, for a given transmitted bit. This

result is significant and will contrast the corresponding second stage result, which we develop shortly.

At this point, we have all the necessary information to write the already well known expression for BER in a conventional BPSK-based CDMA system. Since we are assuming equiprobable signalling, first stage bit-error-rate $BER^{(1)}$ can be written as

$$\begin{aligned}
 BER^{(1)} &= Pr [Z_{1,i}^{(1)} | b_{1,i} = +1] = Pr [Z_{1,i}^{(1)} | b_{1,i} = -1] \\
 &= Q \left(\sqrt{\frac{(E [Z_{1,i}^{(1)} | b_{1,i}])^2}{Var [Z_{1,i}^{(1)} | b_{1,i}]}} \right) \\
 &= Q \left(\left[\frac{1}{2 \frac{E_{b_1}}{N_o}} + \frac{1}{3N} \cdot \frac{\sum_{k=2}^K P_k}{P_1} \right]^{-\frac{1}{2}} \right),
 \end{aligned} \tag{3.24}$$

where $E_{b_1} = P_1 T$ and $Q(z) = \frac{1}{\sqrt{2\pi}} \int_z^\infty e^{-\frac{\lambda^2}{2}} d\lambda$ (the standard Q -function). This results in the standard ‘‘Gaussian Approximation’’ for the performance of a CDMA system which has been shown in many places throughout the literature [7].

3.2.2 Second Stage

Now that first stage analysis is complete, we can analyze the effects of brute parallel interference cancellation upon decision metrics. Our purpose here is merely to show that decision statistics become biased, which can be accomplished by developing the mean of second stage statistics. We forgo the variance computation until the next chapter where we consider a bit-synchronous CDMA system.

We proceed by identifying the constituent parts of the second stage correlation integral in Equation (3.11), much like we did for the first stage statistic. We develop an expression for the second stage metric in terms of first stage metrics. But first, we rewrite the first stage metrics in terms of PN code waveform cross-correlation functions, with the intent of keeping second stage metric expressions from becoming exceedingly unwieldy. Introducing the PN

code waveform cross correlation functions from [4]³, we have

$$R_{l,m}(\tau) = \frac{1}{T} \int_0^\tau a_l(t-\tau)a_m(t)dt \quad \text{and} \quad \hat{R}_{l,m}(\tau) = \frac{1}{T} \int_\tau^T a_l(t-\tau)a_m(t)dt \quad 0 \leq \tau < T. \quad (3.25)$$

We turn the reader’s attention to the fact that the index of the delay parameter τ has been dropped. From here onwards, we shall consider τ a general random delay parameter uniformly distributed over $[0, T)$ attributable to all users.

Before continuing with metric analysis, we state here for reference a few stochastic properties of $R_{l,m}(\tau)$ and $\hat{R}_{l,m}(\tau)$ which we shall use shortly. With regard to first moments, it is easily seen that for random codes we have

$$E [R_{l,m}(\tau)] = E [\hat{R}_{l,m}(\tau)] = E [R_{l,m}(\tau)\hat{R}_{l,m}(\tau)] = E [R_{l,m}(\tau)] \cdot E [\hat{R}_{l,m}(\tau)] = 0$$

and

$$E \left[\int_0^T a_l(t-\tau)a_m(t)dt \right] = E [R_{l,m}(\tau) + \hat{R}_{l,m}(\tau)] = 0.$$

Further, it can be shown from [25, 37, 38] that

$$E [R_{l,m}^2(\tau) + \hat{R}_{l,m}^2(\tau)] = Var \left[\frac{1}{T} \int_0^T a_l(t-\tau)a_m(t)dt \right] = \frac{2}{3N}.$$

To illustrate how we use PN code cross-correlation functions, we refer to the diagram below where we depict the asynchronous time relationship between users in the system. The $(i-1)^{th}$, i^{th} , and $(i+1)^{th}$ bits of several users are shown, with their respective time delays. With this pictorial framework in mind and continuing with user 1 as our desired user, we can rewrite the first stage decision statistic in terms of PN code cross-correlations like so

³Just as with decision statistics, we choose to normalize by the bit duration T here as well so as to remove the dependence upon T of the cross-correlation functions.

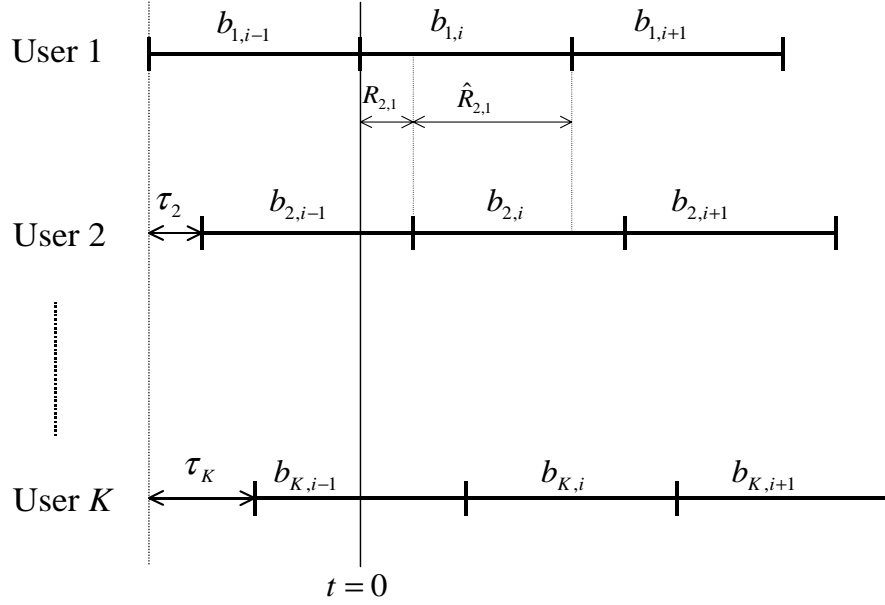


Figure 3.3: Asynchronous Time Relationship Between Users

$$\begin{aligned}
 Z_{1,i}^{(1)} &= \frac{1}{T} \int_{iT}^{(i+1)T} \Re \left\{ \left[\sum_{l=1}^K \sqrt{P_l} b_l(t - \tau_l) a_l(t - \tau_l) e^{j\phi_l} + n(t) \right] a_1(t) e^{-j\phi_1} \right\} dt \\
 &= \sqrt{P_1} b_{1,i} + \frac{1}{T} \int_{iT}^{(i+1)T} \sum_{l=2}^K \sqrt{P_l} b_l(t - \tau_l) a_l(t - \tau_l) a_1(t) \cos(\phi_l - \phi_1) dt + \eta \\
 &= \sqrt{P_1} b_{1,i} + \frac{1}{T} \sum_{l=2}^K \sqrt{P_l} \left[\int_{iT}^{iT+\tau_l} b_{l,i-1} a_l(t - \tau_l) a_1(t) dt + \int_{iT+\tau_l}^{(i+1)T} b_{l,i} a_l(t - \tau_l) a_1(t) dt \right] \\
 &\quad \cdot \cos(\phi_l - \phi_1) + \eta \\
 &= \underbrace{\sqrt{P_1} b_{1,i}}_{\text{Desired User}} + \underbrace{\sum_{l=2}^K \sqrt{P_l} \cos(\phi_l - \phi_1) [b_{l,i-1} R_{l,1}(\tau) + b_{l,i} \hat{R}_{l,1}(\tau)]}_{\text{MAI}} + \underbrace{\eta}_{\text{Noise}} \tag{3.26}
 \end{aligned}$$

As elaborated in the previous section, once the receiver has completed first stage processing and obtained amplitude estimates for all users, MAI signal reconstruction commences

according to Equation (3.8)

$$\hat{s}_l^{(2)}(t - \tau_l) = \left[\sum_{i=-\infty}^{\infty} Z_{l,i}^{(1)} p_T(t - \tau_l - iT) \right] a_l(t - \tau_l) e^{j\phi_l}. \quad (3.27)$$

MAI is then cancelled following Equation (3.10). User 1's new reconstructed received signal is written as

$$\hat{r}_1^{(2)}(t) = r(t) - \sum_{l=2}^K \hat{s}_l^{(2)}(t - \tau_l). \quad (3.28)$$

The second stage finishes by producing a set of improved decision statistics according to Equation (3.11). User 1's second stage metric is computed according to

$$Z_{1,i}^{(2)} = \frac{1}{T} \int_{iT}^{(i+1)T} \Re \left\{ \hat{r}_1^{(2)}(t) a_1(t) e^{-j\phi_1} \right\} dt. \quad (3.29)$$

Substituting Equation (3.28) into Equation(3.29) gives

$$\begin{aligned} Z_{1,i}^{(2)} &= \frac{1}{T} \int_{iT}^{(i+1)T} \Re \left\{ \left[r(t) - \sum_{l=2}^K \hat{s}_l^{(2)}(t - \tau_l) \right] a_1(t) e^{-j\phi_1} \right\} dt \\ &= \frac{1}{T} \int_{iT}^{(i+1)T} \Re \left\{ r(t) a_1(t) e^{-j\phi_1} \right\} dt - \frac{1}{T} \int_{iT}^{(i+1)T} \Re \left\{ \sum_{l=2}^K \hat{s}_l^{(2)}(t - \tau_l) a_1(t) e^{-j\phi_1} \right\} dt \\ &= Z_{1,i}^{(1)} - \frac{1}{T} \int_{iT}^{(i+1)T} \Re \left\{ \sum_{l=2}^K \left[\left\{ Z_{l,i-1}^{(1)} p_T(t - \tau_l + T) \right\} \right. \right. \\ &\quad \left. \left. + Z_{l,i}^{(1)} p_T(t - \tau_l) \right\} a_l(t - \tau_l) e^{j\phi_l} \right] a_1(t) e^{-j\phi_1} \right\} dt \\ &= Z_{1,i}^{(1)} - \sum_{l=2}^K \cos(\phi_l - \phi_1) \left[Z_{l,i-1}^{(1)} \frac{1}{T} \int_{iT}^{iT+\tau_l} a_l(t - \tau_l) a_1(t) dt \right. \\ &\quad \left. + Z_{l,i}^{(1)} \frac{1}{T} \int_{iT+\tau_l}^{(i+1)T} a_l(t - \tau_l) a_1(t) dt \right] \\ &= \underbrace{Z_{1,i}^{(1)}}_{\text{Conv. Receiver}} - \underbrace{\sum_{l=2}^K \cos(\phi_l - \phi_1) \left[Z_{l,i-1}^{(1)} R_{l,1}(\tau) + Z_{l,i}^{(1)} \hat{R}_{l,1}(\tau) \right]}_{\text{Interference Cancellation}}. \end{aligned} \quad (3.30)$$

We now have an expression for the second stage statistic in terms of first stage statistics. Upon substitution of the expressions for first stage metrics into the above expression, we will be able to find the bias produced through brute parallel interference cancellation. Moving

on with such a substitution, we now plug Equation (3.26) into Equation (3.30)⁴

$$\begin{aligned}
 Z_{1,i}^{(2)} &= \sqrt{P_1}b_{1,i} + \sum_{l=2}^K \sqrt{P_l} \cos(\phi_l - \phi_1) [b_{l,i-1}R_{l,1}(\tau) + b_{l,i}\hat{R}_{l,1}(\tau)] + \eta \\
 &\quad - \sum_{l=2}^K \cos(\phi_l - \phi_1) \left\{ \left[\sqrt{P_l}b_{l,i-1} \right. \right. \\
 &\quad \left. \left. + \sum_{m=1}^{l-1} \sqrt{P_m} \cos(\phi_m - \phi_l) [b_{m,i-1}\hat{R}_{m,l}(\tau) + b_{m,i}R_{m,l}(\tau)] \right. \right. \\
 &\quad \left. \left. + \sum_{m=l+1}^K \sqrt{P_m} \cos(\phi_m - \phi_l) [b_{m,i-2}R_{m,l}(\tau) + b_{m,i-1}\hat{R}_{m,l}(\tau)] + \eta \right] R_{l,1}(\tau) \right. \\
 &\quad \left. + \left[\sqrt{P_l}b_{l,i} + \sum_{m=1}^{l-1} \sqrt{P_m} \cos(\phi_m - \phi_l) [b_{m,i}\hat{R}_{m,l}(\tau) + b_{m,i+1}R_{m,l}(\tau)] \right. \right. \\
 &\quad \left. \left. + \sum_{m=l+1}^K \sqrt{P_m} \cos(\phi_m - \phi_l) [b_{m,i-1}R_{m,l}(\tau) + b_{m,i}\hat{R}_{m,l}(\tau)] + \eta \right] \hat{R}_{l,1}(\tau) \right\}. \quad (3.31)
 \end{aligned}$$

Simplifying and collecting like terms yields

$$\begin{aligned}
 Z_{1,i}^{(2)} &= \sqrt{P_1}b_{1,i} - \sum_{l=2}^K \sum_{m=1}^{l-1} \sqrt{P_m} \cos(\phi_l - \phi_1) \cos(\phi_m - \phi_l) \left[b_{m,i-1}\hat{R}_{m,l}(\tau)R_{l,1}(\tau) \right. \\
 &\quad \left. + b_{m,i} [R_{m,l}(\tau)R_{l,1}(\tau) + \hat{R}_{m,l}(\tau)\hat{R}_{l,1}(\tau)] + b_{m,i+1}R_{m,l}(\tau)\hat{R}_{l,1}(\tau) \right] \\
 &\quad - \sum_{l=2}^K \sum_{m=l+1}^K \sqrt{P_m} \cos(\phi_l - \phi_1) \cos(\phi_m - \phi_l) \left[b_{m,i-2}\hat{R}_{m,l}(\tau)R_{l,1}(\tau) \right. \\
 &\quad \left. + b_{m,i-1} [R_{m,l}(\tau)R_{l,1}(\tau) + \hat{R}_{m,l}(\tau)\hat{R}_{l,1}(\tau)] + b_{m,i}R_{m,l}(\tau)\hat{R}_{l,1}(\tau) \right] \\
 &\quad + \eta \left[1 - \sum_{l=2}^K \cos(\phi_l - \phi_1) [R_{l,1}(\tau) + \hat{R}_{l,1}(\tau)] \right]. \quad (3.32)
 \end{aligned}$$

Now with a closed form expression for the second stage statistic in hand, we are ready to take the expectation conditioned upon the desired user's i^{th} transmitted bit $b_{1,i}$. In taking the conditional expectation, the first term in the expression above remains intact while the last term, the noise term, vanishes. When considering the two double summation terms,

⁴We can only substitute Equation (3.26) in its current written form for the $Z_{1,i}^{(1)}$ term in Equation (3.30). For $Z_{l,i-1}^{(1)}$ and $Z_{l,i}^{(1)}$, l is the desired user and we designate user m as the interferer. Interferer m can be any user in $\{1, \dots, l-1\} \cup \{l+1, \dots, K\}$, and as such, user m 's bit indices can be $i-1$, i , or $i+1$, and not just i and $i-1$ as when the interferers are users 2 through K .

one realizes that the only components that can survive the conditional expectation operator are those where the indices $m = 1$ and $l \in \{2, \dots, K\}$. When $m = 1$, the products of cosine terms and the products of PN code cross-correlation terms become squared terms and thus survive the expectation operation. We also note that when $m = 1$, the second double summation contributes nothing. Grouping terms gives

$$\begin{aligned}
 E \left[Z_{1,i}^{(2)} \middle| b_{1,i} \right] &= \sqrt{P_1} b_{1,i} - E \left[\sqrt{P_1} \sum_{l=2}^K \cos^2(\phi_l - \phi_1) b_{1,i} \left[R_{l,1}^2(\tau) + \hat{R}_{l,1}^2(\tau) \right] \right] \\
 &= \sqrt{P_1} b_{1,i} - \sqrt{P_1} b_{1,i} E \left[\sum_{l=2}^K \cos^2(\phi_l - \phi_1) \right] E \left[R_{l,1}^2(\tau) + \hat{R}_{l,1}^2(\tau) \right] \\
 &= \sqrt{P_1} b_{1,i} - \sqrt{P_1} b_{1,i} \frac{1}{2} (K-1) \frac{2}{3N} \\
 &= \underbrace{\sqrt{P_1} b_{1,i}}_{\text{Des. Amp. Est}} - \underbrace{\frac{1}{3N} \sqrt{P_1} b_{1,i} (K-1)}_{\text{Bias Term}}, \tag{3.33}
 \end{aligned}$$

Equation (3.33) demonstrates the presence of a bias proportional to the number of interferers in second stage amplitude estimates. In contrast to the first stage, second stage MAI is not zero-mean and therefore, on the ensemble average, corrupts second stage amplitude estimates, which in turn corrupts MAI signal estimates, ultimately hurting second stage BER. The following section presents the harmful effects this bias can have on system performance.

3.3 Discussion of Bias

The last section showed that while first stage metrics are unbiased, second stage metrics are biased in direct proportion to system loading. We explain in this section how the bias arises and gauge the decline in system performance with a few simulation examples. We conclude the section as well as the chapter by motivating the soft cancellation idea.

The bias emanates from the fact that the second stage's MAI amplitude re-estimation process involves matched-filtering of remnants of previous matched-filter outputs, namely those of first stage MAI. The presence of the MAI term in Equation (3.26) indicates that the interferers' signals are correlated with the desired user's signal (user 1's signal) at the first

stage. At the second stage, we use the interferers' first stage decision metrics as estimates of their signal amplitudes, then reconstruct estimates of the interferer's transmitted signals, and subtract these from the original received signal to form $\hat{r}_1^{(2)}(t)$. The reconstructed received signal $\hat{r}_1^{(2)}(t)$ is then matched-filtered in an effort to gauge its degree of correlation with user 1's PN sequence. However, each interferer's first stage metric itself contains correlation byproducts from the other $K - 1$ users, including user 1. Consequently, all $K - 1$ reconstructed interfering signals are also correlated with user 1. Therefore, when cancelling MAI, an amount of the desired signal (user 1) is removed from $r(t)$, resulting in the bias. The bias exists for all desired users in the system and can be substantiated for them by a similar argument.

The significance of Equation (3.33) is that on the ensemble average, the more the system is loaded, the more decision statistic values will stray from the actual desired user's signal amplitude. This bias in signal amplitude estimates directly causes the received signal points to drift towards the decision boundary. One way to see this is to view the magnitude of the decision statistic when loading is intensified. Figure 3.4 shows an average of the magnitude of the second stage metric across different system loads, in a system under perfect power control with $P_k = 1$ W for all users, with $N = 15$ and $E_b/N_o = 10$ dB.

The degradation in the mean of second stage decision statistics has a direct impact upon second stage BER. The impact can be particularly severe under heavy system loading⁵. Figure 3.5 shows the effect of interference cancellation on a perfect power control system with $N = 15$, loaded with $K = 15$ users.

In such an extreme case, interference cancellation actually worsens performance. However, loading need not be extreme for performance to suffer as compared to a system capable of producing unbiased estimates. Taking from Kaul's analysis in [25], we show in Figure 3.6 a comparison of BER after cancellation between analytical BER from [25] (using unbiased estimates) and simulation BER (using the actual biased estimates from the matched-filter

⁵We consider a *heavy* system load as one which approaches the processing gain N .

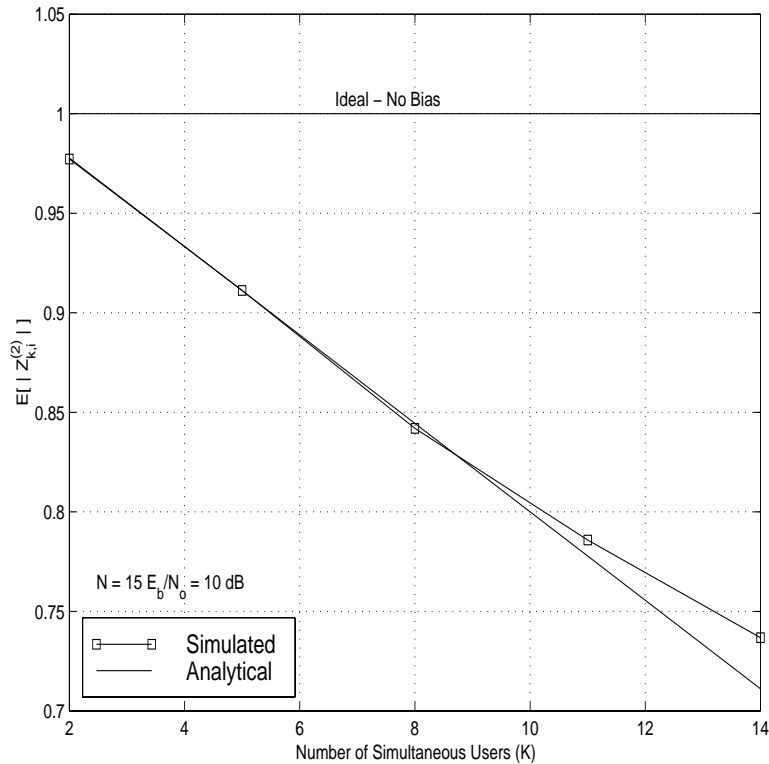


Figure 3.4: Average Magnitude of Second Stage Metric versus Number of Simultaneous Users (K) for Perfect Power Control ($P_k = 1$ W for all Users) with Processing Gain $N = 15$ and $E_b/N_o = 10$ dB

outputs). Indeed, the bias hurts performance across all system loads, and exacerbates the performance discrepancy particularly in greater system loads.

Given how problematic the bias can be, we would ideally like to eliminate it altogether. However, the bias results from our matched-filter estimator, and replacing the matched-filter estimator with an equivalent low-complexity unbiased estimator is not trivial. Even if such an unbiased structure were found, it would likely be more complex than the multiply-add-accumulate scheme characterizing the matched-filter, and possibly even non-linear. We therefore seek to simultaneously preserve the matched-filter structure and find an effective low-complexity bias mitigation solution.

To this end, one may reason that if MAI estimates are unreliable, then perhaps using them

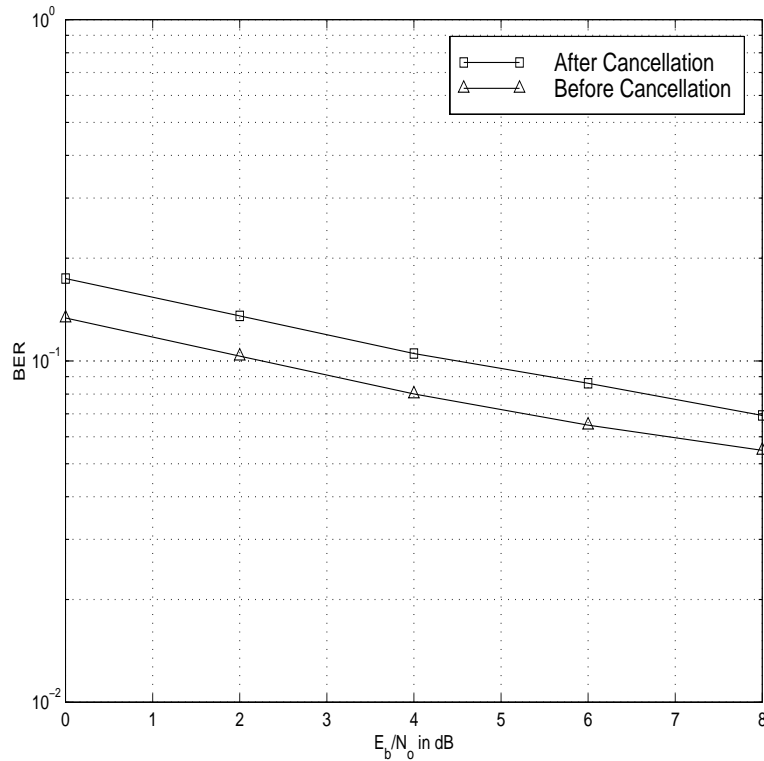


Figure 3.5: BER versus Number of Simultaneous Users (K) in Perfect Power Control System ($P_k = 1$ W for all Users) with Processing Gain $N = 15$ and $K = 15$ Users

partially instead of integrally may advance the cause of BER reduction. More specifically, we can postulate that weighting MAI estimates in proportion to their reliability will abate the effects of the bias on BER. In essence, we propose to cancel only a certain percentage of MAI, scaling down each interferer prior to cancellation by a soft cancellation factor (SCF) between zero and unity. The exact percentage would depend upon the degree of MAI estimate reliability and on general system parameters (processing gain, signal powers etc...). The following chapter models and analyzes this soft interference cancellation idea for a bit-synchronous system, and Chapter 5 details simulation results showing the potential performance enhancements over brute interference cancellation.

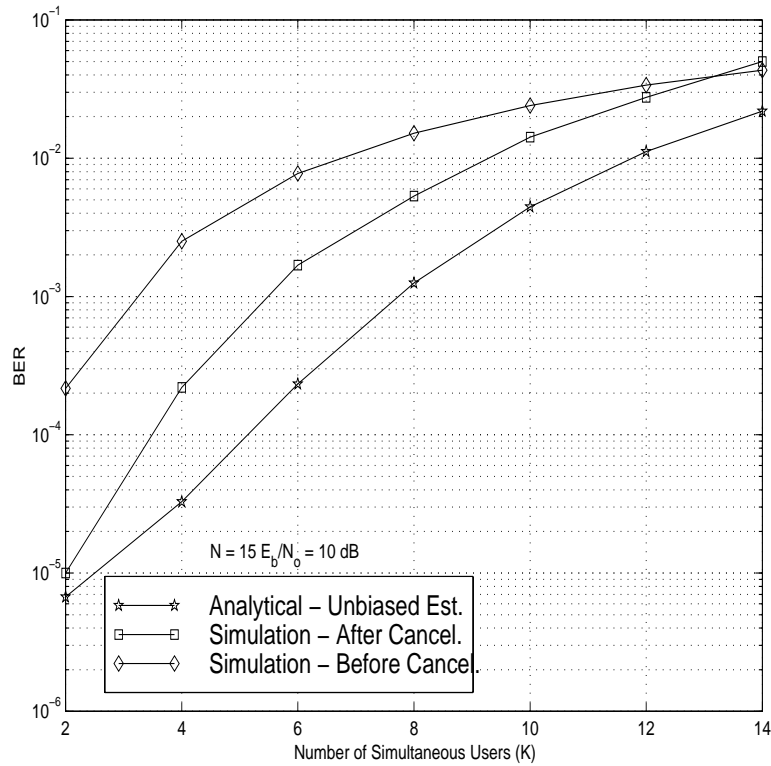


Figure 3.6: BER versus E_b/N_o in Perfect Power Control Asynchronous System ($P_k = 1$ W for all Users) with Processing Gain $N = 15$ and $K = 15$ Users

3.4 Summary

This chapter has presented a model of a brute parallel interference cancellation CDMA receiver, and has analyzed its decision statistics. We have shown that second stage decision statistics are biased in proportion to the number of interfering users. This bias can have very harmful effects on system BER, particularly for large system loads. We motivated the need for an effective low-complexity bias mitigation solution, and have opted to analyze soft interference cancellation in the next chapter based upon several successful simulation trials in the past.

Chapter 4

Analysis of Soft Parallel Interference Cancellation

We analyzed a brute parallel interference cancellation CDMA receiver structure in Chapter 3 and showed that second stage metrics are biased proportionally to system loading as a consequence of interference cancellation using a matched-filter estimator. The bias can force decision statistic values to stray markedly from actual transmitted signal amplitudes. We demonstrated the harmful impact of the bias upon BER performance, particularly for heavy system loads. In this chapter, we analyze our proposed bias mitigation technique, termed *soft interference cancellation*.

In the system model and analysis from the last chapter, the cancellation of interference is carried out using unweighted decision statistics. Here, we extend the work begun in [1, 2] where decision statistics are weighted by a *soft cancellation factor (SCF)* and then used in cancellation, resulting in soft interference cancellation. Moving beyond mere simulation trials, this chapter models the SCF and analyzes the receiver algorithm adjusted for soft cancellation.

In effort to make the analysis more tractable, we consider here a bit-synchronous CDMA

system, thereby dispensing with the modelling of the propagation delay τ through the channel. A bit-synchronous CDMA system can be regarded as operating under worse conditions than an asynchronous system. The inter-user asynchronism in time in an asynchronous system decreases the magnitude of MAI, making users interfere with each other less on average, thereby allowing for lower BER. A bit-synchronous system does not share this benefit. Therefore, analyzing soft cancellation in a bit-synchronous system will in effect provide a lower bound on the performance improvement that a more realistic asynchronous system would exhibit.

We begin this chapter by briefly revisiting our CDMA transmitter model, this time adjusting for bit-synchronism by removing all appearances of the τ terms from the model. We then present the receiver structure and the interference cancellation algorithm, both modified for soft interference cancellation. An analysis of the algorithm ensues in much the same way as in the previous chapter. We derive first and second stage metric moments, this time determining the variance at the second stage, all of which are functions of SCFs. The mean and variance pair allows us to formulate second stage BER in terms of SCFs. This in turn allows us to derive the set of optimal SCFs minimizing BER. We show how the optimal SCFs reduce the bias and proceed to demonstrate via simulation examples the performance enhancements afforded by soft cancellation.

4.1 Model of Soft Parallel Interference Cancellation

This section essentially repeats in compressed form the presentation in Section 3.1, accounting for the introduction of the SCFs. We begin with the bit-synchronous transmitter structure, moving quickly through the CDMA signal models. Then we adjust the receiver algorithm for soft cancellation.

4.1.1 Transmitter Model

Figure 4.1, much like Figure 3.1, is a block diagram of our bit-synchronous CDMA transmitter. We have K users simultaneously transmitting over a linear AWGN channel a binary

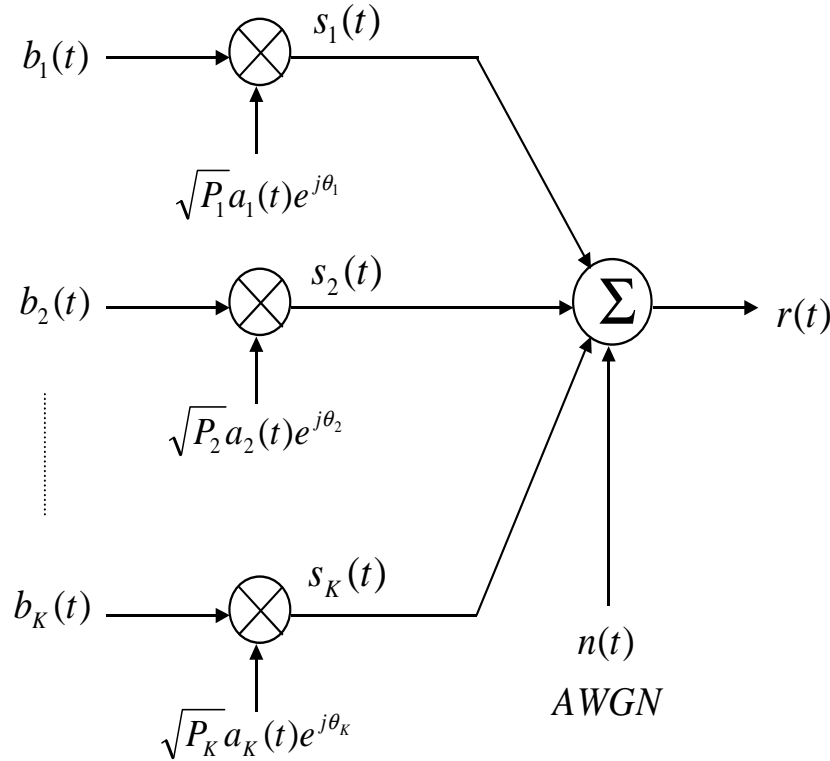


Figure 4.1: CDMA Bit-Synchronous Transmitter Model

data stream modelled as

$$b_k(t) = \sum_{i=-\infty}^{\infty} b_{k,i} p_T(t - iT). \tag{4.1}$$

Each user's data stream is spread by its own high rate PN code waveform, expressed as

$$a_k(t) = \sum_{j=-\infty}^{\infty} a_{k,j} p_{T_c}(t - jT_c), \tag{4.2}$$

where $\{b_{k,i}\}$ and $\{a_{k,j}\}$ are modelled as before with $b_{k,i} \in \{-1, +1\}$, $a_{k,j} \in \{-1, +1\}$, and $Pr[b_{k,i} = -1] = Pr[b_{k,i} = +1] = Pr[a_{k,j} = -1] = Pr[a_{k,j} = +1] = 1/2$. The bit duration is

T and the chip duration is T_c . The ratio $N = T/T_c$ is defined as the processing gain.

Each user transmits a signal modelled by

$$s_k(t) = \sqrt{P_k} b_k(t) a_k(t) e^{j\theta_k}, \quad (4.3)$$

where P_k is the baseband power of the k^{th} user's signal and θ_k is the associated carrier phase, modelled as a random variable uniformly distributed over $[0, 2\pi)$.

Each user's transmitted signal travels through a linear AWGN channel producing a received signal $r(t)$ given as

$$\begin{aligned} r(t) &= \sum_{k=1}^K s_k(t) + n(t) \\ &= \sum_{k=1}^K \sqrt{P_k} b_k(t) a_k(t) e^{j\theta_k} + n(t). \end{aligned} \quad (4.4)$$

The noise $n(t)$ is a zero-mean ergodic and stationary complex AWGN process with one-sided power spectrum magnitude N_o . In such a bit-synchronous model, the received phase is identical to the transmitted phase.

4.1.2 Soft Interference Cancellation Receiver

We now present in Figure 4.2 our interference cancellation receiver modified for bit-synchronism and soft cancellation. The soft cancellation is represented by scaling each reconstructed signal estimate with its own SCF ξ_k .

First Stage:

As before, the first stage is a conventional CDMA correlation receiver. The decision statistic produced for the k^{th} user's i^{th} bit $Z_{k,i}^{(1)}$ is given by

$$Z_{k,i}^{(1)} = \frac{1}{T} \int_{iT}^{(i+1)T} \Re \{ r(t) a_k(t) e^{-j\theta_k} \} dt. \quad (4.5)$$

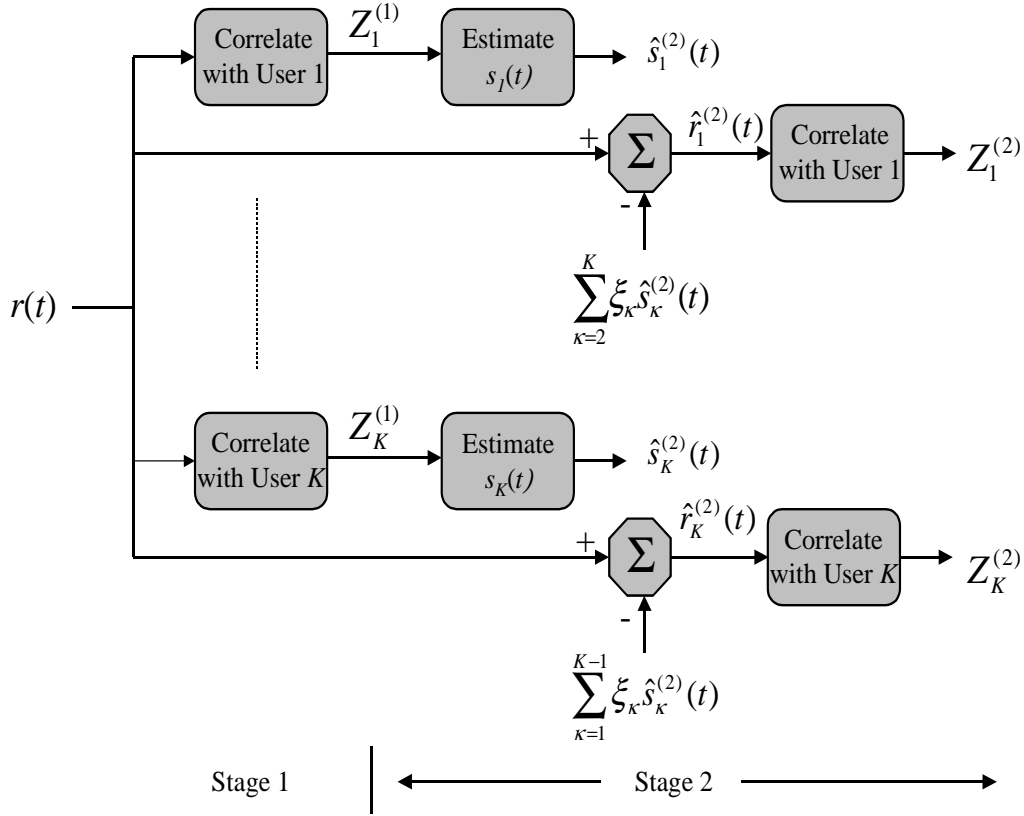


Figure 4.2: CDMA Bit-Synchronous Soft Interference Cancellation Receiver Model

Second Stage:

The second stage begins here as well by reconstructing estimates of transmitted signals. Each reconstructed signal takes the form

$$\hat{s}_k^{(2)}(t) = \left[\sum_{i=-\infty}^{\infty} Z_{k,i}^{(1)} p_T(t - iT) \right] a_k(t) e^{j\theta_k}. \tag{4.6}$$

We now attribute an SCF ξ_k for each interferer and form a new reconstructed received signal

for each user according to

$$\hat{r}_k^{(2)}(t) = r(t) - \sum_{\substack{\kappa=1 \\ \kappa \neq k}}^K \xi_\kappa \hat{s}_\kappa^{(2)}(t). \quad (4.7)$$

Each reconstructed received signal is then passed through a bank of correlators identical to that in the first stage to obtain a cleaner set of decision statistics for each user, given by

$$Z_{k,i}^{(2)} = \frac{1}{T} \int_{iT}^{(i+1)T} \Re \left\{ \hat{r}_k^{(2)}(t) a_k(t) e^{-j\theta_k} \right\} dt. \quad (4.8)$$

Through soft cancellation, we hope to better reduce the level of interference in $\hat{r}_k^{(2)}(t)$ as compared to brute cancellation, such that the correlator following the cancellation operation will better detect $a_1(t)$ in $\hat{r}_k^{(2)}(t)$.

In performing soft cancellation, our objective is to use the SCFs which minimize second stage BER. Turning to user 1 as our desired user as before, we now seek the set $\{\xi_l\} \ l \in \{2, \dots, K\}$, such that

$$\{\xi_l\} = \arg \left\{ \min_{\substack{0 \leq \xi_l \leq 1 \\ \forall l \in \{2, \dots, K\}}} BER^{(2)}(\{\xi_l\}) \right\}, \quad (4.9)$$

where

$$BER^{(2)}(\{\xi_l\}) = Q \left(\sqrt{\frac{\left(E \left[Z_{1,i}^{(2)} \mid b_{1,i} \right] \right)^2}{Var \left[Z_{1,i}^{(2)} \mid b_{1,i} \right]}} \right) = Q \left(\sqrt{\frac{\left(E \left[Z_{1,i}^{(2)} \mid b_{1,i} \right] \right)^2}{E \left[\left(Z_{1,i}^{(2)} \mid b_{1,i} \right)^2 \right] - \left(E \left[Z_{1,i}^{(2)} \mid b_{1,i} \right] \right)^2}} \right). \quad (4.10)$$

Now that we have specified our system model and objective, we continue with an analysis of the receiver metrics and ultimately determine the set of optimal SCFs minimizing $BER^{(2)}$ for a given system.

4.2 Metric Characterization and Bias Analysis

Our metric analysis here can be derived in part from the last chapter's analysis of the asynchronous case. To convert the metrics to those of a synchronous system, one need only set $\tau = 0$ in the metric expressions of the previous chapter, which leads to $R_{l,m}(0) = 0$. This

leaves only $\hat{R}_{l,m}(0)$ to account for PN code cross-correlations. To make notation in subsequent analysis less cumbersome, we define the synchronous normalized cross-correlation of the PN code waveforms as

$$\Gamma_{m,l} = \frac{1}{T} \int_0^T a_m(t) a_l(t) dt = \hat{R}_{l,m}(0). \quad (4.11)$$

This definition is taken from [36], where Divsalar and Simon have computed several moments of $\Gamma_{m,l}$ which will prove most useful in the second stage variance computation, and have been reproduced in the Appendix.

4.2.1 First Stage

The first stage statistic in an asynchronous system was given by Equation (3.26) as

$$Z_{1,i}^{(1)} = \sqrt{P_1} b_{1,i} + \sum_{l=2}^K \sqrt{P_l} \cos(\phi_l - \phi_1) [b_{l,i-1} R_{l,1}(\tau) + b_{l,i} \hat{R}_{l,1}(\tau)] + \eta. \quad (4.12)$$

Substituting for synchronism yields

$$Z_{1,i}^{(1)} = \sqrt{P_1} b_{1,i} + \sum_{l=2}^K \sqrt{P_l} b_{l,i} \Gamma_{1,l} \cos(\phi_l - \phi_1) + \eta. \quad (4.13)$$

Taking the conditional expectation of the first stage metric gives the same result as in the asynchronous case, namely

$$E [Z_{1,i}^{(1)} | b_{1,i}] = \sqrt{P_1} b_{1,i}, \quad (4.14)$$

showing that first stage metrics are unbiased amplitude estimates in the synchronous case as well.

To compute the conditional variance of first stage statistic, we take advantage once again of the statistical independence of its desired user, MAI, and noise components. The desired user contribution is zero again and we computed the noise contribution in the previous chapter to be $Var [\eta | b_{1,i}] = \frac{N_0}{2T}$.

In computing the conditional variance of the MAI component, we keep in mind that the MAI is zero mean and that $E [\Gamma_{l,m}^2] = 1/N$ (see Appendix). The conditional variance of the

first stage statistic is then computed as

$$\begin{aligned}
 \text{Var} \left[Z_{1,i}^{(1)} \middle| b_{1,i} \right] &= E \left[\left(\sum_{l=2}^K \sqrt{P_l} b_{l,i} \Gamma_{1,l} \cos(\phi_l - \phi_1) \right)^2 \middle| b_{1,i} \right] + \frac{N_o}{2T} \\
 &= \sum_{l=2}^K E \left[\left(\sqrt{P_l} b_{l,i} \Gamma_{1,l} \cos(\phi_l - \phi_1) \right)^2 \right] + \frac{N_o}{2T} \\
 &= \frac{1}{2N} \sum_{l=2}^K P_l + \frac{N_o}{2T}. \tag{4.15}
 \end{aligned}$$

Comparing with the asynchronous first stage variance in Equation (3.23), we see that the synchronous first stage variance is greater due to bit-synchronism, and therefore increases first stage BER.

4.2.2 Second Stage

The second stage metric for user 1 is expressed as

$$\begin{aligned}
 Z_{1,i}^{(2)} &= \frac{1}{T} \int_{iT}^{(i+1)T} \Re \left\{ \hat{r}_1^{(2)}(t) a_1(t) e^{-j\theta_1} \right\} dt \\
 &= \frac{1}{T} \int_{iT}^{(i+1)T} \Re \left\{ \left[r(t) - \sum_{l=2}^K \xi_l \hat{s}_l^{(2)}(t) \right] a_1(t) e^{-j\theta_1} \right\} dt \\
 &= \frac{1}{T} \int_{iT}^{(i+1)T} \Re \left\{ r(t) a_1(t) e^{-j\theta_1} \right\} dt - \frac{1}{T} \int_{iT}^{(i+1)T} \Re \left\{ \sum_{l=2}^K \xi_l \hat{s}_l^{(2)}(t) a_1(t) e^{-j\theta_1} \right\} dt \\
 &= Z_{1,i}^{(1)} - \frac{1}{T} \int_{iT}^{(i+1)T} \Re \left\{ \left[\sum_{l=2}^K \xi_l Z_{l,i}^{(1)} p_T(t - iT) a_l(t) e^{j\theta_l} \right] a_1(t) e^{-j\theta_1} \right\} dt \\
 &= Z_{1,i}^{(1)} - \sum_{l=2}^K \xi_l Z_{l,i}^{(1)} \cos(\theta_l - \theta_1) \frac{1}{T} \int_{iT}^{(i+1)T} a_l(t) a_1(t) dt \\
 &= \underbrace{Z_{1,i}^{(1)}}_{\text{Conv. Rec.}} - \underbrace{\sum_{l=2}^K \xi_l Z_{l,i}^{(1)} \Gamma_{1,l} \cos(\theta_l - \theta_1)}_{\text{Interference Cancellation with SCF}}. \tag{4.16}
 \end{aligned}$$

Substituting Equation (4.12) into Equation (4.16) gives

$$\begin{aligned}
 Z_{1,i}^{(2)} &= \sqrt{P_1}b_{1,i} + \sum_{l=2}^K \sqrt{P_l}b_{l,i}\Gamma_{1,l} \cos(\theta_l - \theta_1) + \eta \\
 &\quad - \sum_{l=2}^K \xi_l \left[\sqrt{P_l}b_{l,i} + \sum_{\substack{m=1 \\ m \neq l}}^K \sqrt{P_m}b_{m,i}\Gamma_{l,m} \cos(\theta_m - \theta_l) + \eta \right] \cdot \Gamma_{1,l} \cos(\theta_l - \theta_1) \\
 &= \sqrt{P_1}b_{1,i} + \sum_{l=2}^K (1 - \xi_l) \sqrt{P_l}b_{l,i}\Gamma_{1,l} \cos(\theta_l - \theta_1) \\
 &\quad - \sum_{l=2}^K \sum_{\substack{m=1 \\ m \neq l}}^K \left[\xi_l \sqrt{P_m}b_{m,i}\Gamma_{1,l}\Gamma_{l,m} \cos(\theta_m - \theta_l) \cos(\theta_l - \theta_1) \right] \\
 &\quad + \eta \left[1 - \sum_{l=2}^K \xi_l \Gamma_{1,l} \cos(\theta_l - \theta_1) \right]. \tag{4.17}
 \end{aligned}$$

Now that we have an expression for the second stage statistic we are ready to begin mean and variance computations.

Conditioning the second stage statistic upon $b_{1,i}$ and taking the expectation, we see that the first term, the desired term, in Equation (4.17) remains intact while the last term, the noise term, vanishes. The second term in the second stage statistic vanishes as well in the expectation. The double summation term only contributes in the expectation when $m = 1$, when the cosine and PN code cross-correlation terms become squared terms. Taking the conditional expectation gives

$$\begin{aligned}
 E \left[Z_{1,i}^{(2)} \middle| b_{1,i} \right] &= \sqrt{P_1}b_{1,i} - E \left[\sum_{l=2}^K \xi_l \sqrt{P_1}b_{1,i}\Gamma_{1,l}^2 \cos^2(\theta_m - \theta_l) \middle| b_{1,i} \right] \\
 &= \sqrt{P_1}b_{1,i} - \sqrt{P_1}b_{1,i} \sum_{l=2}^K \xi_l E \left[\Gamma_{1,l}^2 \cos^2(\theta_1 - \theta_l) \right] \\
 &= \underbrace{\sqrt{P_1}b_{1,i}}_{\text{Des. Amp. Est.}} - \underbrace{\frac{1}{2N} \sqrt{P_1}b_{1,i} \sum_{l=2}^K \xi_l}_{\text{Reduced Bias Term}}. \tag{4.18}
 \end{aligned}$$

We see that in the synchronous soft cancellation case the bias exists as well. However, it is worthwhile to comment on the new form that the bias term takes in Equation (4.18) as compared to Equation (3.33). One difference is the factor of 1/2 instead of 1/3, which arises from the change to synchronism. The second and more important difference though,

is the appearance of the summation of the SCFs of the interferers, due to the use of soft cancellation.

When using brute cancellation in a synchronous system, the bias term would take the form $\sqrt{P_1}b_{1,i}(K - 1)/(2N)$ (amounting to $\xi_l = 1$ for all interferers). Even though the SCFs are defined to be between zero and unity, their summation in Equation (4.18) is in fact always less¹ than $K - 1$. Therefore, the bias magnitude in soft cancellation is less than that in brute cancellation.

The decrease in bias magnitude may lead one to hastily conclude that a solution to the effects of the bias would be to systematically set all SCFs to zero, eliminating the bias altogether. Indeed, setting all SCFs to zero would cure the system of the bias, but in doing so would in effect reduce the receiver to a conventional correlator, not cancelling any interference at all since all MAI signal estimates would be zeroed. We will see further on that in general, non-zero SCFs minimize $BER^{(2)}$.

We now commence the second stage metric variance derivation. This variance can be defined as

$$Var [Z_{1,i}^{(2)} | b_{1,i}] = E \left[\left(Z_{1,i}^{(2)} | b_{1,i} \right)^2 \right] - \left(E [Z_{1,i}^{(2)} | b_{1,i}] \right)^2. \quad (4.19)$$

We have already computed $E [Z_{1,i}^{(2)} | b_{1,i}]$ in Equation (4.18), and will now determine $E \left[\left(Z_{1,i}^{(2)} | b_{1,i} \right)^2 \right]$.

¹A given system will never have all SCFs minimizing $BER^{(2)}$ equal to unity, hence $\sum_{l=2}^K \xi_l < K - 1$.

Reproducing the expression for $Z_{1,i}^{(2)}$ and assigning terms, we have

$$\begin{aligned}
 Z_{1,i}^{(2)} &= \underbrace{\sqrt{P_1} b_{1,i}}_{\Psi_1} \\
 &+ \underbrace{\sum_{l=2}^K (1 - \xi_l) \sqrt{P_l} b_{l,i} \Gamma_{1,l} \cos(\theta_l - \theta_1)}_{\Psi_2} \\
 &- \underbrace{\sum_{l=2}^K \sum_{\substack{m=1 \\ m \neq l}}^K \left[\xi_l \sqrt{P_m} b_{m,i} \Gamma_{1,l} \Gamma_{l,m} \cos(\theta_m - \theta_l) \cos(\theta_l - \theta_1) \right]}_{\Psi_3} \\
 &+ \underbrace{\eta \left[1 - \sum_{l=2}^K \xi_l \Gamma_{1,l} \cos(\theta_l - \theta_1) \right]}_{\Psi_4}. \tag{4.20}
 \end{aligned}$$

Expressing the desired expectation in terms of Ψ_1 , Ψ_2 , Ψ_3 , and Ψ_4 gives

$$\begin{aligned}
 E \left[\left(Z_{1,i}^{(2)} | b_{1,i} \right)^2 \right] &= E \left[\{ (\Psi_1 + \Psi_2 - \Psi_3 + \Psi_4) | b_{1,i} \}^2 \right] \\
 &= E \left[(\Psi_1 | b_{1,i})^2 \right] + E \left[(\Psi_2 | b_{1,i})^2 \right] + E \left[(\Psi_3 | b_{1,i})^2 \right] + E \left[(\Psi_4 | b_{1,i})^2 \right] \\
 &+ 2E \left[\Psi_1 \Psi_2 | b_{1,i} \right] - 2E \left[\Psi_1 \Psi_3 | b_{1,i} \right] + 2E \left[\Psi_1 \Psi_4 | b_{1,i} \right] - 2E \left[\Psi_2 \Psi_3 | b_{1,i} \right] \\
 &+ 2E \left[\Psi_2 \Psi_4 | b_{1,i} \right] - 2E \left[\Psi_3 \Psi_4 | b_{1,i} \right]. \tag{4.21}
 \end{aligned}$$

Now that we have subdivided our task into several more tractable calculations, we compute each component in order of appearance in Equation (4.21). Beginning then with the squared terms, we have

$$\begin{aligned}
 E \left[(\Psi_1 | b_{1,i})^2 \right] &= P_1 \\
 E \left[(\Psi_2 | b_{1,i})^2 \right] &= E \left[\left(\sum_{l=2}^K (1 - \xi_l) \sqrt{P_l} b_{l,i} \Gamma_{1,l} \cos(\theta_l - \theta_1) \right)^2 \right] \\
 &= \sum_{l=2}^K E \left[\left((1 - \xi_l) \sqrt{P_l} b_{l,i} \Gamma_{1,l} \cos(\theta_l - \theta_1) \right)^2 \right] \\
 &= \frac{1}{2N} \sum_{l=2}^K (1 - \xi_l)^2 P_l \\
 &= \frac{1}{2N} \sum_{l=2}^K P_l - \frac{1}{N} \sum_{l=2}^K \xi_l P_l + \frac{1}{2N} \sum_{l=2}^K \xi_l^2 P_l.
 \end{aligned}$$

The calculation of $E[(\Psi_3|b_{1,i})^2]$ is more involved and we will decompose it. We consider first the squared terms in this expectation, that is, the terms contained in

$$E \left[\sum_{l=2}^K \sum_{\substack{m=1 \\ m \neq l}}^K \left\{ \xi_l \sqrt{P_m} b_{m,i} \Gamma_{1,l} \Gamma_{l,m} \cos(\theta_m - \theta_l) \cos(\theta_l - \theta_1) \right\}^2 \middle| b_{1,i} \right]. \quad (4.22)$$

Within this expectation of squares, we start with the terms where $m = 1$ and $l \in \{2, \dots, K\}$.

Substituting $m = 1$ gives

$$\begin{aligned} E \left[\sum_{l=2}^K \left\{ \xi_l \sqrt{P_1} b_{1,i} \Gamma_{1,l} \Gamma_{l,1} \cos(\theta_1 - \theta_l) \cos(\theta_l - \theta_1) \right\}^2 \middle| b_{1,i} \right] &= E \left[\sum_{l=2}^K \xi_l^2 P_1 \Gamma_{1,l}^4 \cos^4(\theta_1 - \theta_l) \right] \\ &= \sum_{l=2}^K \xi_l^2 P_1 E \left[\Gamma_{1,l}^4 \cos^4(\theta_1 - \theta_l) \right] \\ &= \frac{3}{8} P_1 \left(\frac{3}{N^2} - \frac{2}{N^3} \right) \sum_{l=2}^K \xi_l^2 \\ &= P_1 \left(\frac{9}{8N^2} - \frac{3}{4N^3} \right) \sum_{l=2}^K \xi_l^2, \end{aligned}$$

where we have used the fact that $E[\Gamma_{1,l}^4] = \left(\frac{3}{N^2} - \frac{2}{N^3} \right)$ as shown in the Appendix, and that $E[\cos^4(\theta_1 - \theta_l)] = \frac{3}{8}$.

The remainder of the squared terms inside the expectation take the form

$$\begin{aligned} &E \left[\sum_{l=2}^K \sum_{\substack{m=2 \\ m \neq l}}^K \left\{ \xi_l \sqrt{P_m} b_{m,i} \Gamma_{1,l} \Gamma_{l,m} \cos(\theta_m - \theta_l) \cos(\theta_l - \theta_1) \right\}^2 \right] \\ &= E \left[\sum_{l=2}^K \xi_l^2 \sum_{\substack{m=2 \\ m \neq l}}^K P_m \Gamma_{1,l}^2 \Gamma_{l,m}^2 \cos^2(\theta_m - \theta_l) \cos^2(\theta_l - \theta_1) \right] \\ &= \sum_{l=2}^K \xi_l^2 \sum_{\substack{m=2 \\ m \neq l}}^K P_m E \left[\Gamma_{1,l}^2 \Gamma_{l,m}^2 \right] \cdot E \left[\cos^2(\theta_m - \theta_l) \cos^2(\theta_l - \theta_1) \right] = \frac{1}{4N^2} \sum_{l=2}^K \sum_{\substack{m=2 \\ m \neq l}}^K \xi_l^2 P_m. \end{aligned}$$

We therefore have

$$\begin{aligned} E \left[\sum_{l=2}^K \sum_{\substack{m=1 \\ m \neq l}}^K \left\{ \xi_l \sqrt{P_m} b_{m,i} \Gamma_{1,l} \Gamma_{l,m} \cos(\theta_m - \theta_l) \cos(\theta_l - \theta_1) \right\}^2 \middle| b_{1,i} \right] \\ = \frac{3}{8} P_1 \left(\frac{3}{N^2} - \frac{2}{N^3} \right) \sum_{l=2}^K \xi_l^2 + \frac{1}{4N^2} \sum_{l=2}^K \sum_{\substack{m=2 \\ m \neq l}}^K \xi_l^2 P_m. \end{aligned} \quad (4.23)$$

We now come to the cross-terms inside $E[(\Psi_3|b_{1,i})^2]$. We first calculate the expectation of the cross-terms involving only $m = 1$ components. That is, we compute

$$\begin{aligned}
 & E \left[\sum_{l=2}^K \sum_{\substack{n=2 \\ n \neq l}}^K \left[\xi_l \sqrt{P_1} b_{1,i} \Gamma_{1,l}^2 \cos^2(\theta_1 - \theta_l) \right] \cdot \left[\xi_n \sqrt{P_1} b_{1,i} \Gamma_{1,n}^2 \cos^2(\theta_1 - \theta_n) \right] \middle| b_{1,i} \right] \\
 &= E \left[\sum_{l=2}^K \sum_{\substack{n=2 \\ n \neq l}}^K \xi_l \xi_n P_1 \Gamma_{1,l}^2 \Gamma_{1,n}^2 \cos^2(\theta_1 - \theta_l) \cos^2(\theta_1 - \theta_n) \right] \\
 &= \sum_{l=2}^K \sum_{\substack{n=2 \\ n \neq l}}^K \xi_l \xi_n P_1 E[\Gamma_{1,l}^2 \Gamma_{1,n}^2] \cdot E[\cos^2(\theta_1 - \theta_l) \cos^2(\theta_1 - \theta_n)] = \frac{1}{4N^2} P_1 \sum_{l=2}^K \sum_{\substack{n=2 \\ n \neq l}}^K \xi_l \xi_n.
 \end{aligned}$$

To complete the set of cross-terms inside $E[(\Psi_3|b_{1,i})^2]$, we determine

$$\begin{aligned}
 & E \left[\sum_{l=2}^K \sum_{\substack{m=2 \\ m \neq l}}^K \sum_{\substack{n=2 \\ n \neq l}}^K \sum_{\substack{q=2 \\ q \neq n}}^K \left[\xi_l \sqrt{P_m} b_{m,i} \Gamma_{1,l} \Gamma_{l,m} \cos(\theta_m - \theta_l) \cos(\theta_l - \theta_1) \right] \right. \\
 & \quad \left. \cdot \left[\xi_n \sqrt{P_q} b_{q,i} \Gamma_{1,n} \Gamma_{n,q} \cos(\theta_q - \theta_n) \cos(\theta_n - \theta_1) \right] \right]. \tag{4.24}
 \end{aligned}$$

The only terms in the above expectation that have non-zero contributions are those where $q = m$. Adjusting indices, we now have

$$\begin{aligned}
 & E \left[\sum_{l=2}^K \sum_{\substack{m=2 \\ m \neq l}}^K \sum_{\substack{n=2 \\ n \neq l, m}}^K \left[\xi_l \sqrt{P_m} b_{m,i} \Gamma_{1,l} \Gamma_{l,m} \cos(\theta_m - \theta_l) \cos(\theta_l - \theta_1) \right] \right. \\
 & \quad \left. \cdot \left[\xi_n \sqrt{P_m} b_{m,i} \Gamma_{1,n} \Gamma_{n,m} \cos(\theta_m - \theta_n) \cos(\theta_n - \theta_1) \right] \right] \\
 &= \sum_{l=2}^K \sum_{\substack{m=2 \\ m \neq l}}^K \sum_{\substack{n=2 \\ n \neq l, m}}^K P_m \xi_l \xi_n E[\Gamma_{1,n} \Gamma_{n,m} \Gamma_{1,l} \Gamma_{l,m}] \\
 & \cdot E[\cos(\theta_m - \theta_n) \cos(\theta_n - \theta_1) \cos(\theta_m - \theta_l) \cos(\theta_l - \theta_1)] = \frac{1}{8N^3} \sum_{l=2}^K \sum_{\substack{m=2 \\ m \neq l}}^K \sum_{\substack{n=2 \\ n \neq m, l}}^K P_m \xi_l \xi_n,
 \end{aligned}$$

where we have used the fact that $E[\Gamma_{1,l} \Gamma_{l,m} \Gamma_{1,n} \Gamma_{n,m}] = \frac{1}{N^3}$ and that

$$E[\cos(\theta_m - \theta_n) \cos(\theta_n - \theta_1) \cos(\theta_m - \theta_l) \cos(\theta_l - \theta_1)] = \frac{1}{8}.$$

We can finally write

$$\begin{aligned}
 E \left[(\Psi_3 | b_{1,i})^2 \right] &= \frac{3}{8} P_1 \left(\frac{3}{N^2} - \frac{2}{N^3} \right) \sum_{l=2}^K \xi_l^2 + \frac{1}{4N^2} \sum_{l=2}^K \sum_{\substack{m=2 \\ m \neq l}}^K \xi_l^2 P_m \\
 &+ \frac{1}{4N^2} P_1 \sum_{l=2}^K \sum_{\substack{m=2 \\ m \neq l}}^K \xi_l \xi_m + \frac{1}{8N^3} \sum_{l=2}^K \sum_{\substack{m=2 \\ m \neq l}}^K \sum_{\substack{n=2 \\ n \neq m, l}}^K P_m \xi_l \xi_n. \tag{4.25}
 \end{aligned}$$

Moving on to the final squared term, we have

$$\begin{aligned}
 E \left[(\Psi_4 | b_{1,i})^2 \right] &= E \left[\left(\eta \left[1 - \sum_{l=2}^K \xi_l \Gamma_{1,l} \cos(\theta_l - \theta_1) \right] \right)^2 \right] \\
 &= \text{Var}[\eta] \cdot E \left[\left(\left[1 - \sum_{l=2}^K \xi_l \Gamma_{1,l} \cos(\theta_l - \theta_1) \right] \right)^2 \right] \\
 &= \frac{N_o}{2T} \left[1 + \frac{1}{2N} \sum_{l=2}^K \xi_l^2 \right].
 \end{aligned}$$

The cross-terms give

$$\begin{aligned}
 2E \left[\Psi_1 \Psi_2 | b_{1,i} \right] &= 2E \left[\sqrt{P_1} b_{1,i} \sum_{l=2}^K (1 - \xi_l) \sqrt{P_l} b_{l,i} \Gamma_{1,l} \cos(\theta_l - \theta_1) \middle| b_{1,i} \right] \\
 &= 0. \\
 2E \left[\Psi_1 \Psi_3 | b_{1,i} \right] &= 2E \left[\sqrt{P_1} b_{1,i} \sum_{l=2}^K \sum_{\substack{m=1 \\ m \neq l}}^K \left[\xi_l \sqrt{P_m} b_{m,i} \Gamma_{1,l} \Gamma_{l,m} \cos(\theta_m - \theta_l) \cos(\theta_l - \theta_1) \right] \middle| b_{1,i} \right] \\
 &= 2E \left[\sqrt{P_1} b_{1,i} \sum_{l=2}^K \xi_l \sqrt{P_1} b_{1,i} \Gamma_{1,l} \Gamma_{l,1} \cos(\theta_1 - \theta_l) \cos(\theta_l - \theta_1) \middle| b_{1,i} \right] \\
 &= 2P_1 \sum_{l=2}^K \xi_l E \left[\Gamma_{1,l}^2 \cos^2(\theta_l - \theta_1) \right] \\
 &= \frac{1}{N} P_1 \sum_{l=2}^K \xi_l. \tag{4.26}
 \end{aligned}$$

$$2E \left[\Psi_1 \Psi_4 | b_{1,i} \right] = 2E \left[\sqrt{P_1} b_{1,i} \cdot \eta \left[1 - \sum_{l=2}^K \xi_l \Gamma_{1,l} \cos(\theta_l - \theta_1) \right] \middle| b_{1,i} \right] = 0.$$

$$\begin{aligned}
2E[\Psi_2\Psi_3|b_{1,i}] &= 2E\left[\sum_{n=2}^K(1-\xi_n)\sqrt{P_n}b_{n,i}\Gamma_{1,n}\cos(\theta_n-\theta_1)\right. \\
&\quad \cdot \left.\sum_{l=2}^K\sum_{\substack{m=1 \\ m\neq l}}^K\xi_l\sqrt{P_m}b_{m,i}\Gamma_{1,l}\Gamma_{l,m}\cos(\theta_m-\theta_l)\cos(\theta_l-\theta_1)\right|b_{1,i}] \\
&= 2\sum_{l=2}^K\sum_{\substack{m=2 \\ m\neq l}}^K(1-\xi_m)\xi_lP_mE[\cos(\theta_m-\theta_1)\cos(\theta_m-\theta_l)\cos(\theta_l-\theta_1)] \\
&\quad \cdot E[\Gamma_{1,m}\Gamma_{1,l}\Gamma_{l,m}] \\
&= \frac{1}{2N^2}\sum_{l=2}^K\sum_{\substack{m=2 \\ m\neq l}}^K(1-\xi_m)\xi_lP_m, \\
&= \frac{1}{2N^2}\sum_{l=2}^K\sum_{\substack{m=2 \\ m\neq l}}^K\xi_lP_m - \frac{1}{2N^2}\sum_{l=2}^K\sum_{\substack{m=2 \\ m\neq l}}^K\xi_l\xi_mP_m,
\end{aligned}$$

where we have used the fact that $E[\cos(\theta_m-\theta_1)\cos(\theta_m-\theta_l)\cos(\theta_l-\theta_1)] = \frac{1}{4}$ and that $E[\Gamma_{1,m}\Gamma_{1,l}\Gamma_{l,m}] = \frac{1}{N^2}$.

Finally, we have that

$$2E[\Psi_2\Psi_4|b_{1,i}] = 2E[\Psi_3\Psi_4|b_{1,i}] = 0, \quad (4.27)$$

because these terms both include $E[\eta]$ components, which are zero, multiplying the rest.

At this point, we can write the variance of the second stage metric. Following Equation (4.19), we have

$$\begin{aligned}
\text{Var}[Z_{1,i}^{(2)}|b_{1,i}] &= E\left[\left(Z_{1,i}^{(2)}|b_{1,i}\right)^2\right] - \left(E\left[Z_{1,i}^{(2)}|b_{1,i}\right]\right)^2 \\
&= E\left[\left(Z_{1,i}^{(2)}|b_{1,i}\right)^2\right] - \left[\sqrt{P_1}b_{1,i} - \frac{1}{2N}\sqrt{P_1}b_{1,i}\sum_{l=2}^K\xi_l\right]^2 \\
&= E\left[\left(Z_{1,i}^{(2)}|b_{1,i}\right)^2\right] - \left[P_1 - \frac{1}{N}P_1\sum_{l=2}^K\xi_l + \frac{1}{4N^2}P_1\left(\sum_{l=2}^K\xi_l\right)^2\right].
\end{aligned}$$

Cancelling like terms yields at last

$$\begin{aligned}
 \text{Var} \left[Z_{1,i}^{(2)} \middle| b_{1,i} \right] &= \frac{1}{2N} \sum_{l=2}^K P_l + \frac{1}{2N} \sum_{l=2}^K \xi_l^2 P_l + P_1 \left(\frac{9}{8N^2} - \frac{3}{4N^3} \right) \sum_{l=2}^K \xi_l^2 + \frac{1}{4N^2} \sum_{l=2}^K \sum_{\substack{m=2 \\ m \neq l}}^K \xi_l^2 P_m \\
 &+ \frac{1}{4N^2} P_1 \sum_{l=2}^K \sum_{\substack{m=2 \\ m \neq l}}^K \xi_l \xi_m - \frac{1}{2N^2} \sum_{l=2}^K \sum_{\substack{m=2 \\ m \neq l}}^K \xi_l P_m + \frac{1}{2N^2} \sum_{l=2}^K \sum_{\substack{m=2 \\ m \neq l}}^K \xi_l \xi_m P_m \\
 &+ \frac{1}{8N^3} \sum_{l=2}^K \sum_{\substack{m=2 \\ m \neq l}}^K \sum_{\substack{n=2 \\ n \neq m, l}}^K P_m \xi_l \xi_n - \frac{1}{N} \sum_{l=2}^K \xi_l P_l - \frac{1}{4N^2} P_1 \left(\sum_{l=2}^K \xi_l \right)^2 \\
 &+ \frac{N_o}{2T} \left[1 + \frac{1}{2N} \sum_{l=2}^K \xi_l^2 \right],
 \end{aligned}$$

where the last term is the noise contribution to the variance, and all preceding terms are due to MAI.

It is interesting to note that while in general, BER after cancellation is lower than before cancellation, the noise contribution to the variance is magnified due to the use of the matched-filter estimator in the cancellation process. However, the cancellation process generally removes more MAI than it enhances noise, thereby making the second stage variance as a whole smaller than first stage variance. The smaller variance at the second stage is indicative of second stage amplitude estimates wandering about their mean to a lesser degree than at the first stage, hence allowing for bit estimates to be correct more often.

We now have all the requisite items to minimize $BER^{(2)}$. Since $BER^{(2)}$ is expressed in terms of the Q -function, minimizing $BER^{(2)}$ is equivalent to maximizing the Q -function argument. Therefore, to find the optimal SCF for a given interferer ($\xi_\kappa, \kappa \in \{2, \dots, K\}$), we can proceed by taking the partial derivative of the Q -function argument with respect to ξ_κ , setting it to zero, and solving for ξ_κ , as denoted by

$$\{\xi_\kappa\} : \quad \frac{\partial}{\partial \xi_\kappa} \left[\frac{\left(E \left[Z_{1,i}^{(2)} \middle| b_{1,i} \right] \right)^2}{\text{Var} \left[Z_{1,i}^{(2)} \middle| b_{1,i} \right]} \right] = 0, \quad \text{where} \quad \kappa \in \{2, \dots, K\}. \quad (4.28)$$

Differentiation yields two extrema: a minimum and a maximum. As we desire the latter, we discard the former, leaving us with the result

$$\xi_\kappa = \frac{\mathcal{A}}{\mathcal{B}}, \quad (4.29)$$

where

$$\begin{aligned} \mathcal{A} = & 8N^3 \left(P_\kappa - \frac{N_o}{2T} \right) - \sum_{\substack{l=2 \\ l \neq \kappa}}^K \xi_l^2 \left[P_1(7N - 6) + (2N - 1) \left(\sum_{\substack{m=2 \\ m \neq \kappa, l}}^K P_m + 2NP_l \right) \right] \\ & - 2N(2N - 1) \sum_{\substack{l=2 \\ l \neq \kappa}}^K \xi_l [2P_\kappa - P_l] - (2N - 1) \left[\sum_{\substack{l=2 \\ l \neq \kappa}}^K \sum_{\substack{m=2 \\ m \neq \kappa, l}}^K \xi_l \xi_m (P_l - P_\kappa) \right] \\ & - 4N^2 \frac{N_o}{2T} \sum_{\substack{l=2 \\ l \neq \kappa}}^K \xi_l^2, \end{aligned} \quad (4.30)$$

and

$$\begin{aligned} \mathcal{B} = & 8N^3 \left(P_\kappa + \frac{N_o}{2T} \right) - \sum_{\substack{l=2 \\ l \neq \kappa}}^K \xi_l \left[P_1(7N - 6) + (2N - 1) \left(\sum_{\substack{m=2 \\ m \neq \kappa, l}}^K P_m + 2NP_\kappa \right) \right] \\ & - 2N(1 - 2N) \left[\sum_{\substack{m=2 \\ m \neq \kappa}}^K P_m + (6 - 7N)P_1 \right] - 4N^2 \frac{N_o}{2T} \sum_{\substack{l=2 \\ l \neq \kappa}}^K \xi_l. \end{aligned}$$

Our expression for the optimal SCF minimizing $BER^{(2)}$ in its above most general form does not lend itself easily to immediate interpretation. We therefore devote the next chapter to an analysis of the SCF and its implications.

4.3 Chapter Summary

This chapter presented and analyzed a bit-synchronous soft interference cancellation CDMA receiver model. Receiver metrics were developed in terms of the SCFs which allowed us to formulate BER after cancellation in terms of the SCFs. As our objective was to minimize BER after interference cancellation, we performed a minimization operation on $BER^{(2)}$ to determine this optimal set of SCFs.

Chapter 5

Interpretation of the Soft Cancellation Factor and Simulation Results

Thus far, we have presented our soft interference cancellation receiver model and have optimized its BER performance within the means of soft cancellation. In this chapter, we demonstrate both quantitatively and qualitatively the performance enhancements afforded by the use of soft cancellation over brute cancellation.

We first seek general insights into the optimal SCFs as expressed in Equation (4.29). We examine certain limiting cases and attempt to make sense of the SCFs yielded in these limiting cases. We examine performance enhancements under perfect power control and in the near-far situation.

5.1 Evaluation of the SCF

We reproduce for convenience the expression for optimal SCFs from the end of the previous chapter. In keeping still with user 1 as our desired user, we attribute to the κ^{th} interferer the SCF ξ_κ ,

$$\xi_\kappa = \frac{\mathcal{A}}{\mathcal{B}}, \quad (5.1)$$

where

$$\begin{aligned} \mathcal{A} = & 8N^3 \left(P_\kappa - \frac{N_o}{2T} \right) - \sum_{\substack{l=2 \\ l \neq \kappa}}^K \xi_l^2 \left[P_1(7N - 6) + (2N - 1) \left(\sum_{\substack{m=2 \\ m \neq \kappa, l}}^K P_m + 2NP_l \right) \right] \\ & - 2N(2N - 1) \sum_{\substack{l=2 \\ l \neq \kappa}}^K \xi_l [2P_\kappa - P_l] - (2N - 1) \left[\sum_{\substack{l=2 \\ l \neq \kappa}}^K \sum_{\substack{m=2 \\ m \neq \kappa, l}}^K \xi_l \xi_m (P_l - P_\kappa) \right] \\ & - 4N^2 \frac{N_o}{2T} \sum_{\substack{l=2 \\ l \neq \kappa}}^K \xi_l^2, \end{aligned}$$

and

$$\begin{aligned} \mathcal{B} = & 8N^3 \left(P_\kappa + \frac{N_o}{2T} \right) - \sum_{\substack{l=2 \\ l \neq \kappa}}^K \xi_l \left[P_1(7N - 6) + (2N - 1) \left(\sum_{\substack{m=2 \\ m \neq \kappa, l}}^K P_m + 2NP_\kappa \right) \right] \\ & - 2N(1 - 2N) \left[\sum_{\substack{m=2 \\ m \neq \kappa}}^K P_m + (6 - 7N)P_1 \right] - 4N^2 \frac{N_o}{2T} \sum_{\substack{l=2 \\ l \neq \kappa}}^K \xi_l. \end{aligned}$$

Conceptually, the approach followed to minimize $BER^{(2)}$ via differentiation is the simplest. However as a consequence, the SCF for a given interferer is expressed in terms of the SCFs of the other interferers. Despite this, Equation (5.1) does converge after a certain number of iterations for each interferer if given an initial set of SCFs between zero and unity. The chosen number of iterations depends upon the desired level of SCF accuracy, as more iterations lead to increased SCF precision. In general, computation to two or three decimal places is sufficient. To maintain a given level of SCF accuracy, additional users require additional iterations.

Another issue concerning SCF accuracy is that Equation (5.1) assumes knowledge of signal and noise powers. While perfect knowledge of these quantities is usually not available in practice, they can be estimated in a number of ways varying in complexity and effectiveness [39, 40]. As we seek to expose the full potential of the soft cancellation factor technique, all

simulations and results in this chapter exploit perfect knowledge of signal and noise powers. The convergence of Equation (5.1) makes the implementation of the soft cancellation factor technique feasible in a digital receiver. Equation (5.1) can be used to tabulate a look-up table which the receiver can update according to changing conditions, and consult when cancelling interference.

We saw in Equation (3.33) that the cause of biased MAI estimates was in fact the MAI itself, and that using SCFs decreased the bias magnitude as seen in Equation (4.18). Equation (5.1) indicates however that optimal SCFs are not only functions of MAI parameters, but of noise power as well. The explanation for this is that even though noise does not contribute on an average basis to MAI estimates, noise does contribute to the oscillation of MAI estimates about their mean (i.e. contributes to their variance). Therefore, since noise impacts the variance of reconstructed MAI, which in turn impacts $BER^{(2)}(\{\xi_l\})$, optimal SCFs have to account for noise.

As we examine certain limiting cases in the next section, we will see the fundamental dependence of SCF upon MAI reliability. Namely, the more MAI estimates deviate from their true values due to either AWGN or other users accessing the channel, the smaller SCFs become so as to further down-scale unreliable MAI estimates.

5.2 Limiting Cases

Initial insights into the behavior of the SCFs can be gained by first observing certain extreme cases. We first investigate a system with hypothetically infinite processing gain. Such a system has infinite immunity to MAI and will only be impaired by AWGN. A quick inspection of Equation (5.1) shows that

$$\lim_{N \rightarrow \infty} \xi_\kappa = \frac{P_\kappa - \frac{N_o}{2T}}{P_\kappa + \frac{N_o}{2T}}. \quad (5.2)$$

Under full MAI immunity then, the SCFs depend only upon the given interferer's power and the noise power. Intuitively, the more noise present in the system, the less reliable

MAI estimates become, and consequently the more MAI estimates require scaling-down. Equation (5.1) is consistent with intuition as ξ_κ decreases with increased N_o . Further, for a given value of N_o , the stronger the interferer power P_κ , the more reliable the interferer's amplitude estimate, and correspondingly, the higher the SCF used to cancel the interferer becomes.

Continuing along this line of thought, if we consider the above infinite processing gain system with the additional hypothetical amenity of noise absence, we obtain a system with perfect MAI estimates. With ideal knowledge of interference uncorrupted by noise from AWGN, we would need no MAI down-scaling, corresponding to an SCF of unity. Examination of Equations (5.1) and (5.2) confirms that

$$\lim_{\substack{N \rightarrow \infty \\ N_o \rightarrow 0}} \xi_\kappa = 1. \quad (5.3)$$

It is interesting to note however that if the system is fully immune to MAI and there is no noise, any value of SCF (not just $\xi_\kappa = 1$) will lead to $BER^{(2)} = 0$, as the variance of the matched-filter outputs (at both stages) will be zero. Notwithstanding this, the fact that ξ_κ approaches unity under these conditions is indicative that less down-scaling is needed as MAI estimates become more and more reliable.

More general insight can be gained by considering a perfect power control system, thereby setting all signal powers equal to P . After some manipulation of Equation (5.1), one arrives at the result that under perfect power control, all interferers bear the same SCF, as determined by¹

$$\begin{aligned} \xi &= \frac{P(4N^2 - 2N) - 4N^2 \frac{N_o}{2T}}{P(4N^2 + 2K(2N - 1) - 3N - 2) + 4N^2 \frac{N_o}{2T}} \\ &= \frac{\frac{E_b}{N_o}(4N^2 - 2N) - 2N^2}{\frac{E_b}{N_o}(4N^2 + 2K(2N - 1) - 3N - 2) + 2N^2}. \end{aligned} \quad (5.4)$$

When all users are received with the same power, MAI estimates across all users share the same degree of reliability, and are thus all scaled-down by the same amount. As before, we

¹Analysis in the previous chapter was carried out assuming the presence of MAI, implying $K \geq 2$. Therefore, the constraint $K \geq 2$ must also be applied to the expression of ξ for perfect power control.

see in Equation (5.4) the same dependence of SCF upon N_o , namely the greater the noise power, the smaller the SCF.

Another important relationship revealed in Equation (5.4) is that of SCF with system loading: as system loading increases, SCF decreases. Specifically, the relationship of SCF with loading is inversely linear; however, the coefficients of Equation (5.4) are such that a plot of SCF versus loading would in fact look roughly linear, as we will soon see. This finding is in accord with earlier literature to the effect that the performance of CDMA systems degrades approximately linearly with system loading.

Equations (5.3) and (5.4) both serve to illustrate the fundamental dependence of SCF upon MAI reliability. Figure 5.1 shows a plot of Equation (5.4) with $N = 15$, and Figure 5.2 depicts the same for an $N = 31$ system. Indeed, as MAI fidelity drops, so does SCF, reflecting a lesser degree of reliability in MAI estimates. We can note that Figure 5.2 is essentially a version of Figure 5.1 stretched out over twice as many users. This is consistent with the fact that increasing the processing gain in a CDMA system amounts to enhancing the system's inherent MAI suppression ability. In effect, when doubling the processing gain for a given system load, the SCFs will need only down-scale MAI estimates by about half as much.

Further insight is gained in the following Monte-Carlo simulation experiments of specific cases.

5.3 Perfect Power Control

We begin our analysis of the SCF performance enhancement by picking-up the example in Figure 3.4 of a perfect power control system with $N = 15$ where we investigated the decay of decision statistic fidelity due to the bias as a function of loading. Employing optimal SCFs for each value of loading, we obtain a revised plot for the amplitude estimates in a synchronous system in Figure 5.3. We see that the bias has indeed been reduced as compared to brute

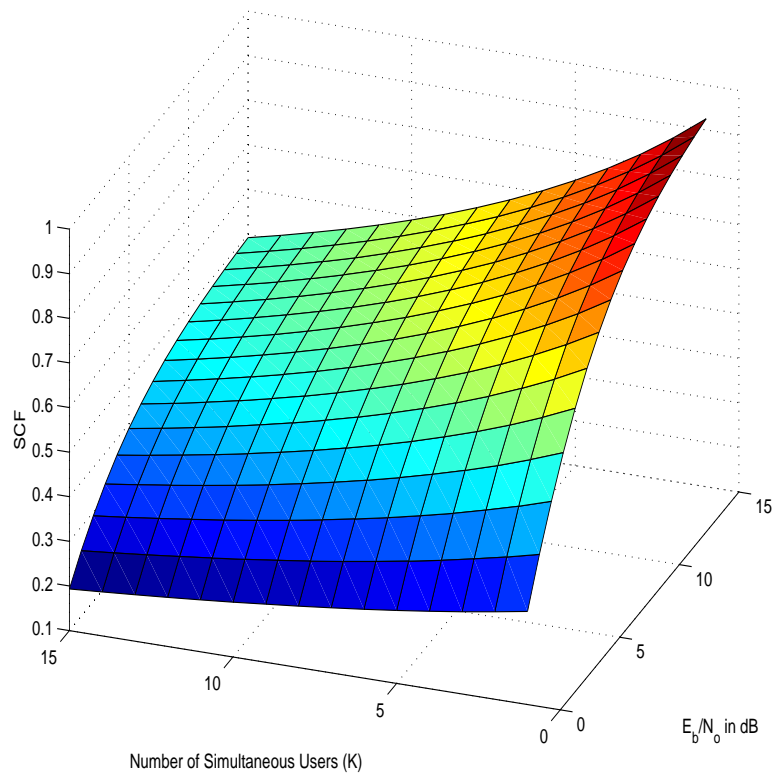


Figure 5.1: Soft Cancellation Factor (SCF) versus Number of Simultaneous Users (K) and versus $\frac{E_b}{N_o}$ for Processing Gain $N = 15$

cancellation where ξ is always unity. The bias magnitude is decreased more for heavier loads since MAI estimates are weighted down more in heavy loads due to their decreased reliability. Even though the bias has not been eliminated, we will see shortly that the SCF values corresponding to such a bias reduction are indeed those which minimize $BER^{(2)}$.

Moving on to actual BER improvements, we now look at a synchronous version the $N = 15$ and $K = 15$ asynchronous system considered earlier in Figure 3.5. The optimal SCFs for such a system, as computed with Equation (5.4), are plotted in Figure 5.4 against E_b/N_o . The SCF evolution exhibited is expected as SCF rises with E_b/N_o ; we can further note that the SCF evolution with E_b/N_o is roughly linear. Figure 5.5 depicts the resulting improvement in BER, as well as BER in cases where the SCFs used are not the optimal ones.

The BER sensitivity to different SCFs values is dependent on how far the SCFs used stray

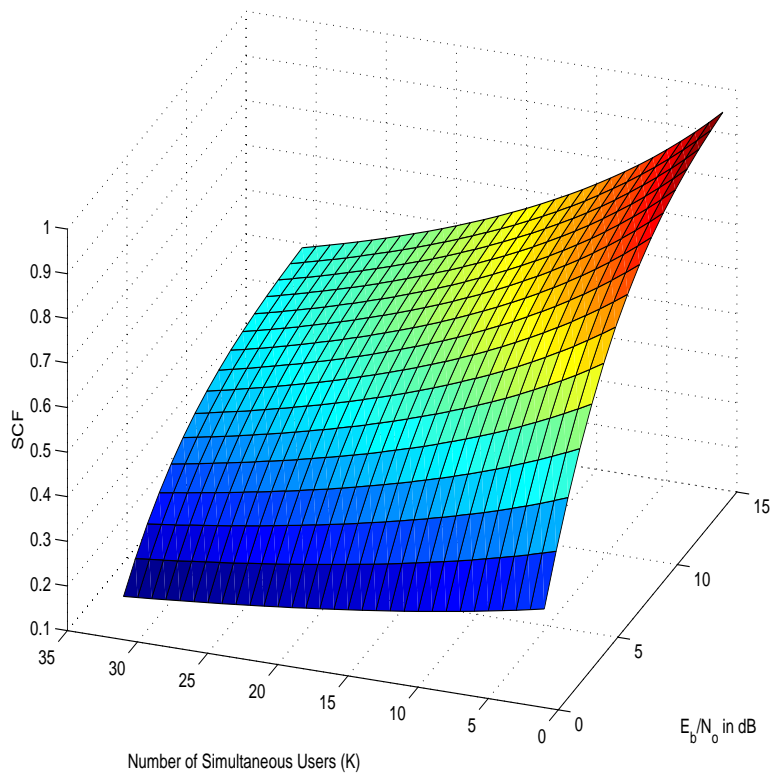


Figure 5.2: Soft Cancellation Factor (SCF) versus Number of Simultaneous Users (K) and versus $\frac{E_b}{N_o}$ for Processing Gain $N = 31$

from the optimal ones. The optimal ones minimizing BER are plotted in Figure 5.4 against E_b/N_o . When brute cancellation is used ($\xi = 1$ for all E_b/N_o), the difference is significant, corresponding to an extreme of MAI estimate unreliability. When $\xi = 0.8$, we approach more the range of optimal SCF values shown in Figure 5.4, and correspondingly, BER approaches the optimal BER. At $\xi = 0.3$, we are much closer to optimal SCF values, particularly for $0 \text{ dB} \leq E_b/N_o \leq 2 \text{ dB}$, and so BER is close to optimal in that E_b/N_o range.

We continue by evaluating the performance enhancement for our synchronous $N = 15$ system across different system loads. Figure 5.6 shows the optimal SCFs for system loads of 2 users to 15 users at a constant $E_b/N_o = 10 \text{ dB}$ for all users, and Figure 5.7 shows the resulting BER improvement across these loads. Indeed, as the number of users intensifies, MAI fidelity weakens and more down-scaling becomes necessary. The SCF dependence upon loading is

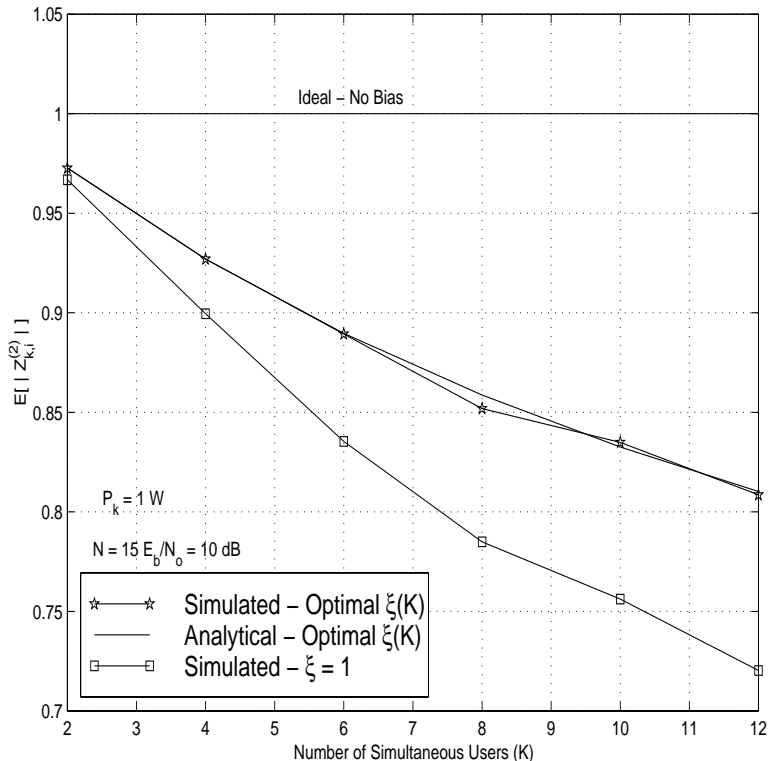


Figure 5.3: Average Second Stage Decision Metric $E \left[\left| Z_{k,i}^{(2)} \right| \right]$ versus Number of Simultaneous Users (K) for Processing Gain $N = 15$, $P_k = 1$ W for all Users, and $E_b/N_o = 10$ dB

now seen to be indeed approximately linear, just as it was with respect to E_b/N_o .

Figure 5.7 indicates that the BER enhancement for small loads is less marked since the system's unscaled MAI estimates are still reasonably reliable, but as the number of users approaches the system processing gain, the gain in BER becomes more pronounced. We provide in this plot as well a comparison with analytical BER derived under the premise of unbiased estimates². We see that even under such circumstances, the performance of the system is still surpassed by the use of optimal SCFs with a biased estimator. This is truly indicative of the potential of the soft cancellation technique. The reason for this performance advantage over the unbiased system is that an unbiased estimator's variance of

²Such unbiased estimates could not be provided by a matched-filter as we have established that the matched-filter is a biased estimator. Rather, an unbiased estimator would need to be employed.

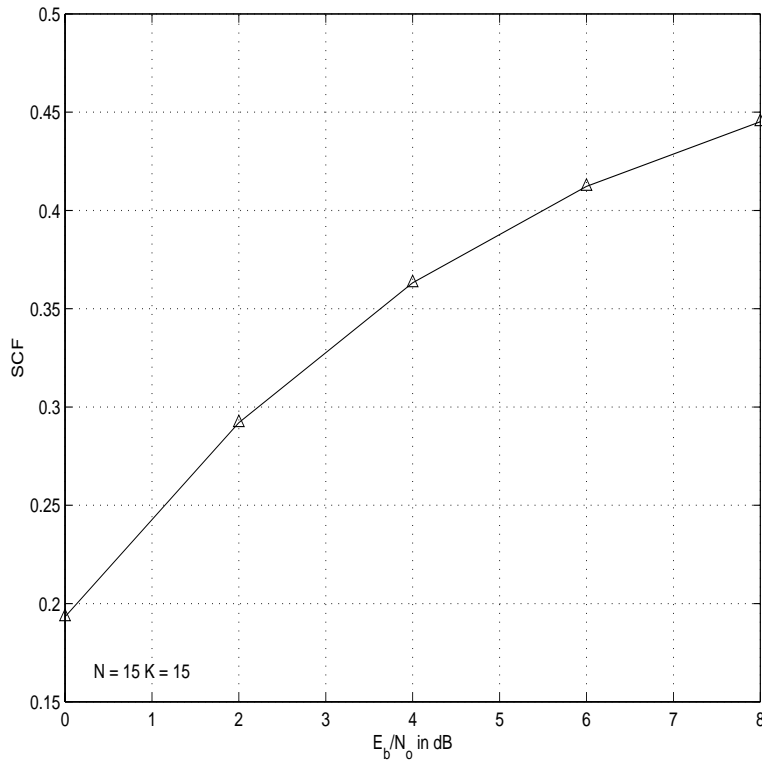


Figure 5.4: Soft Cancellation Factor versus $\frac{E_b}{N_0}$ for $N = 15$ and $K = 15$

MAI estimates (with brute cancellation) about their mean is still greater than that of the biased estimator using SCFs.

The fact that a biased system employing SCFs can perform better than an unbiased one using brute cancellation may prompt one to ask if an unbiased system with soft cancellation could do even better. Certainly, even in an unbiased system, the finite processing gain would hamper MAI estimate reliability to some extent, and soft cancellation may very well be capable of improving BER. It is the author's opinion that soft cancellation in an unbiased system would indeed improve performance beyond that of our biased system with soft cancellation.

Moving along with the performance analysis of our receiver, we now consider the sensitivity of BER to different SCFs, and consider as well how the SCFs analytically derived for the synchronous case improve performance for the asynchronous case. Figure 5.8 shows BER versus SCF across three different system loads for an $N = 31$ and $E_b/N_0 = 10$ dB system

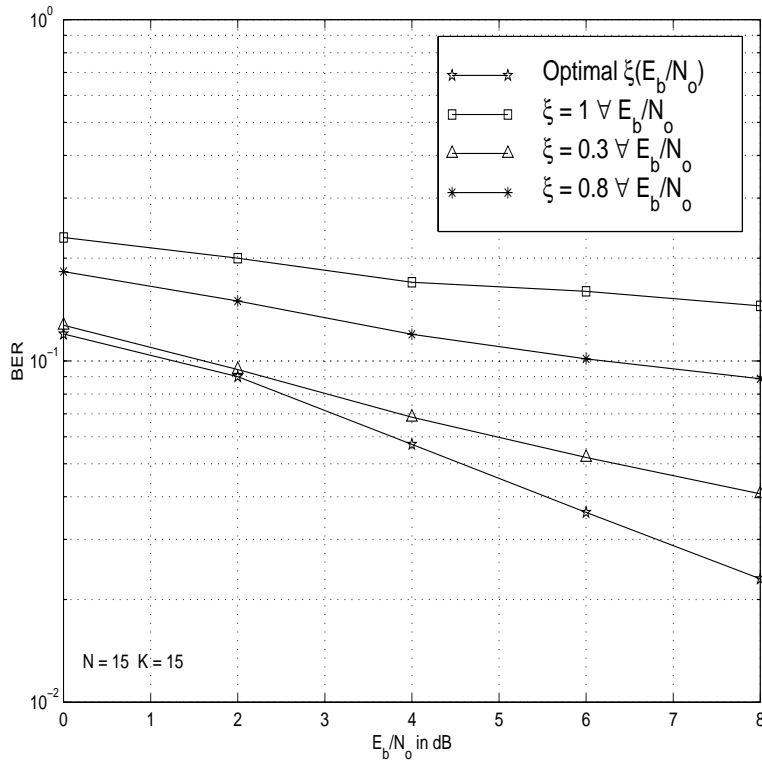


Figure 5.5: BER Comparison with Several SCFs for Processing Gain $N = 15$ and for Number of Simultaneous Users $K = 15$

for both the asynchronous and synchronous cases. We first treat the BER curves for the synchronous case which we have analyzed and then compare them to the corresponding curves for the asynchronous case.

For the case of a modest load, $K = 10$ users, in a synchronous system, $BER^{(2)}$ is minimized when $\xi = 0.7$, exactly as depicted satisfyingly in simulation. Under such a load, we see that BER is relatively sensitive to changes in SCF. We attribute this sensitivity to the fact that the bias magnitude in this modest load is relatively small, and as such MAI estimates are still fairly reliable and useful in cancellation. Therefore, over- or under-compensating for their unreliability induces changes in BER as soon as the non-optimal SCF value is used. For the slightly heavier load of $K = 15$ users, we see a close match between the optimal analytical SCF of $\xi = 0.62$ and lowest simulation BER occurring at an SCF of 0.6 (it should be noted

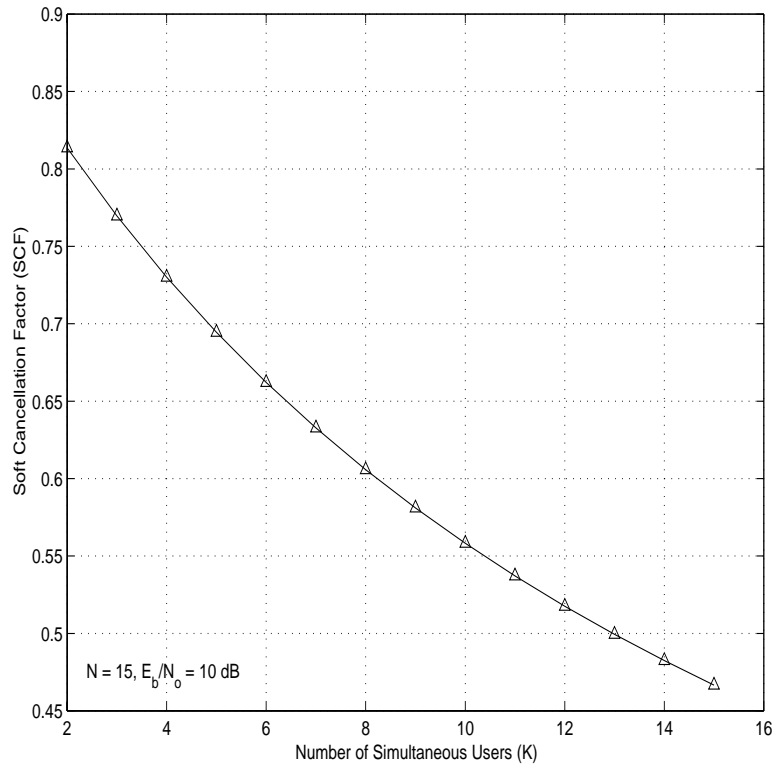


Figure 5.6: Soft Cancellation Factor versus Number of Simultaneous Users (K) for Processing Gain $N = 15$ and for $\frac{E_b}{N_o} = 10$ dB

though that simulations were run in 0.1 increments for SCF). The BER sensitivity to SCF when $K = 15$ is about the same as for $K = 10$, as expected. For $K = 30$, optimal analytical SCF occurs at $\xi = 0.47$ which is consistent with depicted simulation results. We note that under this heavy load, BER is less sensitive to changes in SCF than for lighter loads. When loading is heavy, MAI estimates are corrupted to a greater degree and are naturally less effective in cancellation. Consequently, wandering around the optimal SCF value bears less impact upon BER as for lesser loads.

Shifting now to the comparison between the synchronous and asynchronous systems, we see in Figure 5.8 that for the modest load of $K = 10$ users, the SCFs minimizing BER for both synchronous and asynchronous systems roughly match, but as loading grows, a mismatch sets in with the optimal SCF for asynchronous systems being higher than that for synchronous

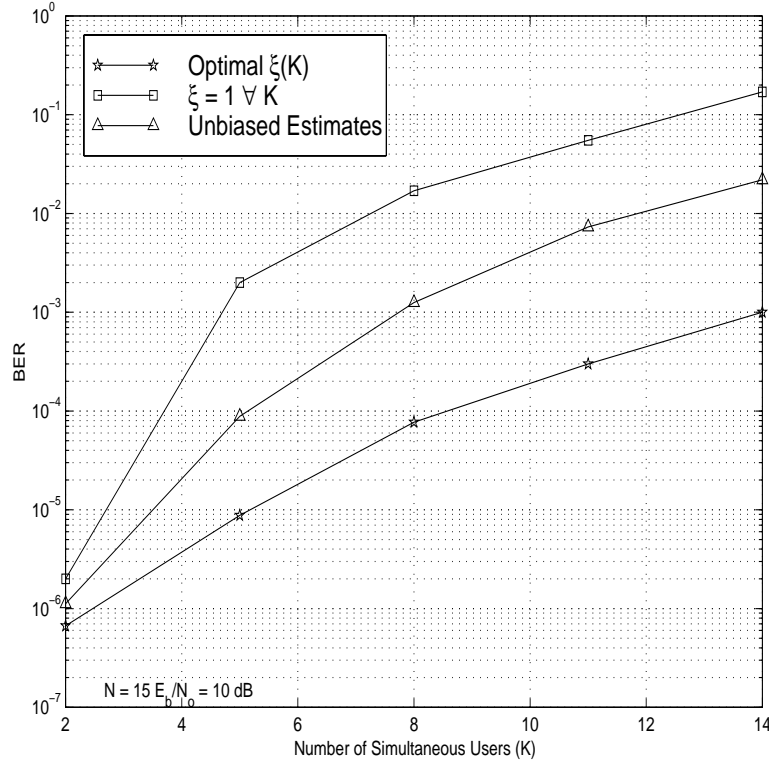


Figure 5.7: BER Comparison of Soft Cancellation, Cancellation when $\xi = 1$, and Cancellation when $\xi = 1$ with Unbiased Estimates for Processing Gain $N = 15$ and for $\frac{E_b}{N_o} = 10$ dB

systems. We explain this discrepancy by referring the reader to the bias magnitudes for synchronous and asynchronous systems for user signals with unity power, produced below

$$|\text{Bias}_{\text{Synch.}}| = \frac{K-1}{2N} \quad |\text{Bias}_{\text{Asynch.}}| = \frac{K-1}{3N}. \quad (5.5)$$

The magnitude of the difference between the two is then

$$|\text{Bias}_{\text{Synch.}} - \text{Bias}_{\text{Asynch.}}| = \frac{K-1}{6N}. \quad (5.6)$$

When loading is low, we can see that the two magnitudes are more similar to each other than when loading is higher. For low system loads then, the amount of MAI estimate corruption is on average roughly similar between the two cases. Therefore, the two types of systems share about the same degree of optimal adjustment (SCF values) for MAI estimate unreliability

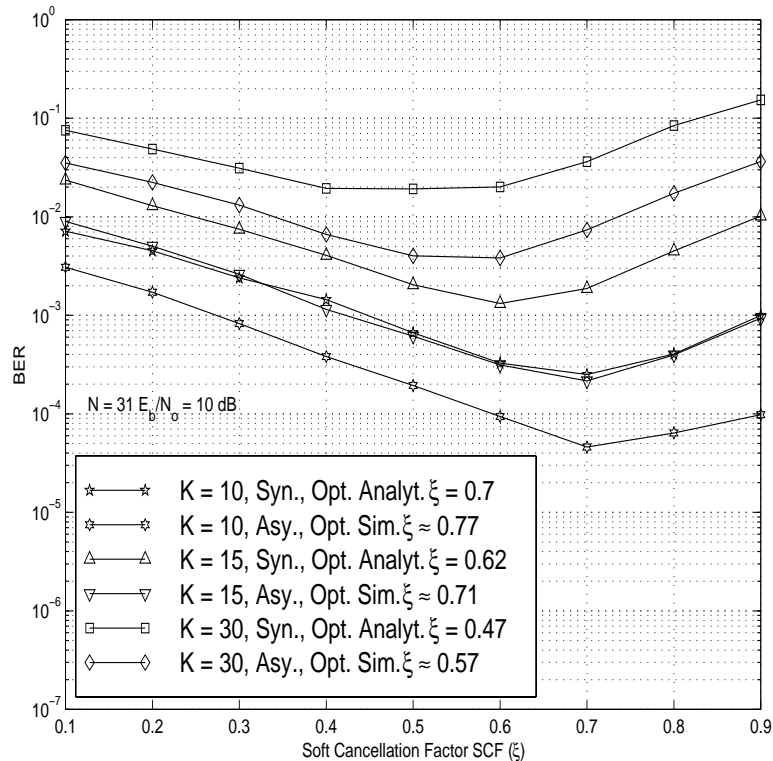


Figure 5.8: BER versus Soft Cancellation Factor (SCF) Across Various System Loads (K) for Both Synchronous and Asynchronous Systems with Processing Gain $N = 31$ and $E_b/N_0 = 10$ dB

for low loading. For a given higher loading however, the bias magnitude of the synchronous system is greater than in the asynchronous system, leading consequently to a lower SCF for the synchronous system.

However, despite the fact that for heavier system loads the optimal SCFs differ in the synchronous and asynchronous cases, BER for these heavier loads is not very sensitive locally around the optimal SCF value. Therefore, one could in fact use the optimal SCFs derived for the synchronous case in the asynchronous case without incurring any genuine degradation in BER.

5.4 The Near-Far Case

When users are received with significantly different powers, the weaker users often suffer from higher BERs than their stronger counterparts since the lower power signals are drowned in the pool of higher power signals. Figure 5.9 depicts the SCFs and the BERs for a system with $N = 31$, $K = 20$ users, and $E_b/N_o = 10$ dB. The 20 users are separated into 2 power groups: 10 weak users and 10 strong users. The BERs of the two groups with and without SCF usage are compared as their power disparity is taken from 0 dB to 15 dB.

Figure 5.9 shows the evolution of SCF as the power disparity grows for the two groups of users. Since in this case there are only two distinct powers (the weaker power attributed to 10 users and the stronger power attributed to the other 10 users), all users within a power group bear the same SCF. Figure 5.9 depicts the SCF used to cancel users from a given group when the desired user is from the other group. When the desired user is a weak user and we wish to cancel a strong user, the SCF used to cancel the strong user rises as the strong user's power increases because the greater its power, the more reliable its amplitude estimate becomes. When the desired user is a strong user and we wish to cancel a weak user, the SCF used to cancel the weak user diminishes as the power gap widens, because the weak user's amplitude estimate reliability worsens with the power disparity. Figure 5.10 demonstrates the resulting BER enhancement using SCFs. The strong users benefit the most since their power is greater to begin with. The weak users' BER still degrades, but not as severely as it would without SCFs.

Despite a simulated power disparity of up to 15 dB, a cellular system usually benefits from power control and is thus assured that received power variations are maintained relatively small. Therefore, referring to Figure 5.10, a cellular system using soft cancellation can see the BER of its weaker users increase by about an order of magnitude over brute cancellation.

We conclude this chapter with an implementation note. It was observed in Section 5.2

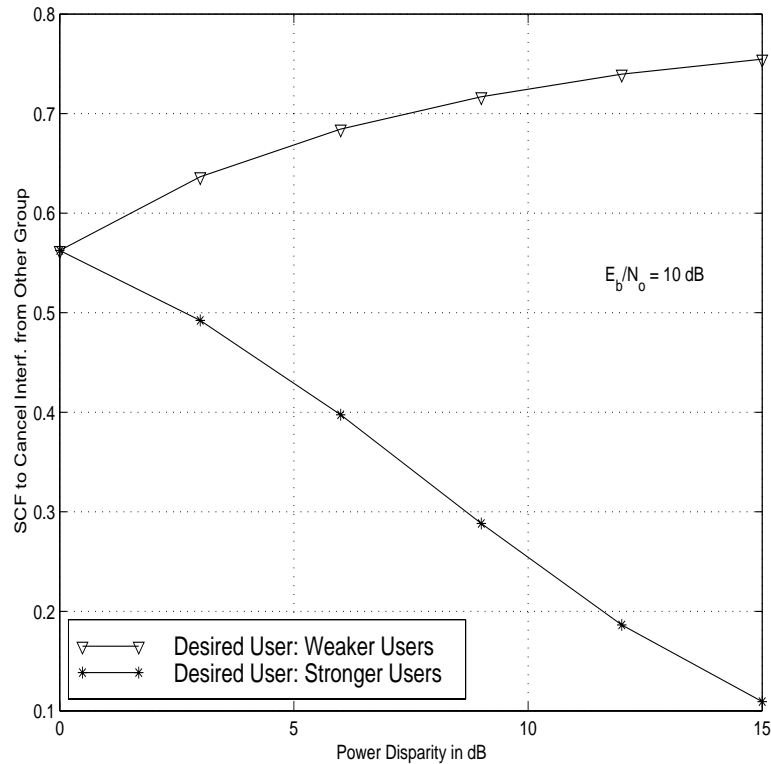


Figure 5.9: Soft Cancellation Factor versus Power Disparity in dB for Processing Gain $N = 31$ and for $\frac{E_b}{N_o} = 10$ dB

that for perfect power control, all interferers bear identical SCFs. This in turn means that, regardless of the desired user, all users in a given system will be cancelled with a unique SCF. Given this, it is possible to implement the cancellation process by cancelling all users at once, and then for each desired user, adding in the corresponding reconstructed signal estimate for matched-filtering. This implementation is linear in K , in contrast to the more computationally expensive quadratic in K implementation in Figures 3.2 and 4.2.

If however, signals are received with differing power levels, each user's SCF will be different and will furthermore depend upon which user is the desired user. Therefore, for optimal soft interference cancellation, the quadratic in K complexity implementation must be used. An interesting topic of future research in this area would be to investigate how to choose a unique SCF to attribute to each interferer so as to minimize the difference between the

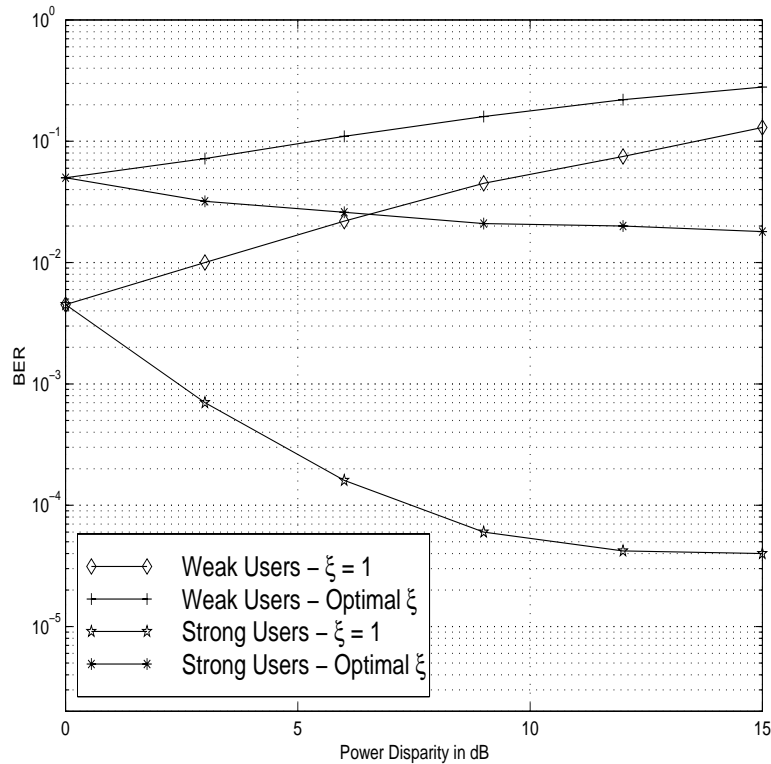


Figure 5.10: BER Comparison of Soft Cancellation versus Brute Cancellation ($\xi = 1$) for Processing Gain $N = 31$ and for $\frac{E_b}{N_o} = 10$ dB

resulting BER and the optimal one, and under what conditions of power disparities would such an approximation be acceptable.

5.5 Chapter Summary

This chapter presented both quantitatively and qualitatively the BER performance enhancements allowable with the use of soft interference cancellation. We saw that under the conditions of perfect power control and under the near-far effect as well, substantial BER gains are achievable as compared to blunt cancellation; sometimes even, system BER can improve by over an order of magnitude.

Chapter 6

Conclusions

In this final chapter, we summarize the work and contributions detailed throughout this thesis and make recommendations for future research in the area of soft interference cancellation for CDMA.

6.1 Summary and Contributions

Chapter 2 briefly described Verdù's optimal CDMA detector yielding lowest possible probability of error. Such a detector is not practical for implementation, but this result spawned the quest for detection algorithms that approach optimal performance with reasonable complexity. We presented some of the fruits of this quest and have since concentrated on a particular variety of such sub-optimal CDMA receivers, namely parallel interference cancellation.

Chapter 3 presented a parallel interference cancellation structure first introduced by Striglis *et al.* [24, 35]. We showed that the use of matched-filters to form amplitude estimates results in biased amplitude estimates, which can have devastating effects on BER (after cancellation), particularly under severe system loads. We motivated the need for an effective

low-complexity bias mitigation solution and cited previous empirical results [2, 1] of the success of soft rather than brute cancellation.

Chapter 4 continued in the direction of soft cancellation by modelling and analyzing soft interference cancellation in our receiver structure. We determined the mean and variance of second stage statistics in terms of SCFs and then expressed second stage BER in terms of the SCFs. We derived the optimal set of SCFs for a given system that minimizes BER after cancellation.

We verified the BER performance enhancements from soft cancellation in Chapter 5. Beginning with generalities, we considered issues in evaluation of the optimal SCF and analyzed the expression for optimal SCF in limiting cases to check for soundness. We then delved into simulation trials for perfect power control and in the near-far situation. We found that soft cancellation does indeed improve performance in all circumstances over brute cancellation (no MAI estimate down-scaling). The degree of improvement was generally found to be dependent upon loading and noise levels, with higher loading and E_b/N_o leading to greater improvements. We also compared our results to empirical trials of soft cancellation in asynchronous systems under perfect power control. Results indicated that with lighter loading came a greater similarity in optimal SCFs between synchronous and asynchronous systems. Despite a slight difference in SCF values between the synchronous and asynchronous cases, we found that in general, optimal SCFs for the synchronous case can be applied to the asynchronous case. When in the near-far situation, system performance for both weak and strong users improved as compared to brute cancellation. However, the BER of the weak users was still found to decay with increasing power disparity, albeit to a lesser degree than with brute cancellation. It was noted however that we can assume rough power control in a cellular system, and the improvement for lower power users can still be an order of magnitude.

The principle contribution of this work is the first analytical expression for optimal soft cancellation factors for parallel interference cancellation in a synchronous AWGN CDMA channel. This thesis is able to analytically substantiate performance gains observed during

empirical work in the past, and further, identify and track the dependencies of these improvements. While analyzed for synchronous systems, we have shown in some generality that the results can be applied to asynchronous systems as well.

6.2 Future Work

The work in this thesis leaves room for continued research in a number of directions. Of greatest interest to the author is the analytical modelling of soft cancellation in an asynchronous system. It would most interesting to see analysis corroborate simulation results once again, and to gain insights into the differences between synchronous and asynchronous performance using soft interference cancellation. Further insights could also be gained by investigating the performance of soft cancellation in a system with an unbiased amplitude estimator; the author predicts that performance of such a system would surpass that of all others considered here.

Moreover, as suggested at the end of the preceding chapter with regard to the near-far situation, a study of how to attribute a unique SCF to each interferer such that the difference in BER compared to using optimal SCFs is minimized. Use of a unique SCF permits the linear in K implementation of the receiver. Finally, since we have analyzed soft cancellation in a relatively benign type of channel (AWGN), it would be interesting to see how or if soft cancellation would help in multipath fading conditions.

Bibliography

- [1] R. M. Buehrer and B. D. Woerner. *The Application of Multiuser Detection to Cellular CDMA*. PhD thesis, Virginia Polytechnic Institute and State University, Blacksburg, VA, June 1996.
- [2] N. S. Correal, R. M. Buehrer, and B. D. Woerner. Improved cdma performance through bias reduction for parallel interference cancellation. In *Personal Indoor Mobile Radio Communications (PIMRC)*, pages 565–569, Helsinki, Finland, Sep 1997.
- [3] D. Divsalar, M. K. Simon, and D. Raphaeli. Improved parallel interference cancellation for cdma. *IEEE Trans. Commun.*, 46(2):258–268, Feb 1998.
- [4] M. B. Pursley. Performance evaluation of phase-coded spread spectrum multiple-access communications-part i: System analysis. *IEEE Trans. Commun.*, COM-25(8):795–799, Aug 1977.
- [5] Theodore S. Rappaport. PCS: An academic perspective. In *PCS'97 Track 7*, Sep 1997. Keynote Address.
- [6] W. W. Erdman. Wireless communications: A decade of progress. *IEEE Communications Magazine*, 31(12):48–51, May 1993.
- [7] Theodore S. Rappaport. *Wireless Communications, Principles and Practice*. Prentice Hall PTR, 1996.

- [8] W. C. Y. Lee. Overview of cellular cdma. *IEEE Transactions on Vehicular Technology*, 40(2):87–98, Jan 1991.
- [9] K. S. Gilhousen. On the capacity of a cellular cdma system. *IEEE Transactions of Vehicular Technology*, 40(2):303–312, May 1991.
- [10] P. Jung, P. W. Baier, and A. Steil. Advantages of cdma and spread spectrum over fdma and tdma in cellular mobile radio applications. *IEEE Transactions on Vehicular Technology*, 42(3):357–364, Aug 1993.
- [11] D. J. Goodman. Trends in cellular and cordless communications. *IEEE Commun. Magazine*, 29(6):31–39, June 1991.
- [12] R. A. Scholtz. The origins of spread spectrum communications. *IEEE Commun. Magazine*, COM-30:822–854, May 1982.
- [13] R. Price and P. E. Green. A communication technique for multipath channels. In *Proc. IRE*, volume 46, pages 555–570, Mar 1958.
- [14] D. L. Schilling. Broadband cdma for personal communication systems. *IEEE Commun. Magazine*, 29(11):86–93, Nov 1991.
- [15] G. E. Cooper and R. W. Nettleton. A spread-spectrum technique for high capacity mobile communications. *IEEE Trans. Veh. Tech.*, VT-27(4):264–275, Nov 1978.
- [16] B. Gudmundson and J. Skold. A comparison of cdma and tdma systems. In *Proc. 42nd IEEE Veh. Tech. Conf.*, pages 732–735, Denver, CO, May 1992.
- [17] A. J. Viterbi. When not to spread-spectrum. a sequel. *IEEE Commun. Magazine*, 23:12–17, Apr 1985.
- [18] R. A. Cameron and B. D. Woerner. An analysis of cdma with imperfect power control. In *Proc. 42nd IEEE Veh. Tech. Conf.*, pages 977–980, Denver, CO, May 1992.

- [19] L. W. Couch II. *Digital and Analog Communication Systems*. MacMillan, fourth edition, 1993.
- [20] A. Duel-Hallen, J. Holtzman, and Z. Zvonar. Multiuser detection for cdma systems. *IEEE Commun. Magazine*, pages 46–58, Apr 1995.
- [21] S. Moshavi. Multi-user detection for ds-cdma communications. *IEEE Commun. Magazine*, pages 124–136, Oct 1996.
- [22] S. Verdu. Minimum probability of error for asynchronous gaussian multiple access channels. *IEEE Trans. Inform. Theory*, IT-32(1):85–96, Jan 1986.
- [23] M. K. Varanasi and B. Aazhang. Multistage detection in asynchronous code division multiple-access communications. *IEEE Trans. Commun.*, 38(4):509–519, Apr 1990.
- [24] S. Striglis, A. Kaul, N. Yang, and B. D. Woerner. A multistage rake receiver for improved capacity of cdma systems. In *Proc. 44th IEEE Veh. Tech. Conf.*, pages 789–793, Stockholm, Sweden, June 1994.
- [25] A. Kaul and B. D. Woerner. An adaptive multistage interference cancellation receiver for cdma. Master’s thesis, Virginia Polytechnic Institute and State University, Blacksburg, VA, Mar 1995.
- [26] R. C. Dixon. *Spread Spectrum Systems*. Wiley, New York, 1984.
- [27] H. Taub and D. L. Schilling. *Principles of communication systems*. McGraw Hill Book Company, second edition, 1986.
- [28] Telecommunications industry association, Washington DC. *TIA/EIA Interim Standard, Mobile base station compatibility standard for dual-mode wideband spread spectrum cellular system*, July 1993.
- [29] V. Aue and J.H. Reed. An interference robust cdma demodulator that uses spectral correlation properties. In *Proc. 44th IEEE Veh. Tech. Conf.*, pages 563–567, Stockholm, Sweden, June 1994.

- [30] R. D. Holley and J. H. Reed. Using spectral correlation to reduce multiple access interference in cdma systems. In *Second workshop on cyclostationary signals*, pages 15.1–15.14, Monterey, CA, July 31-Aug 2 1994.
- [31] J. D. Laster and J. H. Reed. A survey of adaptive single channel interference rejection techniques for wireless communications. In *Proc. Fourth Virginia Tech Symposium on Wireless Personal communications*, pages 2.1–2.25, Blacksburg, VA, June 1994.
- [32] K. S. Schneider. Optimum detection of code division multiplexed signals. *IEEE Trans. Aero. Electronic Sys.*, AES-15(1):181–185, Jan 1979.
- [33] J. M. Holtzman. Ds/cdma successive interference cancellation. In *Proc. Third IEEE ISSSTA*, pages 69–76, Oulu, Finland, July 4-6 1994.
- [34] R. M. Buehrer, N. S. Correal, and B. D. Woerner. A comparison of multiuser receivers for cellular cdma. In *IEEE Global Telecommunications Conference*, pages 1571–1577, United Kingdom, Nov 1996.
- [35] S. Striglis. A multistage rake receiver for cdma systems. Master's thesis, Virginia Polytechnic Institute and State University, Blacksburg, VA, Aug 1994.
- [36] D. Divsalar and M. Simon. Improved cdma performance using parallel interference cancellation. Technical Report JPL Publication 95-21, California Institute of Technology, Jet Propulsion Laboratory (JPL), Pasadena, CA, Oct 1995.
- [37] Jr. R. K. Morrow and J. S. Lehnert. Bit-to-bit error dependence in slotted ds/ssma packet systems with random signature sequences. *IEEE Trans. Commun.*, 37(10):1052–1061, Oct 1989.
- [38] J. S. Lehnert and M. B. Pursley. Error probabilities for binary direct-sequence spread spectrum communications with random signature sequences. *IEEE Trans. Commun.*, COM-35(1):87–98, Jan 1987.

- [39] T. K. Moon, Z. Xie, C. K. Rushforth, and R. T. Short. Parameter estimation in a multi-user communication system. *IEEE Trans. Commun.*, 42(8):2553–2560, Aug 1994.
- [40] N. Celandroni, E. Ferro, and F. Potorti. Quality estimation of psk modulated signals. *IEEE Commun. Magazine*, pages 50–55, July 1997.

Appendix

In this appendix, we reproduce the various moments of the synchronous PN code waveform/sequence cross-correlations from [36]. For convenience, we reproduce the definitions of the PN code waveforms.

The k^{th} user's binary data stream $b_k(t)$ is spread by its unique signature code waveform $a_k(t)$, given by

$$a_k(t) = \sum_{n=-\infty}^{\infty} a_{k,n} p_{T_c}(t - nT_c), \quad (6.1)$$

where $\{a_{k,n}\}$ is a set of (*i.i.d.*) Bernoulli random variables, with $a_{k,n} \in \{-1, +1\}$ and $Pr[a_{k,n} = -1] = Pr[a_{k,n} = +1] = 1/2$. The unit pulse of duration T is $p_{T_c}(t)$. The processing gain of the system N is defined as the ratio of the bit duration to the chip duration $N = T/T_c$.

The synchronous cross-correlation of the PN codes of users i and j is defined to be

$$\Gamma_{i,j} = \frac{1}{T} \int_0^T a_i(t) a_j(t) dt = \frac{1}{N} \sum_{m=1}^N a_{i,m} a_{j,m}. \quad (6.2)$$

We have the following moment computations

$$\begin{aligned} E[\Gamma_{i,j}] &= \frac{1}{N} \sum_{m=1}^N E[a_{i,m} a_{j,m}] = 0 \\ E[\Gamma_{i,j}^2] &= \frac{1}{N^2} \sum_{m=1}^N \sum_{n=1}^N E[a_{i,m} a_{j,m} a_{i,n} a_{j,n}] = \frac{1}{N^2} \sum_{m=1}^N E[a_{i,m}^2 a_{j,m}^2] = \frac{1}{N} \\ E[\Gamma_{i,j} \Gamma_{j,m} \Gamma_{i,m}] &= \frac{1}{N^3} \sum_{l=1}^N \sum_{k=1}^N \sum_{n=1}^N E[a_{i,l} a_{j,l} a_{j,k} a_{m,k} a_{i,n} a_{m,n}] = \frac{1}{N^3} \sum_{l=1}^N E[a_{i,l}^2 a_{j,l}^2 a_{m,l}^2] = \frac{1}{N^2} \end{aligned}$$

$$E \left[\Gamma_{i,j}^3 \right] = \frac{1}{N^3} \sum_{k=1}^N \sum_{l=1}^N \sum_{m=1}^N E \left[a_{i,k} a_{j,k} a_{i,l} a_{j,l} a_{i,m} a_{j,m} \right] = 0$$

$$\begin{aligned} E \left[\Gamma_{i,j}^2 \Gamma_{i,k}^2 \right] &= \frac{1}{N^4} \sum_{l=1}^N \sum_{m=1}^N \sum_{n=1}^K \sum_{r=1}^N E \left[a_{i,l} a_{j,l} a_{i,m} a_{j,m} a_{i,n} a_{k,n} a_{i,r} a_{k,r} \right] \\ &= \frac{1}{N^4} \sum_{l=1}^N \sum_{n=1}^N E \left[a_{i,l}^2 a_{j,l}^2 a_{i,n}^2 a_{k,n}^2 \right] = \frac{1}{N^2} \end{aligned}$$

$$\begin{aligned} E \left[\Gamma_{i,j}^4 \right] &= \frac{1}{N^4} \sum_{k=1}^N \sum_{l=1}^N \sum_{m=1}^K \sum_{n=1}^N E \left[a_{i,k} a_{j,k} a_{i,l} a_{j,l} a_{i,m} a_{j,m} a_{i,n} a_{j,n} \right] \\ &= 3 \cdot \frac{1}{N^4} \sum_{m=1}^N \sum_{\substack{k=1 \\ k \neq m}}^N E \left[a_{i,k}^2 a_{j,k}^2 a_{i,m}^2 a_{j,m}^2 \right] + \frac{1}{N^4} \sum_{k=1}^N E \left[a_{i,k}^2 a_{j,k}^4 \right] \\ &= \frac{3N(N-1)}{N^4} + \frac{1}{N^3} = \frac{3}{N^2} - \frac{2}{N^3} \end{aligned}$$

$$\begin{aligned} E \left[\Gamma_{i,k} \Gamma_{j,k} \Gamma_{i,l} \Gamma_{j,l} \right] &= \frac{1}{N^4} \sum_{m=1}^N \sum_{n=1}^N \sum_{r=1}^K \sum_{s=1}^N E \left[a_{i,m} a_{k,m} a_{j,n} a_{k,n} a_{i,r} a_{l,r} a_{j,s} a_{l,s} \right] \\ &= \frac{1}{N^4} \sum_{m=1}^N \sum_{r=1}^N E \left[a_{i,m} a_{j,m} a_{k,m}^2 a_{i,r} a_{j,r} a_{l,r}^2 \right] = \frac{1}{N^4} \sum_{m=1}^N E \left[a_{i,m}^2 a_{j,m}^2 \right] = \frac{1}{N^3}. \end{aligned}$$

Vita

Pascal Renucci was born on May 13th, 1973 in New York City. After spending 18 years in this most relaxed, stress-free city, he enrolled at Carnegie Mellon University in Pittsburgh, Pennsylvania. He graduated with his Bachelor of Science in Electrical and Computer Engineering degree in May 1995, and came to Virginia Tech the following Fall term. During the summer of 1996, Pascal became a member of the Mobile and Portable Radio Research Group (MPRG). At MPRG, he conducted research in the optimization of soft parallel interference cancellation for DS-CDMA receivers, the fruits of which have lead to a journal publication in The IEE Electronics Letters and a conference publication in the proceedings of The International Conference on Telecommunications, June 1998, Greece. His research interests at large include, multiuser detection theory, digital signal processing, and general analysis and simulation of digital communication systems.

Pascal graduated with a Master of Science in Electrical Engineering in May 1998 from Virginia Tech and started work at Hewlett-Packard Laboratories in Palo Alto, California soon thereafter. Pascal is a student member of the IEEE and a member of the Eta Kappa Nu (HKN) Electrical Engineering honor society.